THE ROLE OF HYDROGEN CYANIDE IN CHEMICAL EVOLUTION

by

Rafael Navarro-González

Dissertation submitted to the Faculty of the Graduate School
of The University of Maryland in partial fulfillment
of the requirements for the degree of
Doctor of Philosophy
1989

Advisory Committee:

Professor Cyril Ponnamperuma, Chairman/Advisor
Professor Norman J. Hansen
Professor Joseph Sampugna
Professor Raj K. Khanna
Professor Joseph Silverman
Doctor Mitchell K. Hobish

ABSTRACT

Title of Dissertation: THE ROLE OF HYDROGEN CYANIDE IN CHEMICAL EVOLUTION

Name of degree candidate: Rafael Navarro-González

Degree and year: Doctor of Philosophy, 1989

Dissertation directed by: Cyril Ponnamperuma, Professor and Director Laboratory of Chemical Evolution, Department of Chemistry and Biochemistry

Two major research areas are investigated: The electrosynthesis of hydrogen cyanide; and the role of cyanocomplexes in the free-radical oligomerization of hydrogen cyanide.

The electric discharge production of hydrogen cyanide from a simulated primitive atmosphere composed of methane, nitrogen and water vapor was investigated. The radiation chemical yield (G) of formation of HCN

was determined to be 0.26. A free radical mechanism was proposed to account for the observed chemical changes. Computer simulations of the reaction mechanism could effectively model the early stages of electrolysis of the gas mixture, and permitted the estimation of the rate of electrosynthesis of hydrogen cyanide under various atmospheric conditions.

The possible role of cyanocomplexes of transition elements on the free-radical oligomerization of hydrogen cyanide was investigated. Aqueous, oxygen-free, dilute solutions of hydrogen cyanide and hexacyanoferrate(II) or (III) were submitted to various doses of gamma irradiation. The presence of either cyanocomplex led to a significant decrease in the rate of decomposition of hydrogen cyanide. The major products were ammonia and carbon dioxide. Computer simulations of these systems permitted the elucidation of the reaction mechanism and the derivation of rates of reactions of free-radicals with the cyanocomplexes. The results obtained provide an insight into the possible role of cyanocomplexes of transition elements in chemical evolution.

DEDICATION

To my wife, Fabiola Aceves-Diaz, my son Rafael Navarro-Aceves, my mother, Carmen González de Navarro, and all members of our families.

To the memory of my father,

Rafael Navarro-Contreras

1932-1985

ACKNOWLEDGEMENT

I am especially indebted to my advisor, Professor Cyril Ponnamperuma for his constant support and encouragement throughout this study. He fostered creativity in my research by providing right degree of autonomy. I am thankful to Professor Joseph Silverman for allowing me have complete use of his ionizing radiation facilities, and to his graduate students Byron Lambert and Fuh-Wei Tang for their constant assistance during the irradiation of samples. I appreciate the great interest and help of Dr. Yasuhiro Honda during the development of the dosimetric methods and preparation of samples for electric discharges. I am also very thankful to Dr. Mitchell K. Hobish for his great interest and help at several stages in this study.

I am indebted to my Mexican advisor, Professor Alicia Negrón-Mendoza, Chairman of the Chemistry Department of the Institute of Nuclear Sciences, U.N.A.M., for her constant interest and support throughout this study; I am thankful to Professor

Marcos Rosenbaum P., Director of this Institute, for his interest and advises during my academic training at Maryland. I conducted a portion of this work in their Institute, and am grateful for their consideration to use the ionizing radiation sources and the laboratory facilities during my short stays at Mexico City. I want to acknowledge a fellowship from The National Autonomous University of Mexico (U.N.A.M.) during my graduate studies at Maryland.

I wish to thank all members of the Laboratory of Chemical Evolution for providing a friendly and scientific atmosphere.

Finally to my wife, Fabiola Aceves-Diaz, and my son Rafael Navarro-Aceves, for their constant encouragement and patient endurance, I am grateful in measure beyond words.

College Park, Md
Spring, 1989

Rafael Navarro-González

TABLE OF CONTENTS

LIST OF TABLES

LIST OF FIGURES

CHAPTER 1

THE ABIOTIC CHEMISTRY OF HYDROGEN CYANIDE

1.1 Introduction

Modern scenarios of the origin of life on Earth are based on ideas generated independently by Oparin (1924) and Haldane (1929). According to these authors the appearance of the first living cells was preceded by abiotic syntheses and accumulation of organic compounds of increasing complexity on the primitive Earth. These compounds were essential for the origin and evolution of phase-separated systems that eventually led to the emergence of the first populations of living cells (Oparin, 1924, 1938, 1957, 1972; and Haldane, 1938).

The earliest published experiment expressly designated as demonstrating the formation of organic compounds from a hypothetical primitive atmosphere was

that by Groth and Suess (1938). They exposed a CO_2-H_2O gas mixture with ultraviolet light at 147 nm, and identified formaldehyde and glyoxal as products. These results were interpreted as "giving an explanation for the formation of certain carbon compounds that were probably prerequisite for the appearance of life" (Groth and Suess, 1938). Later, Calvin and coworkers (Garrison *et al.*, 1951) simulated the atmosphere-hydrosphere interface, by irradiating with α-rays an aqueous solution containing ferrous ion in equilibrium with a CO_2-H_2 gas mixture. Formaldehyde, formic acid and succinic acid were identified among the products. Shortly after, Miller (1953, 1957a,b) reported the synthesis of amino acids such as glycine, alanine and β-alanine, among others, from the electric discharge of a CH_4-NH_3-H_2-H_2O gas mixture. Based on the observation that HCN and aldehydes were formed in the early phase of the experiments, Miller suggested that α-amino acids were formed by the Strecker mechanism (Miller, 1957b), which consists of the condensation of HCN, RCHO, and NH_3 (Reaction 1.1), followed by hydrolysis of the α-amino nitrile (Reaction 1.2):

$$RCHO + NH_3 + HCN \longrightarrow RCH(NH_2)CN + H_2O \qquad (1.1)$$

$$RCH(NH_2)CN + 2H_2O \longrightarrow RCH(NH_2)CO_2H + NH_3 \qquad (1.2)$$

The first direct evidence of the possible importance of HCN in chemical evolution was indicated by the studies of Oró and coworkers, who found that adenine (Oró, 1960, Oró and Kimball, 1961) and amino acids such as glycine, alanine, and aspartic acid (Oró and Kamat, 1961) were formed when an aqueous concentrated ammoniacal solution of HCN was heated. Such results were not only confirmed, but also the number of identified products was extended to include formic acid, urea, hypoxanthine (Lowe *et al.*, 1963), and several other amino acids (Lowe *et al.*, 1963, Matthews and Moser, 1966).

These findings have such a significant impact in understanding the abiogenesis of biological precursors from simple molecules, that a reexamination of the data was suggested by Sidle (1967) to ensure that these were not due to low level contamination from the reagents and/or the environment. Over hundred scientific articles published in the last two decades have not only demonstrated the versatility of HCN in promoting syntheses of a large array of biologically important compounds, but also contributed to a profound understanding of the chemistry involved (see, for instance,

Ferris and Hagan, 1984, and references therein).

This chapter reviews the current status of studies of the abiotic chemistry of hydrogen cyanide, and directs attention to areas where further research is needed. The material examined below has been grouped into three major areas of research; these consist of the synthesis (section 1.2) and the distribution (Section 1.3) of HCN in the primitive Earth, and the chemistry involved in the formation of biomolecules using HCN as the starting material (section 1.4). Particular emphasis was given to include reaction mechanisms, chemical yields of products, and kinetic data in order to get a quantitative perspective of the possible significance of HCN in the process chemical evolution that preceded the appearance of life on Earth. The last section (1.5) on this chapter introduces the research objectives of this dissertation.

1.2 Abiotic synthesis of HCN

HCN has been obtained in a number of studies in abiotic chemistry. The first investigations utilized

highly reducing atmospheres of different ratios of CH_4 and NH_3 in the presence or absence of H_2 and/or H_2O. These studies demonstrated that the production of HCN could be initiated by ultraviolet light (Ponnamperuma *et al.*, 1963; Ferris and Chen, 1975; Toupance *et al.*, 1977; Raulin *et al.*, 1979; Bossard and Toupance, 1980), electric discharges (Miller, 1957a; Ponnamperuma *et al.*, 1969; Yuasa and Ishigami, 1975; Toupance *et al.*, 1975), heat (Harada and Fox, 1964; Koberstein, 1973), shock waves (Bar-Nun and Shaviv, 1975), and ionizing radiation (Palm and Calvin, 1962).

These studies are now considered of little significance to the primitive Earth scenario because ammonia, if present, was probably in small abundance in the atmosphere since it is extremely soluble in water (Bada and Miller, 1968). In addition, the studies of Ferris and Nicodem (1974), and Kuhn and Atreya (1979), indicate that if NH_3 was present in the atmosphere, it would have been immediately photolyzed to N_2. On the other hand, the concentration of H_2 in the primitive atmosphere must have always been small because of its fast escape from the Earth's gravitational force (Mourey *et al.*, 1981).

On the basis of the previous discussion, an atmos-

phere composed mainly of methane, nitrogen and water vapor is now considered reasonable for the initial stages of the history of the Earth (Ferris and Chen, 1975; Bossard *et al.*, 1982). The formation of HCN from these gases has also been demonstrated. A mixture of CH_4 and N_2 in the presence or absence of H_2O has been exposed to ultraviolet light (Dodonova, 1966), electric discharges (Sanchez *et al.*, 1966; Toupance *et al.*, 1975; Kobayashi and Ponnamperuma, 1985b; Stribling and Miller, 1987), shock waves (Rao *et al.*, 1967), and ionizing radiation (Zhdamirov *et al.*, 1971; Balestic, 1974). Addition of H_2S (Raulin and Toupance, 1975b) or H_2 (Stribling and Miller, 1987) to the reaction mixture leads to a significant decrease in the electric discharge-driven production of HCN; however, these gases probably did not affect the synthesis of HCN in the primitive atmosphere since H_2 was rapidly lost (Mourey *et al.*, 1981), and H_2S seems quite unstable in models of primitive environments (Raulin and Toupance, 1975a,b).

Evolution of the atmosphere from CH_4-N_2-H_2O to CO-N_2-H_2O and/or to CO_2-N_2-H_2O likely occurred rapidly (Levine, 1982; Levine *et al.*, 1982); however, the duration of this process is unknown (Ferris and Hagan, 1984). Photochemical considerations indicate that

methane could have been efficiently polymerized; McGovern (1969) estimated that such a process would have occurred in 50-100 million years, while Lasaga *et al.*, (1971) estimated its duration in 1-10 million years. Levine (1982) has shown that photodecomposition of methane depends on altitude, being very unstable at the top of the atmosphere ($t_{1/2} \approx 4$ days), and quite stable at the surface of the Earth (approaching an infinitely long lifetime).

The formation of HCN in a mixture of $CO-N_2-H_2O$ that was subjected to electric discharges has been recently reported by Stribling and Miller (1987). They found that the yield of formation of HCN was at least an order of magnitude less than that obtained under similar conditions when CO was replaced by CH_4 (Stribling and Miller, 1987). Its yield could be increased if H_2 was added (Abelson, 1966; Stribling and Miller, 1987); however, the presence of H_2 in the primitive atmosphere is less likely, particularly at this stage (Mourey *et al.*, 1981). The synthesis of HCN from $CO-NH_3$ mixtures exposed to ultraviolet light (Ferris *et al.*, 1974a), and clay-minerals at high temperatures (Fripiat and Cruz-Cumplido, 1974) has also been reported, although are of little significance to the primitive Earth scenario based on the previous discus-

sion (see page 5, this dissertation). HCN is not synthesized from CO_2-N_2-H_2O mixtures exposed to electric discharges according to Stribling and Miller, 1987. The only synthesis of HCN reported from such a mixture is from the work of Bar-Nun and Shaviv (1975), using shock waves.

Based on the above results, it seems reasonable to conclude that the major production of HCN occurred when the primitive atmosphere was mainly composed of CH_4-N_2-H_2O. Therefore, a detailed analysis of the experiments utilizing these gases is important to get a better insight of the abiotic synthesis of HCN.

1.2.1 Photolysis

Nitrogen is sufficiently stable that its photolysis is negligible, and generally only participates in photochemical reactions as a third body (Canuto *et al.*, 1983; Yung *et al.*, 1984). Methane is photochemically reactive in the vacuum UV. Its absorption spectrum is a continuum beginning at about 145 nm, with two maxima in the absorption curve centered in the region between 100 and 80 nm; there is no minimum at any wavelength down to 0.25 nm (Sun and Weissler, 1955; Ditchburn,

1955). The photochemical decomposition of methane has been studied in detail and its photo-dissociative channels as well as their quantum yields[1] at 121.6 nm are indicated in reactions 1.3 through 1.7 (Gordon and Ausloos, 1967; Rebbert and Ausloos, 1972; Slager and Black, 1982).

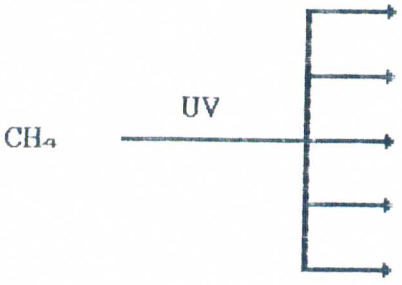

$$CH_3\cdot + H\cdot \qquad (1.3)$$

$$CH_2: + H_2 \qquad \Phi=0.580 \qquad (1.4)$$

$$CH_2: + 2H\cdot \qquad \Phi=0.510 \qquad (1.5)$$

$$\cdot CH: + H_2 + H\cdot \qquad \Phi=0.060 \qquad (1.6)$$

$$:C: + 2H_2 \qquad \Phi=0.004 \qquad (1.7)$$

Reactions 1.4 and 1.5 are the principal photodissociative channels; reactions 1.6 and 1.7 are minor pathways, and reaction 1.3 is the least important (Slager and Black, 1982). The major products from the photolysis of methane are H_2, C_2H_6, C_3H_8, $n\text{-}C_4H_{10}$; other hydrocarbons such as C_2H_4, C_2H_2 are also formed but in low yield (Mahan and Mandal, 1962; Magee, 1963; Braun *et al.*, 1966).

There is only one report of the photochemical syn-

---

[1] Quantum yield is denoted by the symbol Φ, and is defined as the number of species undergoing a process per number of quanta absorbed.

thesis of HCN from CH_4-N_2 mixtures (Dodonova, 1966). The author detected the formation of HCN in very low yield (20 nmoles) after irradiating (125-170 nm) for 10 hours a one to one mixture of CH_4-N_2 at 5-8 Torr. The mechanism of formation was not studied but it was suggested that photoactivated N_2 and its interaction with $\cdot CH:$ radicals could account for its formation (Dodonova, 1966). Chang *et al.* (1979) repeated this experiment using a monochromatic hydrogen lamp emitting at 123.6 nm. HCN or other N-containing organics were not detected. Experiments performed at higher wavelengths did not produce any detectable amount of N-containing organic compounds (Bossard *et al.*, 1981).

Contrary to the unsuccessful efforts of Chang *et al.* (1979) to duplicate the experiments of Dodonova (1966), the formation of HCN from the reaction of $CH_2:$ radicals with N_2 has been demonstrated by Laufer and Bass (1978). These authors studied the kinetics of the reaction (1.8) using flash photolysis on CH_2CO-N_2 and CH_2N_2-N_2 gas mixtures, and determined that its rate of reaction is small ($\leq 6X10^{4}$ dm^3 $mole^{-1}$ s^{-1}).

$$CH_2: + N_2 \longrightarrow HCN + :NH \qquad (1.8)$$

Another possible channel for the formation of HCN

is the reaction of $\cdot CH:$ radicals with N_2. Braun *et al.* (1967) have presented kinetic evidence for the reaction (1.9) using flash photolysis (136 nm) on CH_4-N_2 mixtures. The rate constant was estimated to be $4.3X10^7$ dm^3 $mole^{-1}$ s^{-1}, but the products were not identified (Braun *et al.*, 1967).

$$\cdot CH: + N_2 \longrightarrow \text{products} \qquad (1.9)$$

Ultraviolet light was an abundant source of energy in the primitive Earth. A total flux of 0.32 kJ cm^{-2} y^{-1} of UV light (wavelengths $\leq$200 nm) enters into the upper Earth's atmosphere at the present time (Fox and Dose, 1977). Astronomical observations suggest that the early Sun emitted 10-1,000 times its present value in the spectrum between 100 and 200 nm (Canuto *et al.*, 1982). However, despite the possible great abundance of ultraviolet light, it seems likely that photoproduction of HCN in the primitive Earth was not efficient (Raulin *et al.*, 1982).

1.2.2 Radiolysis

Irradiation of N_2 leads to its dissociation, reaction 1.10 (Harteck and Dondes, 1957, 1958a,b). The ef-

fects of ionizing radiation on methane has been extensively studied, and this system is reasonably well understood (Lind and Bardwell, 1926; Hoing and Sheppard, 1946; Lampe, 1957; Maurin, 1962; Hauser, 1964; Rebbert and Ausloss, 1973; Arai *et al.*, 1981a,b). The mechanism of decomposition of methane involves ionic and radical processes. The principal ion formed at atmospheric pressure is CH_5^+ (Field *et al.*, 1963); its origin and fate during radiolysis are (Maurin, 1962):

$$N_2 \xrightarrow{\text{Irradiation}} \cdot N: + \cdot N: \qquad (1.10)$$

$$CH_4 \xrightarrow{\text{Irradiation}} CH_4^+ + e \qquad (1.11a)$$

$$CH_4 \xrightarrow{\text{Irradiation}} CH_4^* \qquad (1.11b)$$

$$CH_4^* \longrightarrow CH_3\cdot + H\cdot \qquad (1.12)$$

$$CH_4^+ + CH_4 \longrightarrow CH_5^+ + CH_3\cdot \qquad (1.13)$$

$$CH_5^+ + CH_4 \longrightarrow C_2H_5^+ \qquad (1.14)$$

The major products from the radiolysis of methane are H_2, C_2H_6, C_3H_8, $n\text{-}C_4H_{10}$ (Lind and Bardwell, 1926; Hoing and Sheppard, 1946; Lampe, 1957; Maurin, 1962; Hauser, 1964; Rebbert and Ausloss, 1973; Arai *et al.*, 1981a,b).

The radiochemical formation of HCN in a CH_4-N_2

mixture has been studied by Zhdamirov *et al.* (1970). The authors studied the dependance of the radiation chemical yield[2] of HCN as a function of composition of mixture, temperature, pressure and dose rate. *G* (HCN) has a well-marked dependance on the composition of mixture, reaching its maximum value (*G*=0.9) at 5-7% methane content. The temperature dependance of *G* (HCN) over the range 30-400°C is not of the usual Arrhenius type; the graph of log *G* (HCN) *vs* 1/T has two parts, and the energy of activations were estimated to be 2.9 kJ $mole^{-1}$ and 16.2 kJ $mole^{-1}$ at low (30-100°C) and high (200-400°C) temperature, respectively. *G* (HCN) can be increased up to 5.9 at 400°C and atmospheric pressure (Zhdamirov *et al.*, 1970). Although a mechanism was not proposed by the authors, the strong dependance of *G* (HCN) on dose rate[3] suggests that HCN is formed by radical-radical reactions. A likely channel for its formation is:

$$CH_3\cdot + \cdot N: \longrightarrow HCN + H_2 \qquad (1.15)$$

---

[2]Radiation chemical yield is denoted by the symbol *G*, and is the number of molecules formed or destroyed per 100 eV of energy absorbed. The equivalent of 1 G unit is 1.0364 X 10^{-7} mole J^{-1}.

[3]*G*(HCN) increases 4-5 times by changing the dose rate from 10^{13} to 10^{16} eV cm^{-3} s^{-1} (Zhdamirov et al., 1970).

Armstrong and Winkler (1955) studied such a reaction, and determined that its rate coefficient is about $1.3X10^{-6}$ mole s^{-1}. Another source of HCN at low dose rates could be the reaction of active nitrogen with CH_4 (reaction 1.16). Froben (1974) detected the radical $H_2C{=}N\cdot$ from this reaction by electron spin resonance at 77°K .

$$CH_4 + \cdot N: \longrightarrow H_2C{=}N\cdot + H_2 \qquad (1.16a)$$

$$H_2C{=}N\cdot \longrightarrow HCN + H\cdot \qquad (1.16b)$$

Solar wind and cosmic rays were probably the major sources of ionizing radiation on the top of the primitive atmosphere Earth (Oró *et al.*, 1977); their abundances on the contemporary Earth are estimated to be 0.84 J cm^{-2} y^{-1} and 0.0063 J cm^{-2} y^{-1}, respectively (Oró *et al.*, 1977). A dose rate of $5X10^{18}$ eV cm^{-3} y^{-1} can be derived from these values. An estimate of radiochemical production of HCN in the upper parts of the primitive atmosphere would vary from 10^{-6} to 10^{-4} mole dm^{-3} y^{-1} based on the fluctuation of *G* (HCN) determined under various experimental conditions (0.01 to 0.9) by Zhdamirov *et al.* (1970).

Ionizing radiations on the surface of the primitive Earth originated mainly from the decay of radioac-

tive isotopes such as $_{92}U^{235}$, $_{92}U^{238}$, $_{94}Pu^{244}$, $_{90}Th^{232}$, $_{19}K^{40}$. Estimates of their abundance 4 billion years ago depend on the model used. If we assume homogeneous distribution of these elements in the Earth crust, the energy produced per unit time projected per square centimeter of surface is 11.72 (Miller and Orgel, 1974) or 196.65 J cm^{-2} y^{-1} (Fox and Dose, 1977) for 1 or 10 km depth, respectively. A dose rate range from $7X10^{19}$ to $1X10^{21}$ eV cm^{-3} y^{-1} can be derived from these values for the atmosphere at the surface of the Earth. An estimate of radiochemical production of HCN would therefore vary from 10^{-5} to 10^{-1} mole dm^{-3} y^{-1} based on the fluctuation of *G* (HCN) determined under various experimental conditions (0.01 to 0.9) by Zhdamirov *et al.* (1970).

1.2.3 Electrolysis

The mechanism of decomposition of methane is not well understood (Bossard *et al.*, 1982). The major products are H_2, C_2H_2, C_2H_4, C_2H_2, and higher hydrocarbons (Ponnamperuma and Woeller, 1964; Ponnamperuma and Pering, 1966; Ponnamperuma *et al.*, 1969). Their relative yields depend on the pressure of the system and current of the electric discharge. At low

pressures ethane is the most abundant hydrocarbon (glow discharge), but as the pressure is raised to atmospheric levels, acetylene becomes the principal product (spark discharge) (Fujio, 1930; Weiner and Burton, 1953; Sieck and Johnsen, 1963; Borisova and Eremin, 1968). At higher currents (silent and corona discharges), ethane is the most abundant hydrocarbon even at atmospheric pressures (Lind and Glockler, 1929, 1930; Lind and Schltze, 1931; Ponnamperuma and Woeller, 1964; Ponnamperuma and Pering, 1966; Ponnamperuma *et al.*, 1969).

The first report of electrosynthesis of HCN from a simulated atmosphere of CH_4-N_2 is that of Sanchez *et al.* (1966). Toupance *et al.* (1975) carried out a series of investigations on the yield of formation of HCN as a function of N_2 percentage in CH_4-N_2 mixtures. They found that maximum production of HCN occurs in mixtures composed of 70% N_2 and 30% CH_4 (Toupance *et al.*, 1975). Molecular hydrogen formed *in situ* (Raulin *et al.*, 1982) or added prior to electrolysis (Stribling and Miller, 1987) decreases the rate of formation of HCN.

Chemical yields (G) of products formed in electric discharge experiments are usually not reported because

of the difficulty in determining the energy introduced by electric discharges (Navarro-González *et al.*, 1986). In an attempt to measure the yields of HCN from CH_4-N_2 mixtures subjected to electric discharges, Stribling and Miller (1987) estimated the energy introduced by comparing the heat evolved in the experiment with that of a known power source. The ability to reproduce their measurements was determined to be within a factor of two (Stribling and Miller, 1987). However, the authors did not take into account the energy converted into chemical form, light or that not absorbed by the gas. Gases have a low collisional mass stopping power when they are irradiated with low energy electrons (Spinks and Woods, 1976), as in the case of electric discharges. Therefore, their method underestimates the amount of energy supplied by electric discharges.

Electric discharges are generally considered to be very efficient in synthesizing HCN based on the initial amount of CH_4 converted into HCN (Miller and Orgel, 1974; Raulin *et al.*, 1982). However, further work needs to be done in order to understand the mechanism and efficiency of HCN synthesis induced by electric discharges in the primitive atmosphere.

1.2.4 Pyrolysis

The thermal decomposition of methane has been extensively studied under a variety of conditions (Skinner and Ruehrwein, 1959; Kevorkian *et al.*, 1960; Kozlov and Knorre, 1963; Palmer and Hirt, 1963; Kondratiev, 1965; Harting *et al.*, 1971). The rate of decomposition of methane is independent of pressure, reaction conditions (flow, static, or shock wave pyrolysis), and presence of an inert gas; the energy of activation calculated under various conditions is about 423 kJ $mole^{-1}$ in the temperature range of 900-2,000°K (Skinner and Ruehrwein, 1959; Kevorkian *et al.*, 1960; Kozlov and Knorre, 1963; Palmer and Hirt, 1963; Kondratiev, 1965; Harting *et al.*, 1971; Chen *et al.*, 1975).

The dissociation reaction leading to the decomposition of methane is shown in reaction 1.17. Dimerization of $CH_3\cdot$ or $H\cdot$ leads to the formation of the initial products: C_2H_6 or H_2, respectively. Ethane is, however, rapidly consumed during the pyrolysis leading to the formation of ethylene, the secondary product. The latter further reacts to produce acetylene, the tertiary product, as the extent of the reaction is increased (Chen *et al.*, 1975; Roscoe

and Thompson, 1985).

$$CH_4 \xrightarrow{\text{Heat}} CH_3\cdot + H\cdot \qquad (1.17)$$

The shock wave pyrolysis of a CH_4-N_2 atmosphere was studied by Rao *et al.* (1967). Mixtures of 5% CH_4 and 5% N_2 in argon were shock-heated to temperatures between 1500 and 6000°K. Hydrogen cyanide is formed, starting from 2500°K and increasing in yield up to about 20% at 5000°K (Rao *et al.*, 1967). The second order rate of formation for HCN was determined as $k\ (CH_4 + N_2) = 9.32X10^{-3} - 5.02T^{-1}$, in $dm^3\ mole^{-1}\ s^{-1}$. The mechanism of formation was not studied but a possible scheme consistent with the mechanism of methane pyrolysis was suggested (reactions 1.18 to 1.23, followed by reactions 1.15 and 1.16).

$$N_2 \xrightarrow{T \geq 2500°K} N_2^* \qquad (1.18)$$

$$CH_3\cdot + N_2^* \longrightarrow CH_2: + N_2 + H\cdot \qquad (1.19)$$

$$CH_2: + N_2^* \longrightarrow \cdot CH: + N_2 + H\cdot \qquad (1.20)$$

$$\cdot CH: + N_2^* \longrightarrow \cdot CHN_2^* \qquad (1.21)$$

$$\cdot CHN_2^* + \cdot CH: \longrightarrow 2\ HCN \qquad (1.22)$$

$$\cdot CHN_2^* \longrightarrow HCN + \cdot N: \qquad (1.23)$$

The chemical yield calculated for HCN was $G \approx 3.2$ (Bar-Nun and Shaviv, 1975). This value is high compared to that obtained by radiolysis (section 1.2.3) and makes shock waves the most efficient energy source for producing HCN under these conditions. Bar-Nun and Tauber (1972) have estimated that shock waves in the primitive atmosphere were efficiently produced by lighting and meteoritic impact, and an abundance of 4.18 J cm^{-2} y^{-1} has been estimated. A dose rate of $2.6X10^{17}$ eV cm^{-3} y^{-1} can be derived from this value. An estimate of the shock wave production of HCN in the primitive atmosphere is 10^{-2} mole dm^{-3} y^{-1} taking into account a of G=3.2 for HCN.

1.3 Distribution of HCN

HCN is ubiquitous in nature. It has been detected in the interstellar medium (Snyder and Buhl, 1971), comets (Ulich and Conklin, 1974), and in the atmospheres of Jupiter (Tokunaga *et al.*, 1981), and Titan (Hanel *et al.*, 1981, and Owen, 1982). Small amounts of HCN occur on the contemporary Earth; this is biosynthesized from amino acids by several photosynthetic and non-photosynthetic bacteria (Nazly *et al.*, 1981), algae (Vennesland *et al.*, 1981), plants (Nartey, 1981),

and arthropods (Duffey, 1981).

The probable occurrence of HCN on the primitive Earth is supported by its facile formation under a variety of conditions. Table 1.1 summarizes the estimated productions of HCN in the primitive atmosphere induced by different energy sources.

Table 1.1. Estimated productions of HCN in the primitive atmosphere by different energy sources.

Energy source	$G°$ (HCN)	HCN production (mole dm^{-3} y^{-1})
UV light	negligible[1]	negligible
Ionizing radiation:	0.01-0.9[2]	
Upper atmosphere		10^{-6}-10^{-4}
Lower atmosphere		10^{-5}-10^{-1}
Electric Discharges	undetermined	
Shock waves	3.2[3]	10^{-2}
Total		10^{-2}-10^{-1}

1. Raulin *et al.*, 1982; 2. Zhdamirov *et al.*, 1970;
3. Bar-Nun and Shaviv, 1975.

HCN synthesized in the primitive atmosphere would

have been efficiently transported into the oceans by precipitation processes where abiotic syntheses of complex organic molecules may occur (Oró and Kimball, 1961). Fegly *et al*. (1986) have derived a HCN rainout rate of (3-14)X10^{11} mole y^{-1} taking into account a Henry's law constant of 4X10^{3}, a HCN global mixing ratio of 10^{-6}, and a globally rainfall rate of 3.3X10^{-6} g cm^{-2} s^{-1}.

It is difficult to estimate the concentration of HCN or any other compound in the primitive oceans. Miller and Orgel (1974) have attempted to estimate the possible upper limit of organic compounds dissolved in the primitive hydrosphere. They rationalized that it is very unlikely that all of the surface carbon was ever present as organic compounds, but 1 to 20% might have been. If the volume of the primitive oceans was as large as the present ones, this would have given a solution of 0.01 to 0.10 mole dm^{-3} for a one-carbon-atom organic compound such as HCN (modified after Miller and Orgel, 1974). This approximation places only an upper limit since not included in the calculation is the loss of HCN by polymerization and/or hydrolysis in the oceans. Such a high steady-state concentration does not seem likely since hydrolysis to formic acid requires at most a short period of time (10^{3} to

10^4 years) at moderate pH and temperature (Sanchez *et al.*, 1966).

The simplest mechanism that might have operated on the primitive Earth for concentrating organic compounds is evaporation (Miller and Orgel, 1974). Such a mechanism is unlikely to have contributed for the accumulation of a volatile compound such as HCN. Sanchez *et al.* (1966) have suggested the eutectic freezing of HCN-water mixtures as a possible mechanism to increase the concentration of HCN. The eutectic in a HCN-water system occurs at -23.4°C and contains 74.5% w of HCN (Sanchez *et al.*, 1966). This mechanism possibly operated on confined areas on the Earth such as polar regions, but was not dominant on a global perspective for the Earth since many of the physical conditions that prevailed in the early Earth were probably not significantly different from those that exist today (Ferris and Hagan, 1984); in particular, oceans and other bodies of water were subject to similar buffering processes, resulting in a pH that presumably was close to that of modern oceans (pH 8.0-8.5), or at least not far from neutrality (Ferris and Hagan, 1984).

Navarro-González (1983) has suggested the formation of cyanocomplexes as a mechanism to protect HCN

from hydrolysis and to accumulate it in a nonvolatile form. Cyanocomplexes are readily formed when a cyanide solution is in contact with rocks. Beck (1978) has shown that when 1 g of powdered rock is suspended in 10 ml of 0.014 mole dm^{-3} aqueous solution of KCN, a variety of cyanocomplexes of transition elements such as Mn, Fe, Co, Cu, and Mo are formed. Equilibrium conditions are reached within 36 hr, and the steady state concentration of cyano complexes varies from 10^{-5} to 10^{-4} mole dm^{-3} depending on the type of rock; hexacyanoferrate(II) and/or (III) were in most cases the principal cyanocomplex formed (Beck, 1978).

Kobayashi and Ponnamperuma (1985b) found that the yield of HCN in the electric discharge of CH_4-N_2-H_2O mixtures could be increased over 200 times if metal ions such as Fe^{2+}, Zn^{2+}, and MoO_4^{2-} were included in the liquid phase. They proposed the formation of cyanocomplexes in the liquid phase as a mechanism to protect HCN during electrolysis.

Formation of cyanocomplexes of transition metals in the primitive ocean could have been an important mechanism to protect HCN from hydrolysis and to allow its accumulation over extended periods of time. In the absence of such a process, hydrolysis of HCN would

require a short period of time (10^3 to 10^4 years) at moderate pH and temperature (Sanchez *et al.*, 1966).

The source of transition metals for the primordial hydrosphere was the lithosphere (Beck, 1978). Among the different transition elements present in the lithosphere and hydrosphere iron is by far the most abundant (Weast *et al.*, 1985). The concentration of iron in the contemporary hydrosphere is extremely small, e.g., $3.5X10^{-8}$ mole dm^{-3} for sea water (Brewer, 1975) and $1.2X10^{-5}$ mole dm^{-3} for river water (Mackenzie, 1975). This small concentration is a consequence of the low solubility of iron(III) hydroxide, and the absence of complex-forming ligands. During the early stages of the primitive hydrosphere, iron was probably present in its more soluble form, iron(II). Hydrogen cyanide may have played an important role in increasing the dissolution of iron and other metal ions from the lithosphere (Navarro-Gonzlez *et al.*, 1989). Cyanocomplexes of iron are characterized by their high solubilities[4] in water, and

---

[4]Maximum solubility varies from 0.06 to 0.22 mole dm^{-3} for potassium or sodium hexacyanoferrate(II) at 0 and 100C, respectively (Weast, et al., 1985).

high stability constants[5].

1.4 Formation of biomolecules from HCN

It is generally accepted that HCN synthesized in the primitive atmosphere would have been efficiently transported into the oceans where it played a significant role in the process that preceded the emergence of life (Oró and Kimball, 1961; Sanchez *et al.*, 1966; Ferris and Hagan, 1984). A number of studies has been devoted not only to the identification of products resulting from the oligomerization of HCN but also to the elucidation of the mechanisms for their formation. This section reviews the current status of the studies of the oligomerization of HCN in aqueous solution initiated by ionic (section 1.4.1) or radical processes (section 1.4.2). It also examines two possibly competing processes in the primitive oceans: Hydrolysis *vs* oligomerization of HCN (section 1.4.3).

---

[5]The stability constant varies from $2.5X10^{35}$ to $4.0X10^{43}$ for hexacyanoferrate(II) and (III), respectively (Smith and Martell, 1976).

1.4.1 Ionic oligomerization

It has been known since the last century that HCN ionically oligomerizes in basic medium giving rise to a variety of oligomers, generically referred as "azulmic acids" (Volker, 1957, 1960; Schaefer, 1970). Diaminomaleonitrile (DAMN), a tetramer of HCN, is the smallest oligomer isolable from an oligomerizing 0.1-1.0 mole dm^{-3} aqueous HCN solution at room temperature (Sanchez *et al.*, 1967). The initial steps leading to the formation of DAMN are shown in Figure 1.1. The postulated stepwise condensation of HCN to form DAMN is supported by the observation of formation of maleonitrile derivatives from N-alkyiminoacetonitriles in aqueous HCN

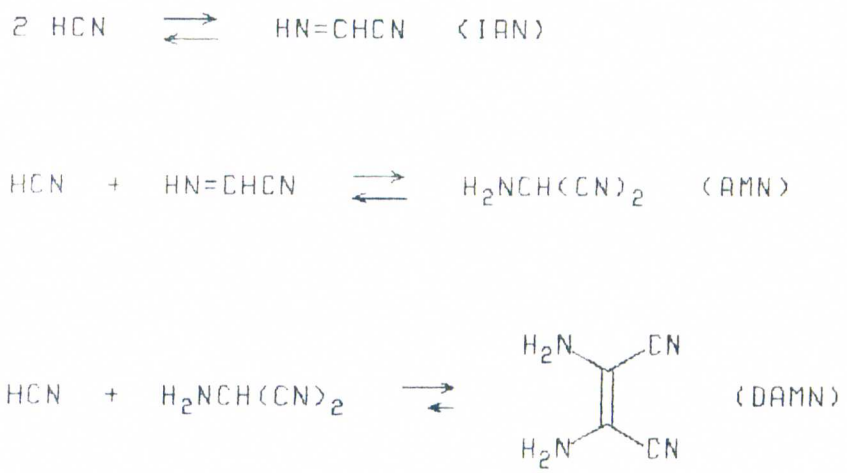

Figure 1.1. Formation of DAMN: Initial Steps in the ionic oligomerization of HCN.

solutions (Ferris *et al.*, 1972); no dimerization of the substituted iminoacetonitriles was observed (Ferris *et al.*, 1972): The suggestion by Kliss and Matthews (1962) that the HCN dimer is a direct precursor to DAMN and larger oligomers therefore does not appear viable (Ferris *et al.*, 1972).

Considerably progress has been made in the characterization of some of the products from the ionic oligomerization of HCN (Ferris and Hagan, 1984). A summary of the data is given below.

HCN dimer. Some controversy has arisen in the literature over the proposed structures of the dimer (Kliss and Matthews, 1962; Loew and Chang, 1971; Loew, 1971; Moffat, 1975; Yang *et al.*, 1976). Since its steady state concentration in an oligomerizing cyanide solution is very low (Ferris and Hagan, 1984), it has never been detected or isolated from solution. A diradical structure, aminocyanocarbene, was suggested (Kliss and Matthews, 1962), but there was never any direct evidence for such species. On the contrary, several different sets of quantum mechanical calculations have shown that iminoacetonitrile (IAN) is the most stable conformation of the dimer (Loew and Chang, 1971; Loew, 1971). Another dimer of HCN, azacyclo-

propenylidene, was also proposed as a stable form based on INDO calculations (Yang *et al.*, 1976), but Moffat (1975) pointed out that such a calculation overestimates the stability of the three-member ring.

Aminomaleonitrile (AMN), the trimer of HCN, is also present in such a low steady state concentration that it has not yet been isolated from an oligomerizing cyanide solution (Sanchez *et al.*, 1967). AMN can be synthesized and stored as the tosylate salt (Ferris *et al.*, 1973). AMN reacts rapidly with HCN to form DAMN; its half-life is of the order 10^2 s in a 1.0 mole dm^{-3} HCN at 25°C and pH 9.2 (Sanchez *et al.*, 1967).

DAMN is formed essentially irreversibly as shown by the lack of exchange of ^{13}C-labelled HCN with DAMN (Ferris and Edelson, 1978). Spectroscopic evidence suggests that the *cis* conformation is formed (Long *et al.*, 1960). Tetramerization of HCN occurs in the pH range 8.5–10.0, reaching a maximum at pH 9.2, which is the pKa of HCN (Sanchez *et al.*, 1967). The tetramerization kinetics have been studied by Sanchez *et al.* (1967) and Toupance *et al.* (1970); and a rate expression,

$$k(HCN + {}^{-}CN) = k_o \exp(-E_a R^{-1} T^{-1}),$$

was derived where, k_o=5.1X10^7 dm^3 mole^{-1} s^{-1}; and E_a=(81.6¥2.1) kJ mole^{-1} (Toupance *et al.*, 1970).

Diiminosuccinonitrile, DISN, is formed by oxidation of DAMN (Ferris and Ryan, 1973; Ferris *et al.*, 1981a, 1982). Reaction 1.24, unbalanced, exemplifies its formation; the oxidizing agent involved during the oligomerization of anoxygenic aqueous solutions of HCN has not yet been identified (Ferris and Ryan, 1973).

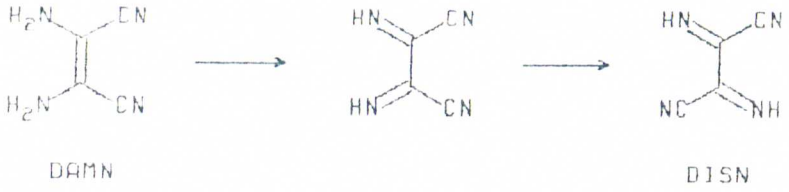

DAMN DISN (1.24)

DISN is a reactive species that undergoes hydrolysis to yield oxalic acid and HCN (Ferries *et al.*, 1982), and ammonolysis to yield urea and oxalic acid (Ferris and Ryan, 1973).

Adenine, a pentamer of HCN, was detected by Oró (1960), Oró and Kimball (1961), and Lowe *et al.* (1963) when 1.5-3.0 mole dm^{-3} ammoniacal solutions of HCN were heated from one to several days at temperatures ranging from 27 to 100°C. Ferris *et al.* (1978) working under milder conditions found that adenine could be detected

only after acid hydrolysis of the solution, a 0.1 mole dm^{-3} NH_4CN aqueous solution at pH 9.2, kept at 25°C for 4-12 months. This observation suggests that adenine is formed as a substituted derivative or is chemically associated with higher HCN oligomers (Ferris *et al.*, 1978). Several mechanisms have been proposed for its formation (Orό 1961; Kliss and Matthews, 1962; Sanchez *et al.*, 1967; Ferris *et al.*, 1978); however, Voet and Schwartz (1983) have recently isolated and identified adenine-8-carboxamide, (adenine-8-CA), in an oligomerizing HCN solution. This purine derivative releases adenine upon hydrolysis. Based on this finding, Voet and Schwartz (1983) have proposed an original mechanism for the formation of adenine (Figure 1.2). Supporting evidence for such a mechanism was based on the isolation and identification of three different imidazole derivatives presumably involved in the reaction mechanism (Voet and Schwartz, 1983).

Higher HCN oligomers. The structure and mechanism of formation of higher oligomers is much less clear. Subsequent oligomerization steps appear to involve a series of internal redox reactions, inferred from the detection of oxidation products (oxalic and urea) as well as reduction products (2,3-diaminosuccinic acid) in the oligomer hydrolysate (Ferris and Hagan, 1984).

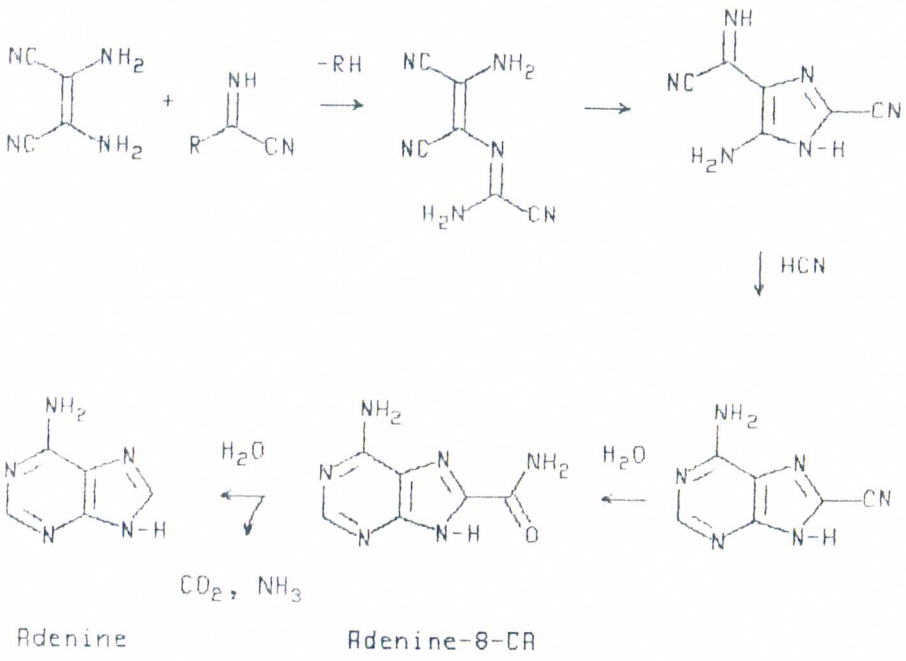

Figure 1.2. Mechanism of Adenine Synthesis according to Voet and Schwartz (1983).

It was suggested that DAMN-DISN interconversion could be mediating these processes (Ferris and Ryan, 1973).

The elucidation of the structure of HCN oligomers is complicated by the heterogenous nature of the material, and only limited progress has been made in this area. Partial characterization of the soluble fraction by ^{13}C-NMR, and differential thermal analysis indicated the presence of carboxamide, -X-C(=O)-NH$_2$, and urea groupings, -X-NH-C(=O)-NH-X- (Ferris *et al.*, 1981b). Pyrolysis of HCN oligomers at 600°C resulted

in the release of gaseous products such as HCN, CO_2, CH_3CN, $HCONH_2$, and pyridine. The pyrolytic formation of these products is consistent with the presence of carboxylic and amide groups in HCN oligomers. Heterocyclic ring systems and structures which are thermalized to heterocycles are indicated by the formation of pyridine and HCN (Ferris *et al.*, 1981b).

At present it is clear that higher oligomers of HCN contain a more complex variety of functional units. This complexity is apparent in the diverse mixture of products that have been identified upon hydrolysis of the oligomers such as:

a. Amino acids: alanine, β-alanine, α-aminoisobutyric, aspartic, α,β-diaminopropionic, and diaminosuccinic acids, glycine, glutamic, and guanidine acetic acids, isoleucine, leucine, and serine (Oró and Kamat, 1961; Lowe *et al.*, 1963; Ferris *et al.*, 1978);

b. Purines: adenine, and hypoxanthine (Lowe *et al.*, 1963; Ponnamperuma, 1965; Ferris *et al.*, 1978);

c. Pyrimidines: 4,5-dihydroxypyrimidine, 5-

hydroxyuracil, uracil, and orotic acid (Ferris and Joshi, 1978; Ferris *et al.*, 1978; Voet and Schwartz, 1982);

d. Hydantoins: hydantoin, 5,5-dimethylhydantoin and 5-carboxymethylidine hydantoin (Ferris *et al.*, 1974b);

d. Urea (Lowe *et al.*, 1963; Ponnamperuma, 1965).

1.4.2 Free-radical oligomerization

The free-radical oligomerization of HCN in aqueous solution has been mainly studied using ionizing radiation as a source of free radicals (Draganic and Draganic, 1977). The interaction of ionizing radiation with liquid water and dilute aqueous solutions is one of the best understood domains of radiation chemistry (Spinks and Woods, 1976). The generally accepted scheme of water radiolysis is summarized by reaction 1.25 (Draganic and Draganic, 1971). In pure water there is scarcely any net decomposition because the radiolytic products undergo very efficient back reactions leading to the re-formation of water (Buxton *et al.*, 1988).

$$H_2O \xrightarrow{\text{Radiation}} e_{aq}^- + H^\cdot + HO^\cdot + H_2 + H_2O_2 + H^+ \qquad (1.25)$$

The radiation chemical yields (G) for this process are G ($-H_2O$)=4.1, G (e_{aq}^-)=2.65, G ($H^\cdot$)=0.55, G ($HO^\cdot$)=2.74, G (H_2)=0.45, G (H_2O_2)=0.68, and G (H^+)=2.65 (Draganic and Draganic, 1971; Buxton *et al.*, 1988).

When dilute aqueous solutions are irradiated practically all the energy absorbed is deposited in the water molecules and the observed chemical changes are brought about indirectly via the molecular products (H_2O_2) and, particularly, the radical products ($H^\cdot$, $HO^\cdot$ and e_{aq}^-). Direct action due to energy deposited directly in the solute is generally unimportant in dilute aqueous solutions, i.e., at solute concentrations below about 1 mole dm^{-3} (Spinks and Woods, 1976).

Other sources of these radicals in liquid water are photolysis at $\leq$ 200 nm , Φ ($H^\cdot$, $\cdot OH$)=0.36; Φ =(e_{aq}^-)$\leq$0.04 (Bamford and Wayne, 1967, Harting and Getoff, 1980), sonolysis (Weissler, 1953, Tain-Jen *et al.*, 1980), and electrolysis (Terasawa and Harada, 1980, Harada *et al.*, 1984).

At present it is difficult to estimate the rate of production of $H^{\cdot}$, $HO^{\cdot}$, and e_{aq}^{-} in the primitive hydrosphere; however, based on the abundance of ultraviolet light, radioactivity and lightning on the primitive Earth, it is likely that these reactive species contributed significantly to free-radical reactions of abiotic significance in the primitive hydrosphere (Niketic, 1984a).

The reaction of $H^{\cdot}$ with HCN has been studied by Ogura (1968) and Draganic *et al.* (1973) using competition kinetics in γ-irradiated aqueous solutions. The rate constant was determined to be: $3.3X10^{7}$ dm^{3} $mole^{-1}$ s^{-1}. The radical(s) produced in this reaction (1.26) have been identified by electron spin resonance in crystal matrices (Cochran *et al.*, 1962) and in aqueous solutions (Neta and Fessenden, 1970; Behar and Fessenden, 1972), and also by fast spectroscopic techniques using pulse radiolysis in aqueous solutions (Buchler *et al.*, 1976; Draganic *et al.*, 1976b).

$$HCN + H^{\cdot} \longrightarrow H_2C{=}N^{\cdot} \qquad (1.26)$$

At pH greater than the pKa for HCN (9.2), cyanide ion reacts with $H^{\cdot}$ (reaction 1.27):

$$^{-}CN + H^{\cdot} \xrightarrow{H_2O} H_2C{=}N^{\cdot} + HO^{-} \qquad (1.27)$$

Anbar and Neta (1967) have reported that the rate of this reaction is $2.6X10^{7}$ dm^{3} $mole^{-1}$ s^{-1}; however, the conditions used to obtained the rate constant are poorly defined (Anbar and Neta, 1967) and the pH (7) used to measure the parameter is smaller than the pKa for HCN; as a consequence the concentration of cyanide was negligible. This value should therefore be used with caution.

The reaction (1.28) of e_{aq}^{-} with HCN has also been studied by Ogura (1968) and Draganic *et al.* (1973) using competition kinetics in γ-irradiated aqueous solutions. The rate constants determined by the different authors are $2.0X10^{8}$ and $6.6X10^{8}$ dm^{3} $mole^{-1}$ s^{-1}, respectively. The latter value may be considered more reliable since it was obtained at lower doses where the reaction mechanism was not complicated by secondary reactions. The same radical(s) is (are) produced as for $H^{\cdot}$ (Draganic *et al.*, 1973). The reaction of cyanide with e_{aq}^{-} is negligible, $k \leq 10^{6}$ dm^{3} $mole^{-1}$ s^{-1} (Anbar and Hart, 1965; Bielski and Allen, 1977).

$$HCN + e_{aq}^{-} \xrightarrow{H_2O} H_2C\dot{N} + HO^{-} \qquad (1.28)$$

Draganic *et al.* (1973) determined the upper limit ($k \leq 5X10^{7}$ dm^3 $mole^{-1}$ s^{-1}) for the rate of reaction (1.29) of HO· with HCN using competition kinetics in γ-irradiated solutions:

$$HCN + HO\cdot \longrightarrow HO{-}CH{=}N\cdot \qquad (1.29)$$

Buchler *et al.* (1976) derived a rate of $6.0X10^{7}$ dm^3 $mole^{-1}$ s^{-1} for reaction 1.29 using pulse radiolysis coupled to fast kinetics spectroscopy, and optimizing the data by computer simulation of the reaction scheme. The structure of the radical produced by this reaction was inferred from the stable products (Draganic *et al.*, 1973) and also from spectroscopy (Buchler *et al.*, 1976; Draganic *et al.*, 1976a).

Several studies have been done to determine the rate of reaction (1.30) of HO· with ^{-}CN using steady-state radiolysis (Kraljic and Trumbore, 1965) and pulse radiolysis (Behar, 1974; Buchler *et al.*, 1976; Bielski and Allen, 1977). The average value obtained from the different studies is $6.5X10^{9}$ dm^3 $mole^{-1}$ s^{-1}. The radical produced have been detected by fast spectros-

copy (Behar, 1974; Buchler *et al.*, 1976).

$$^{-}CN + HO\cdot \longrightarrow HO-\dot{C}=N^{-} \qquad (1.30)$$

At pH >11 the hydroxyl radical dissociates (pK=11.9) producing the hydroxyl radical anion ($\cdot O^{-}$) (Draganic and Draganic, 1971). This radical readily reacts with cyanide ion (reaction 1.31), $k=2.6X10^{9}$ dm^{3} $mole^{-1}$ s^{-1}:

$$^{-}CN + \cdot O^{-} \longrightarrow {}^{-}O-\dot{C}=N^{-} \qquad (1.31)$$

The transient radical produced by this reaction has been detected in pulse radiolysis studies coupled to fast spectroscopy (Behar, 1974; Buchler *et al.*, 1976).

The short-lived intermediates produced in reactions 1.26 to 1.31 react among themselves and/or with HCN/CN^{-} leading to the decomposition of HCN and to the formation of a large variety of compounds. Table 1.2 summarizes the initial radiation chemical yields ($G°$) of decomposition of HCN at various pH's. $G°$ (-HCN) is maximum at pH 6 (Draganic and Draganic, 1980). The variation of $G°$ (-HCN) with pH is primarily due to the

Table 1.2. Initial Radiation Chemical Yields ($G°$) of Decomposition of HCN and $^-$CN at different pH[1].

Compound	pH	$G°$
HCN	2.4	5.8
	6.0	13.8
NH_4CN	9.2	6.5
NaCN (or KCN)	11.3	5.2

1. Draganic and Draganic, 1980.

differences of rates of reactions of $H^{\cdot}$, $HO^{\cdot}$, and e_{aq}^- with HCN/CN^-.

Considerable progress has been made in the characterization of some of the stable products produced in the free-radical oligomerization of dilute[6] aqueous solutions of HCN (Draganic and Draganic, 1980). About 79% of the nitrogen and carbon atoms from HCN molecules decomposed are built into larger molecules, mainly various oligomers. A summary of the products that have been characterized is given below. Section 1.4.2.1 examines the mechanism of formation and

[6]Unless otherwise stated, the data given is for 0.1 mole dm^{-3} HCN aqueous solutions.

chemical yields[7] (G) of low molecular weight products while section 1.4.2.2 deals with larger molecules and/or small molecules released upon their hydrolysis.

1.4.2.1 Formation of low molecular weight products

Molecular hydrogen and hydrogen peroxide originate in decomposition of water molecules (reaction 1.25). Hydrogen, $G°$=0.4, accumulates during irradiation of the HCN solution (Draganic *et al.*, 1973). Hydrogen peroxide, $G°$=0.3 for 0.006 mole dm^{-3} HCN, disappears in reactions with radiolytic products (Draganic *et al.*, 1973; Ogura, 1968).

Carbon dioxide, $G°$=0.8, is formed with a significant yield, but G rapidly decreases with dose in the kGy[8] range to about 0.5. Its mechanism of formation is shown by reactions 1.32 and 1.33.

---

[7]Unless otherwise stated, the chemical yields are the initial values ($G°$): Those determined at the lowest possible doses.

[8]Gray, Gy, is the commonly used unit for radiation dose and its equivalent in SI units is $1.8X10^{-7}$ J $mole^{-1}$.

$$2HO\text{-}CH{=}N^{\cdot} \longrightarrow HC(=NH)OH + HO\text{-}CN \qquad (1.32)$$

$$HO\text{-}CN + H_2O \longrightarrow CO_2 + NH_3 \qquad (1.33)$$

Carbon dioxide accumulates in solution due to its high solubility, and then reacts with hydrated electrons as it is indicated by reaction 1.34 (Draganic *et al.*, 1973; Draganic and Draganic, 1980).

$$CO_2 + e_{aq}^{-} \longrightarrow \cdot CO_2^{-} \qquad (1.34)$$

Ammonia, G°=2.6, is formed with a high yield, and its formation may be explained by reactions 1.33 and 1.35 to 1.37 (Draganic *et al.*, 1973).

$$2H_2C{=}N^{\cdot} \longrightarrow HCN + H_2C{=}NH \qquad (1.35)$$

$$H_2C{=}NH + H_2O \longrightarrow HCHO + NH_3 \qquad (1.36)$$

$$HC(OH){=}NH + H_2O \longrightarrow HCO_2H + NH_3 \qquad (1.37)$$

The ammonia from ammonium cyanide or that produced radiolytically in cyanides is very reactive towards hydroxyl radicals (reaction 1.38), and the radical produced reacts with other intermediates or with solute producing the final products (Draganic *et al.*, 1980).

$$NH_3 + HO^{\cdot} \longrightarrow NH_2^{\cdot} + H_2O \qquad (1.38)$$

Aldehydes and ketones. The most abundant compound formed is formaldehyde, $G°=1.8$, but G rapidly decreases with increasing dose (down to 0.1) (Ogura, 1968; Draganic *et al.*, 1973). Its origin could be explained by reactions 1.35 and 1.36. At high doses of irradiation, CH_2CHO, CH_2COCHO, and $CH_2(CO)_2CH_2$ are formed, and could originate by short-chain oligomerization of the radicals produced by reactions 1.26 to 1.31 (Navarro-González, 1983).

Carboxylic Acids. Formic acid, $G°=0.1$ for 0.006 mole dm^{-3} HCN, may be formed by reactions 1.34 and 1.37 (Ogura, 1968). A large number of mono-, di-, and tricarboxylic acids were identified in HCN (pH=6) and NH_4CN (pH=9.2): aconitic, adipic, 1,2,4-butene-tricarboxylic, butyric, carboxysuccinic, citric, citraconic, 1,2-dimethyl-succinic, fumaric, glutaric, itaconic, maleic, malic, malonic, methyl-malonic, 2-methyl-tricarballylic, oxalic, pimelic, succinic, and tricarballylic (Navarro-González, 1983; Negrón-Mendoza *et al.*, 1982, 1983). Isolated, short-chain oligomerization might explain the formation of carboxylic acids or their amides (Negrón-Mendoza *et al.*, 1983).

Urea is an important product in the aqueous solutions of ammonium cyanide, pH 9.2, ($G=0.65$, 180 kGy),

but is formed in low yield in aqueous solutions of hydrogen cyanide, pH 6 (G=0.03, 130kGy). It may be formed by reactions 1.39 to 1.42 (Draganic and Draganic, 1980; Niketic *et al.*, 1983).

$$\cdot C(OH)=N^- + H_2O \longrightarrow OH^- + \cdot C(OH)=NH \quad (1.39)$$

$$\cdot C(OH)=NH \longrightarrow NH_2\dot{C}=O \quad (1.40)$$

$$NH_2\dot{C}=O + NH_2\cdot \longrightarrow NH_2C(=O)NH_2 \quad (1.41)$$

$$HO-CN + NH_3 \longrightarrow NH_2C(=O)NH_2 \quad (1.42)$$

Carbamyl glycinamide, $H_2NC(=O)NHCH_2C(=O)NH_2$, is formed in low yield in HCN at pH=6 (G=0.02, 130 KGy). It has not yet been detected in NH_4CN solutions, pH 9.2. Carbamyl glycinonitrile, $H_2NC(=O)NHCH_2CN$, forms in low yield (G=0.05) in HCN solutions, pH 6 (130 KGy) and NH_4CN solutions, pH 9.2 (180 KGy). These products could originate by short-chain oligomerization of the radicals produced by reactions 1.26 to 1.30, 1.38 and 1.42 (Niketic *et al.*, 1983).

Amino acids. Trace amounts of amino acids were found in some cases of irradiated solutions. Their origin was attributed to partial hydrolytic breakdown of oligomeric material (Draganic *et al.*, 1976a).

Heterocyclic compounds. A large number of products is formed; however, the identification of most of them still remains to be done. They represent 2-5% of the total mass of all non-volatile products. Adenine, uracil, thymine, and cytosine are formed. There is evidence of the presence of triazines, but they have not yet been identified (Ponnamperuma, 1965; Negrón-Mendoza and Draganic, 1984).

Heterocyclic products are most likely fragments of short side-chains of oligomers which are formed as a result of free radical processes (Negrón-Mendoza and Draganic, 1984).

DAMN is formed with a low radiation chemical yield ($G°=10^{-3}$) in dilute aqueous solutions (Ogura and Kondo, 1967; Draganic and Draganic, 1980); however, as the concentration of HCN is increased (0.5 mole dm^{-3}), it becomes an important product ($G°=0.45$) in the irradiation (Ogura and Kondo, 1967).

1.4.2.2 Formation of larger molecules

Between 50% (NH_4CN, pH=9.2) and 79% (HCN, pH=6) of nitrogen and carbon atoms from decomposed starting

material are built into larger radiolytic products. The oligomeric materials undergo some modifications during the radiolysis, such as hydrolysis and decarboxylation, and these modifications contribute to the formation of a larger variety of oligomeric products (Draganic and Draganic, 1980).

Acid hydrolysis of the nonvolatile products releases several proteinic and nonproteinic amino acids (Table 1.3). The composition of amino acids in the

Table 1.3. $G°$ of formation of amino acids[1].

	System		
Amino acid	HCN pH=6	NH_4CN pH=9.2	NaCN pH=11.3
Ala	0.005	0.004	0.022
Asp	0.012	0.010	0.008
Gly	0.140	0.600	0.240
Glu	<0.001	<0.001	0.002
His	0.002		
Ser	0.002	0.005	0.018
Thr	0.018	<0.001	<0.001
Total	0.190	0.620	0.290

1. Draganic *et al.*, 1976a; and Draganic and Draganic, 1977.

mixture does not depend strongly on the pH of system, but their yields do vary considerably depending on the initial pH of the solution (Table 1.3) (Draganic *et al.*, 1976a, 1977a; Draganic and Draganic, 1977).

Fractionation of the nonvolatile material yields basic (17% (HCN) and 38% (NH_4CN) of total weight), acidic 3% (HCN and NH_4CN) of total weight) and neutral (69% (HCN) and 41% (NH_4CN) of total weight) fractions. The analysis of the acidic fraction indicates the presence of dicarboxylic acids in the unhydrolyzed sample (Draganic *et al.*, 1980; Niketic *et al.*, 1983). Hydrolysis of these fractions releases several amino acids in different percentages: 83.9% in the neutral fraction; 13.8% in the basic fraction; and 2.3% in the acid fraction (Draganic *et al.*, 1980).

The oligomers from ammonium cyanide (pH=9.2) and hydrogen cyanide (pH=6) solutions are very similar (Draganic *et al.*, 1980; Niketic *et al.*, 1982, 1983). At present, the following oligomers have been detected:

Oligoimine, $-(CH_2NH)_n-$, is the main constituent of the neutral fraction, and represents 16.4% of the total mixture of radiolytic products. It releases trace amounts of amino acids upon hydrolysis, but it is not

cleaved by proteolytic enzymes (Draganic *et al.*, 1980; Niketic *et al.*, 1982).

Urea-aldehyde oligomer, $-(NHC(=O)NH(CH_2)_x)_n-$, is present in the neutral fraction, and represents 8.2% of the total mass of the mixture of products. After hydrolysis, glycine is released, constituting 55% of the mass of the oligomer. The oligomer lacks peptidic bonds, and upon hydrolysis ammonia is released (Draganic *et al.*,, 1980).

Other oligomers with urea-aldehyde fragments have peptidic bonds and are isolated in different fractions because of various side-chain modifications present in the oligomers. They represent up to 40% of the non-volatile radiolytic products. The length of the peptidic fragments varies, but it is estimated to be up to 30% of the oligomer mass (M.W. 5,000) in some neutral fractions (Draganic and Draganic, 1980).

Oligomers with peptidic bonds. The presence of these oligomers was established based upon four tests:

a. Amino acid content on acid hydrolysis (Draganic *et al.*, 1976a, 1977a; Draganic and Draganic, 1977).

b. Positive biuret reaction (Draganic *et al.*, 1976a; Draganic and Draganic, 1977).

c. Infrared analysis (Draganic *et al.*, 1977b).

d. Enzymatic cleavage with aminopeptidase M and pronase (Draganic *et al.*, 1980; Niketic *et al.*, 1982).

The oligomers are isolated from the basic fraction and represent 5.3% (NH_4CN) and 14-30% (HCN) of the total weight of the mixture of radiolytic products. Their molecular weights are in the range 1,500-20,000. Enzymatic treatment only cleaves 30% of the peptidic bonds (Draganic and Draganic, 1980; Niketic *et al.*, 1982).

Some of these oligomers show catalytic activity as demonstrated by the hydrolysis of p-nitrophenylacetate (pNPA). The rate of hydrolysis[9] of pNPA varies from 1.0 to 7.8 depending of the oligomer type, and is of the same order of magnitude as that of chymotrypsin[10] (Niketic, 1984b).

---

[9] $X10^{-8}$ mole (pNPA) s^{-1} g^{-1} (substance).

[10] k(pNPA + chymotrypsin)=$3.7X10^{-8}$ mole s^{-1} g^{-1}.

In spite of the progress made in the elucidation of products from the free-radical oligomerization of HCN, further work is still needed to characterize the complex mixture of radiolytic products.

1.4.3 Hydrolysis *vs* oligomerization of HCN

Sanchez *et al.* (1967) investigated the extent of hydrolysis and ionic oligomerization of HCN in a basic medium. They found that hydrolysis is the major reaction channel at concentrations ≤ 0.01 mole dm^{-3} HCN. Ionic oligomerization is important at concentrations ≥ 0.1 mole dm^{-3} HCN; the maximum conversion is centered at pH 9.2, but sharply falls at $8.5 \leq pH \geq 9.8$. Mixed kinetics occur in the range 0.01-0.1 mole dm^{-3} HCN (Sanchez *et al.*, 1967).

Ogura *et al.* (1972) studied the free-radical oligomerization of HCN in the pH range from 1 to 10, and in the concentration range from 0.0005 to 0.1 mole dm^{-3} HCN. They found that the radiation chemical yield of decomposition of HCN is maximum ($G°=6$) in the pH range from 6 to 8 at concentrations of 0.006 mole dm^{-3} HCN, and decreases to about half at $3 \leq pH \geq 10$. The authors also found that $G°$ (-HCN) is not linearly related with

the initial concentration of HCN, and varies from about 3 to 9.5 in the concentration range from 0.0005 to 0.1 mole dm^{-3}. Formic acid, a hydrolyzed product of HCN, is formed in low yield (Ogura, 1968); however, its origin is by free radical reactions (1.29, 1.34, 1.37), and not by based or acid catalyzed reactions (1.43). The base and/or acid catalyzed hydrolysis of HCN is insignificant under the author's conditions since the rate of production of radicals in very high, $\sim 5X10^{-5}$ s^{-1}.

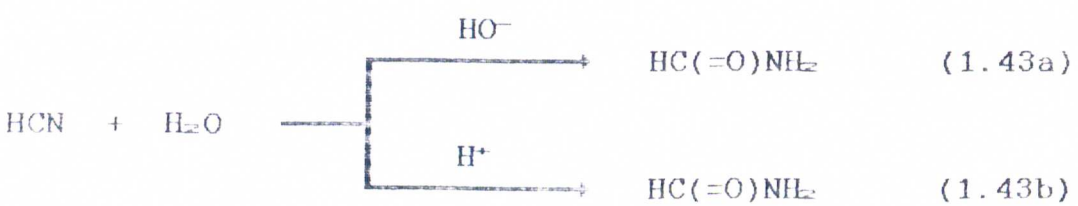

The rate of hydrolysis of HCN by base or acid catalysis is low; however, the latter is more significant. The Arrhenius parameters for these reactions have been recently reported by Stribling and Miller (1987): for $k=k_o \exp(-E_a R^{-1} T^{-1})$, where, $k_o=4.8X10^{11}$ dm^3 $mole^{-1}$ s^{-1}, and $E_a=(85.0)$ kJ $mole^{-1}$, in the base catalyzed reaction (1.43a); and, $k_o=1.8X10^5$ dm^3 $mole^{-1}$ s^{-1}, and $E_a=(90.4)$ kJ $mole^{-1}$, in the acid catalyzed reaction (1.43b).

With the data given in the previous and present sections, we are in a position to evaluate the possible extent of hydrolysis and oligomerization of HCN in the primitive hydrosphere. Such an estimate has not yet been available in the literature; however, the kinetic parameters for the major processes are known. Therefore, we can simplify such processes by a small set of simultaneous chemical equations (Table 1.4), and numerically integrate them with the use of a computer. The details of the computer program (ACUCHEM) are described detail in Chapter 2, section 2.7.

Equations 1 and 2 in Table 1.4 are the equilibrium reactions for the dissociation of liquid water and HCN, respectively. The losses of HCN by base and acid hydrolysis are given by equations 3 and 4, successively. Equation 5 is the reaction leading to the ionic oligomerization of HCN. The production of radicals ($R^{\cdot}$) such as $H^{\cdot}$, $HO^{\cdot}$, and e_{aq}^{-} formed by interaction of various energy sources on the primitive hydrosphere is difficult to determine. If we only consider those produced by radioactivity, and use a moderate energy flux of 20 J cm^{-2} y^{-1} (pages 14-15, this study), the dose rate for the hydrosphere would be about $5X10^{-7}$ kGy s^{-1}. The total yield of radicals from

Table 1.4. Chemical Equations used in Simulation.

No.	Equation	Constant[1]
1.	$H_2O \longrightarrow HO^- + H^+$	$K=1.0X10^{-14}$
2.	$HCN \longrightarrow {}^-CN + H^+$	$K=6.0X10^{-10}$
3.	$HCN + HO^- \xrightarrow{H_2O} HCONH_2 + OH^-$	$k=6.0X10^{-4}$
4.	$HCN + H^+ \xrightarrow{H_2O} HCONH_2 + H^+$	$k=2.6X10^{-11}$
5.	$HCN + {}^-CN \longrightarrow$ Ion-oligomer	$k=2.5X10^{-7}$
6.	$H_2O \longrightarrow R^\cdot$	$k=5.2X10^{-11}$
7.	$HCN/CN^- + R^\cdot \longrightarrow$ FR-oligomer	$k=1.0X10^{8}$
8.	$2R^\cdot \longrightarrow R2$	$k=1.0X10^{10}$

1. Equilibrium or rate constants are distinguished by the symbol K or k, respectively. The units are s^{-1}, and $dm^3\ mole^{-1}\ s^{-1}$ for first and second order rate constants, consecutively. The values are calculated for 25°C from equations given in this chapter.

radiolysis of liquid water is G=6.4; however, if we consider a low production, G=2, a rate of radical formation of $5.2X10^{-11}\ s^{-1}$ is derived (equation 6). This calculation underestimates G ($R^\cdot$) from radiolysis of liquid water, and does not include the contribution of other energy sources, which may have contributed

significantly (page 35). The rates of reactions of these radicals with HCN/CN^- are all known (page 36 to 39), and we use a representative value of 10^9 dm^3 $mole^{-1}$ s^{-1} (equation 7). Dimerization of this generic radical (equation 8) has to be taken into account as a likely competition for equation 7. The rates of radical-radical reactions from transients of water are all known (Buxton *et al.*, 1988), and are typically around 10^{10} dm^3 $mole^{-1}$ s^{-1}; therefore, this value was used in the computer simulation.

The pH used in the simulation is 8, and this value is generally accepted for the primitive hydrosphere (Fox and Dose, 1977). As pointed out on page 22, we are not yet able to estimate the concentration of HCN in the primitive hydrosphere. A concentration range of 0.01-0.1 mole dm^{-3} was used as the upper limit in the computer simulation. Table 1.5 summarizes the net rates of hydrolysis and oligomerization via ions and free-radicals. The integration time was set for a relatively short period of time in geological terms, 2 months in order to avoid over-decomposition of HCN. As it is evident from these results, the decomposition of HCN is primarily *via* free-radical oligomerization reactions, $\geq$88%, at concentrations $\leq 10^{-3}$ mole dm^{-3}. Hydrolysis is unimportant ($\leq$12%), but ionic oligomerization

Table 1.5. Percent Relative Rates of Hydrolysis and Oligomerization of HCN for the Primitive Hydrosphere.

HCN mole dm^{-3}	Hydrolysis	Oligomerization	
		Ionic	Free-Radical
$1.0X10^{-4}$	0.5	<0.1	99.5
$1.0X10^{-3}$	11.5	0.1	88.4
$1.0X10^{-2}$	54.1	2.8	43.1
$1.0X10^{-1}$	60.0	31.5	8.5

is negligible ($\leq$0.1). Oligomerization *via* ions could become significant only at high concentrations ($\approx$0.1 mole dm^{-3}), but under this conditions hydrolysis also enhances.

1.5 Research objectives

Great progress has been achieved in the understanding of mechanisms and efficiencies of HCN production triggered by ultraviolet light, ionizing radiation, and pyrolysis. The contribution of electric discharges to the synthesis of HCN in the primitive atmosphere is generally considered significant (Miller

and Orgel, 1974). Nonetheless, no accurate evaluation of such a contribution has been presented. The major obstacle has been the inability to measure the amount of energy transferred from the high-voltage, high-frequency electric discharges.

Our research goals were centered in obtaining a better insight into two major aspects of role of hydrogen cyanide in chemical evolution. In particular, one of these was to accurately measure the chemical yield of formation of HCN in the electrolysis of a simulated primitive atmosphere and to elucidate its mechanism of synthesis. This work is described in chapter 3.

The other major research goal was to investigate the effect of cyanocomplexes of transition elements on the free-radical oligomerization of HCN. Specifically, we were interested in hexacyanoferrate(II) and (III), since they probably accumulated in the primitive oceans (section 1.3, this study). There is great interest involved in this investigation since only a limited number of studies in abiotic chemistry has been devoted to examine the effects of metal ions in catalyzing reactions of significance to the origins of life (Kobayashi and Ponnamperuma, 1985a). The limited

reports indicate that metal ions could significantly increase the yields of prebiologically and/or biologically important compounds from a variety of abiotic type reactions (Beck, 1978; Kobayashi and Ponnamperuma, 1985b). The systems HCN/Fe were γ-irradiated to trigger free-radical reactions in aqueous solutions, and various mixing ratios for iron were investigated ranging from 100.00 to 0.01%. The results and implications of this work are described in chapter 4.

A general discussion and conclusions of all the data is given is chapter 5.

CHAPTER 2

EXPERIMENTAL PROCEDURES

2.1 General

All chemicals were of the highest purity commercially available, and were used without further purification unless otherwise stated. Their sources were: Aldrich Chem. Co., Inc.; Allied Chemical; Eastman Kodak, Co; Air Products & Chemicals, Inc.; EM Industries, Inc.; Fisher Scientific Co.; J.T. Baker Chem. Co.; Mallinckrodt, Inc.; Matheson Gas Products; Sigma Chem. Co. Methanol and benzene were purified according to the procedures of Perrin *et al*. (1966).

Deionized-distilled water was used for cleaning of glassware and for analysis of irradiated (electric discharge or γ-irradiation) samples. It was purified by flowing tap water through a Millipore system (Millipore, Co.) consisting of charcoal activated and

anion-cation exchanger cylinders, and finally distilled into a glass container.

Triple distilled water was used for preparation and irradiation of samples. This was obtained by successive distillations from an alkaline (pH≈10) solution of 0.01 mole dm^{-3} potassium permanganate, an acid (pH≈2) solution of 0.01 mole dm^{-3} potassium dichromate, and finally distilled without reagents (Draganic and Draganic, 1971). In all cases, only freshly prepared water was used.

All glassware was made of borosilicate glass ("Pyrex"), and was cleaned according to standard procedures used in radiation chemistry (Swallow, 1960). These consisted of immersing the glassware in concentrated sulfuric acid and warm 7 mole dm^{-3} nitric acid, followed by their abundant washing with tap water, deionized-distilled water, and triple distilled water, and finally dried overnight at $\geq$200°C in an oven.

2.2 Preparation of electric discharge samples

Three gaseous systems were investigated. A mixture of CH_4-N_2-H_2O was used to simulate an early primi-

tive atmosphere. This system has been extensively used in this laboratory to obtain basic information on abiotic synthesis of amino acids (Kobayashi and Ponnamperuma, 1985b). The other systems consisted of gaseous CH_4, and air (N_2-O_2); these were used to study the properties of electric discharges.

2.2.1 CH_4-N_2-H_2O system

Electric discharge experiments of a simulated primitive atmosphere were performed using a 4.3 dm^3 dumbbell shaped flask (Figure 2.1). 0.1 dm^3 of 0.05 mole dm^{-3} ammonium chloride buffer at pH 8.7 was

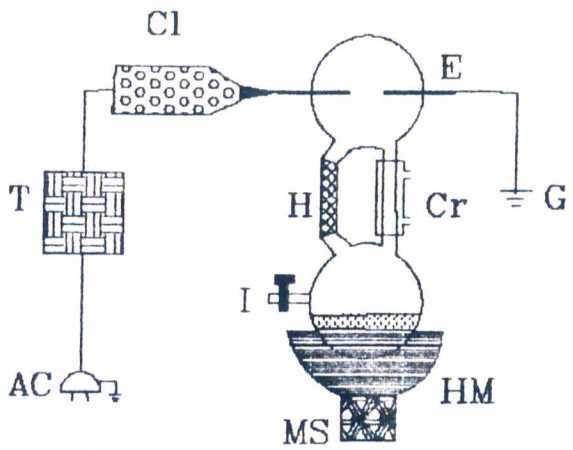

Figure 2.1. Electric Discharge apparatus. AC: Alternating current power; Cl: Coil; Cr: Condenser; E: Electrodes; G: Ground; H: Heating tape; HM: Heating mantle; I: Vacuum and gas inlet; MS: Magnetic stirrer; T: Transformer.

filtered through a Millipore membrane (pore size 0.22 μm, type GS) and then introduced into the flask. The system was air-evacuated by a diffusion vacuum pump. The gases dissolved in the ammonium chloride buffer solution were removed by 4 freeze-thaw cycles while the vacuum pressure was maintained at 30 mTorr. 200 Torr of methane (Matheson Gas Products) and 200 Torr of nitrogen (Air Products & Chemicals, Inc.) of purity ≥99.99%, were introduced into the flask to yield a gaseous solution of 0.0108 mole dm^{-3} of methane, 0.0108 mole dm^{-3} of nitrogen, and 0.00782 mole dm^{-3} of water vapor after allowing the system to equilibrate at 60°C prior to electrolysis.

2.2.2 CH_4, and air (N_2/O_2=3.7) systems

These systems were prepared in a 4.3 dm^3 dumbbell shaped flask (Figure 2.1) or in a 2.1 dm^3 round flask. Air taken directly from the atmosphere was introduced into the flask and the pressure was adjusted from 1 to 760 Torr with a pressure gauge. Methane (Matheson Gas Products) systems were prepared by removing the air from the flasks with a vacuum diffusion pump to about 50 mTorr, followed by filling with methane gas of purity ≥99.99%,, and its re-evacuation. The flasks

were filled with methane at 200 or 760 Torr.

2.3 Preparation of γ-irradiated samples

Aqueous, oxygen-free, 0.1 mole dm^{-3} HCN solutions containing (10^{-3}-10^{-5} mole dm^{-3}) potassium hexacyanoferrate(II) or (III) at pH≈6 can be conveniently prepared using a simple setup (Figure 2.2). 0.3 dm^{3} of triple distilled water or an aqueous solution of (10^{-5}-

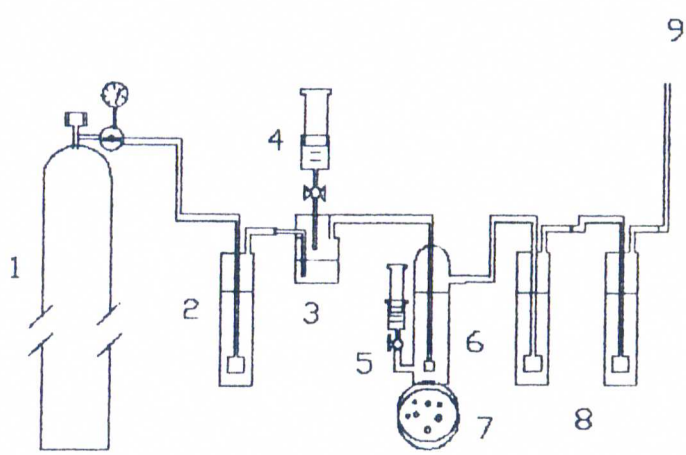

Figure 2.2. Preparation of Oxygen-free Aqueous Solutions of HCN. 1. Argon cylinder; 2. Tank containing triple distilled water; 3. Reactor vessel containing aqueous sulfuric acid (1/1 v); 4. Syringe filled with saturated aqueous KCN or NaCN solution; 5. Syringe for injecting or removing sample solution; 6. Vessel containing HCN sample; 7. NaOH or KOH pellets; 8. Saturated NaOH or KOH solution to trap undissolved HCN; 9. To hood extractor.

10^{-3} mole dm^{-3}) potassium hexacyanoferrate(II) or (III) (Fisher Scientific Co. or Allied Chemical, respectively) is placed into a vessel (6 in figure 2.2), and the solution is degassed at room temperature by bubbling with 99.998% argon (Air Products & Chemicals, Inc.) for at least 30 min. HCN is generated in the reactor vessel (3) by slowly introducing 0.01 dm^3 of a degassed saturated NaCN or KCN (98.5% purity from J.T. Baker Chem. Co.) solution (4) into 0.02 dm^3 of degassed sulfuric acid (J.T. Baker Chem. Co.) solution (1/1, v/v). Gaseous HCN is introduced into the sample flask (6), and the concentration of HCN is monitored by withdrawing aliquots with a syringe (5). Undissolved HCN is trapped in containers (8) with saturated KOH or NaOH.

Aqueous, oxygen-free, 0.02 mole dm^{-3} potassium hexacyanoferrate(II) (Fisher Scientific Co.) solutions (pH 6.7) were prepared using the same setup (Figure 2.2), except that HCN was not generated.

0.01-0.10 dm^3 deoxygenated solutions of HCN and/or hexacyanoferrate(II) or (III) were prepared just prior to irradiation and were kept in special borosilicate glass syringes with caps during irradiation. When larger amounts of sample were needed for analysis, the

solution was introduced into special Pyrex vessels (0.45-0.75 dm^3). These vessels permitted gaseous radiolytic products to escape from the system preventing a build-up of an over-pressure above the liquid phase, and precluding air from entering into the solution.

2.4 Irradiation of samples

2.4.1 Electric discharge experiments

The electric discharge across two electrodes separated by a 0.1 dm gap was produced using high frequency generators (Tesla coils) from Electro-Technic Products, Inc. Three different Tesla coils were used: Two were model BD-50 (A and B) and one was model BD-50E. The electrodes were made from 0.13 mm diameter tungsten rods from Laboratory Supply & Equipment Co.

The intensity of the discharge was controlled by the output adjustment knob of the Tesla coil. In order to determine the amount of energy introduced by an electric discharge, we investigated the properties of the electric discharge at various spark gaps (0-0.1 dm)

and pressures (1-760 Torr) in three gas systems: air, $CH_4-N_2-H_2O$, and CH_4.

Three different methods were developed to determine the amount of energy introduced into the systems by the electric discharge. The first was an indirect method, the *chemical dosimeter* (Navarro-González *et al.*, 1986). This consisted of measuring the extent of decomposition of methane produced by the electric discharge and correlating it with a study where both the energy input and extent of decomposition of methane were measured. The other two were direct methods and consisted of measuring the voltage and current of the electric discharge with an oscilloscope and by calorimetry. The energy input per mole (E_i) was calculated as $E_i = IVtn^{-1}$; where I and V are the discharge current and voltage, respectively, t is the reaction time, and n is the number of moles of the gas present. In order to ascertain the effectiveness of the calorimetric method reported by Stribling and Miller (1987), we also measured the energy input of the electric discharge according their procedure.

Energy measurements using methane as chemical dosimeter. In a chemical dosimeter the energy input is determined from the chemical change produced in a sub-

strate. Calculation of the energy input requires a knowledge of the chemical yield (G) for the reaction or product, which is found by comparing the chemical system with some form of absolute dosimeter. Prior to 1986, absolute dosimetric methods of high voltage high frequency electric discharges were not available. Absolute dosimetry for low voltage electric discharges has long been recognized (Wiener and Burton, 1953), in which the energy input per mole (E_i) was calculated from the discharge current and voltage. Wiener and Burton (1953) studied the electrolysis of methane at atmospheric pressure using a low voltage ($\leq$500 volts) direct current electric discharge. They measured the yields (G) of decomposition of methane and formation of acetylene, the principal product, as a function of energy input. Since this system is very simple to reproduce in the laboratory, we proposed its use as an indirect method to determine the energy in the high voltage electric discharge experiments (Navarro-González *et al.*, 1986). Figure 2.3 shows graphically the raw data obtained by Wiener and Burton (1953). The extrapolation of G° was obtained using different type of polynomial regressions, and the best estimate was

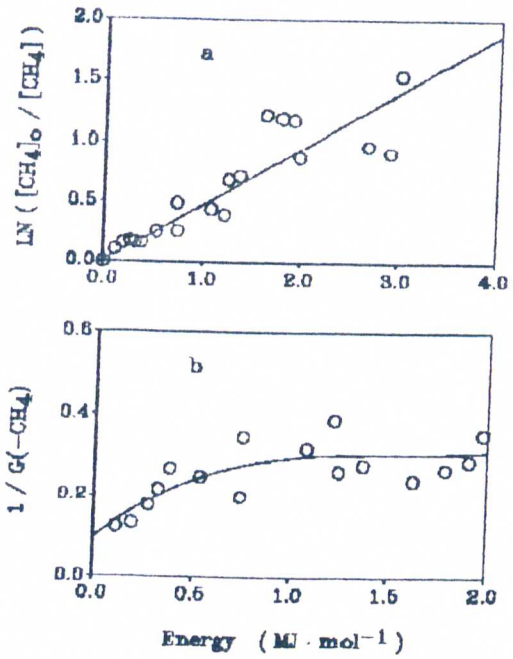

Figure 2.3. Energy Dependance of the Decomposition of Methane (a) and its Chemical Yield (b) in the Atmospheric Electric Discharge of Methane. Raw data was taken from Wiener and Burton, 1953.

$G^{\circ}(-CH_4)=8.34$, with an error of 20%. The power (P) of the high voltage electric discharges can be determined by measuring the rate of disappearance of methane, $k(-CH_4)$, and is calculated according to the following expression:

$$P = \frac{1.6022X10^{-17}\ k\ (-CH_4)}{G^{\circ}\ (-CH_4)}$$

The energy introduced (E_i) by electric discharges is computed by $E_i = P\ t\ n^{-1}$.

Voltage and current measurements with an oscilloscope.

The circuit for measuring the voltage and current of the electric discharge is shown in figure 2.4. Voltage

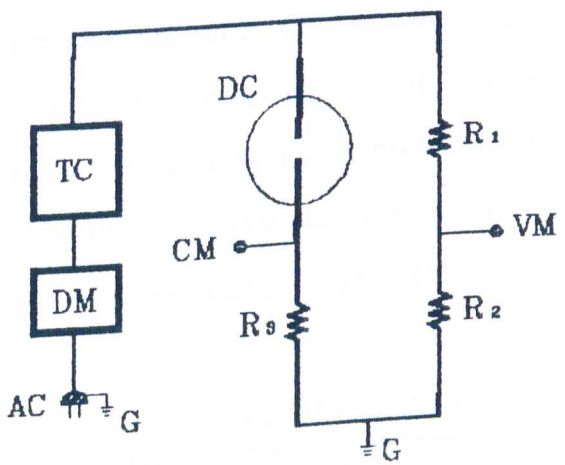

Figure 2.4. Schematic Representation of Electric Circuits for Measuring the Discharge Voltage and Current. AC: Alternating current power; CM: Current measurement; DC: Discharge chamber; DM: Digital multimeter; G: Ground; R: Resistors; TC: Tesla coil; VM: Voltage measurement. $20.0 \leq R_1 \geq 0.5$ M Ω; $10.0 \leq R_2 \geq 2.0$ k Ω; $1000 \leq R_3 \geq 50$ Ω.

measurements of the spark discharge were made with a Tektronix 515A oscilloscope using a tenfold attenuator probe (PG105 Tektronix). The electricity supplied to the Tesla coils was 120 V and 0.1-0.3 A, and was measured with a 8020 B digital multimeter from John Fluke MGL Co., Inc. The resistors (R) used were of 10 W power rating with a tolerance of 2-5%.

Resistor 1 and the electric discharge were connected in parallel to the voltage source and the same voltage was applied to each conducting path. The high voltage of the output was attenuated by resistor 1 and the resultant voltage was measured across resistor 2. Since resistors 1 and 2 were connected in series, the current everywhere in this path was the same. The output voltage of the Tesla coil (V_o) was,

$$V_o = \frac{V_m \ (R_1 + R_2)}{R_2}$$

where, V_m is the potential difference measured across resistor 2. The resistance of R_1 and R_2 was varied from 0.5 to 20.0 M Ω, and 2.0 to 10.0 k Ω, respectively.

The output current (I_o) supplied by the Tesla coil was split between the spark discharge and the path containing R_1 and R_2. The sum of currents in both parallel paths was equal to I_o. Since the spark discharge was connected in series with R_3, the current was the same at every point in this path. The voltage across R_3 was measured in order to determine the current through this path. The current supplied by the Tesla coil was,

$$I_o = \frac{V_m'}{R_3} + \frac{V_o}{R_1 + R_2}$$

where, V_m' is the potential difference measured across resistor 3. The resistance of R_3 was varied from 50 to 1000 Ω.

Voltage and current measurements by calorimetry.

Figure 2.5 shows the set up used to measure the voltage and current of the electric discharge by calorimetry. The heat dissipated (Q_1) from R_1 was monitored by the temperature rise in a calorimetric box made of polyurethane. The temperature was measured with a model 9540 digital platinum resistance thermometer from

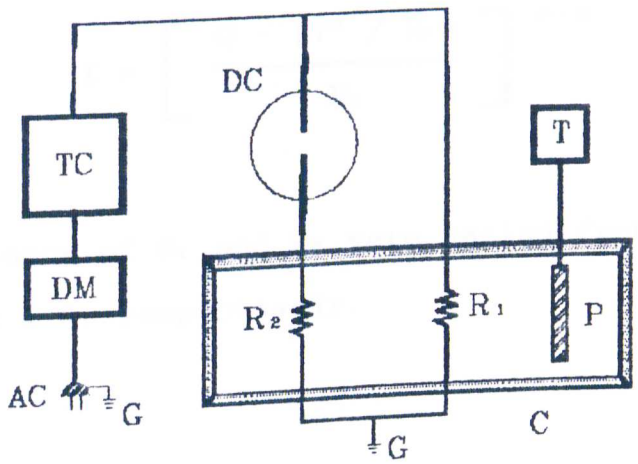

Figure 2.5. Experimental Layout for Measuring the Energy Input of Electric Discharges by Calorimetry. AC: Alternating current power; C: Calorimetric box; DC: Discharge Chamber; DM: Digital multimeter; G: Ground; P: Thermometer probe; R: Resistors; T: Digital thermometer; TC: Tesla Coil. $500 \leq R_1 \geq 20$ k Ω; $R_2 = 5$ k Ω.

Guildline with an accuracy of 0.003°C. The voltage of the discharge was calculated according to the following equation:

$$V = (Q_1 \ R_1)^{0.5}$$

The current of the discharge was obtained from the heat dissipated (Q_{1+2}) from both R_1 and R_2, and was calculated according to the following expression:

$$I = \left[\frac{Q - (V^2 / R_1)}{R_2} \right]^{0.5}$$

The resistance of R_1 and R_2 were varied from 20 to 500 k Ω; and 5 k Ω, respectively.

Energy determination by calorimetry. This method was suggested by Stribling and Miller (1986, 1987). It consists of measuring the rise of temperature in the calorimetric box produced by the sparking of the electric discharge sample (Figure 2.6). The amount of

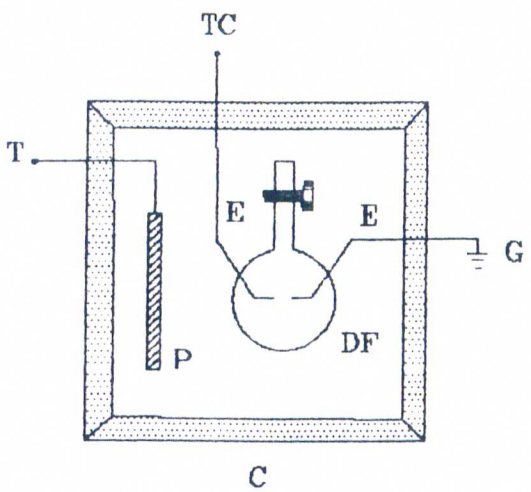

Figure 2.6. Measurement of Heat Generation by the Electric Discharge according to Stribling and Miller (1987). C: Calorimetric box; DF: Discharge Flask; E: Electrode; G: Ground; P: Thermometer probe; T: Thermometer; TC: Tesla Coil.

energy introduced by this method is not accurate since several aspects not taken into account are the energy converted into chemical form, or into light or not absorbed by the gas. Gases have a low collisional mass stopping power when they are irradiated with low energy electrons (Spinks and Woods, 1976), as in the case of electric discharges. Therefore, the method of Miller and Stribling underestimates the amount of energy supplied by electric discharges; however, we also measured the energy of our experiments with this method in order to compare its effectiveness.

2.4.2 γ-Irradiations experiments

γ-Irradiations were carried out using three radioactive ^{60}Co units located at the Institute of Nuclear Sciences, Universidad Nacional Autónoma de México (U.N.A.M.) at México City (dose rates of 0.7 and 20 kGy h^{-1}) and the Department of Chemical and Nuclear Engineering, University of Maryland (U.M.) at College Park (dose rate of 36.6 kGy h^{-1}). The irradiation dose was varied from 0.014 to 600 kGy.

The irradiations were initiated at room temperature. The temperature of the samples did not increase during its irradiation at low dose rate (0.7 kGy h^{-1}, U.N.A.M.); however, it increased up to 45°C or 55°C when the samples received a total dose of 80 kGy using dose rates of 20 kGy h^{-1} or 36.6 kGy h^{-1}, respectively. Figure 2.7 shows the variation of temperature as a function of dose produced by the ^{60}Co source located at U.M. The increase in temperature during the irradiation of the aqueous solutions does not lead to a significant effect on the radiation chemical yield of decomposition of liquid water, G° ($-H_2O$); G° ($-H_2O$)

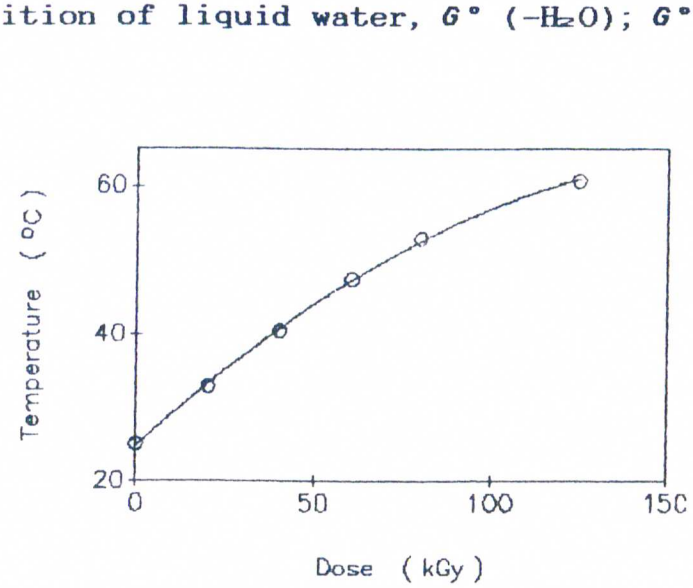

Figure 2.7. Dose dependance of temperature in the γ-irradiation of aqueous dilute solutions. ^{60}Co source: Department of Chemical and Nuclear Engineering, University of Maryland at College Park.

varies slightly from 4.41 at 23°C to 4.54 at 65°C and increases 0.07% per degree (Draganic and Draganic, 1971). The effect of temperature on reaction rate constants is also not large, increasing only by a few tenths of a percent per degree (Draganic and Draganic, 1971).

2.5 Control experiments

Control samples were prepared and analyzed simultaneously to irradiated samples except that they were not submitted to electrolysis or radiolysis. The analysis of these samples corroborated the absence of contamination during the preparation and the analysis of the samples.

2.6 Analyses of samples

The samples submitted to irradiation and their controls were analyzed immediately after irradiation according to procedures described below.

2.6.1 Determination of gas products

An aliquot of 0.05 dm^3 of gas from the electric discharge sample was transferred from the discharge flask to a high-vacuum sealed gas container and analyzed by a model 21-620A mass spectrometer from Consolidated Electrodynamics Co. The gases were identified by their fragmentation pattern. Supporting evidence of their identity was obtained by gas chromatography of the gas sample, and was reported previously by Kobayashi and Ponnamperuma (1985b). The gas products were quantified by the intensity of the molecular ion or a predominant fragment ion when the former overlapped with a fragment produced by a different gas. Table 2.1 summarizes the sensitivities of the different ions in the mass spectrometry. Ethylene was not quantified because its molecular ion ($C_2H_4^+$, 28) and the predominant fragment ($C_2H_3^+$, 27) overlapped with those of ethane and also nitrogen (N_2^+, 28).

Dissolved gases were extracted from solution and injected into a mass spectrometer (Consolidate Electrodynamics Co.) or into a Varian 1400 gas chromatograph equipped with a thermal conductivity detector (Varian Associates) by a modified Toepler pump according to a procedure already described (Torres *et al.*, 1982;

Table 2.1. Sensitivity factors for ions in the mass spectrometry analysis.

Parent Molecule	Fragment (MW)	Sensitivity Factor[1]
CH_4	CH_4^+ (16)	2.1
C_2H_2	C_2H^+ (25)	3.1
	$C_2H_2^+$ (26)	14.1
C_2H_4	$C_2H_4^+$ (28)	8.3
C_2H_6	$C_2H_6^+$ (30)	2.7
N_2	N_2^+ (28)	2.9

1. Sensitivity factor is defined as the peak height per pressure of gas samples.

Castillo, 1983). A column (12 dm long, 0.06 dm e.d.) packed with silica-gel (40/60 mesh) from Varian Associates was used to chromatograph hydrogen or carbon dioxide using argon or helium (Air Products & Chemicals Inc.) with a flow rate of 0.03 dm^3 min^{-1}. The temperature regime was isothermal at 50° or 55°C, consecutively.

NH_3 and CO_2 were identified by mass spectrometry; H_2 and CO_2 were identified and quantified by gas chromatography. Figures 2.8 and 2.9 show the calibra-

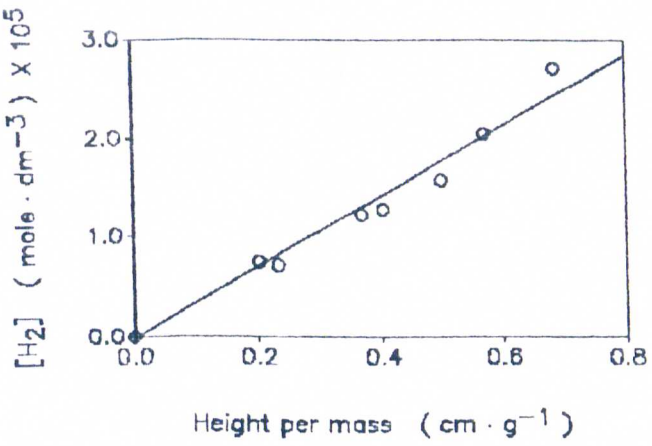

Figure 2.8. Calibration Curve for the Microdetermination of dissolved H_2 in Irradiated Aqueous Solutions. Calibration system: 0.02 mole dm^{-3} ethanol (pH 7).

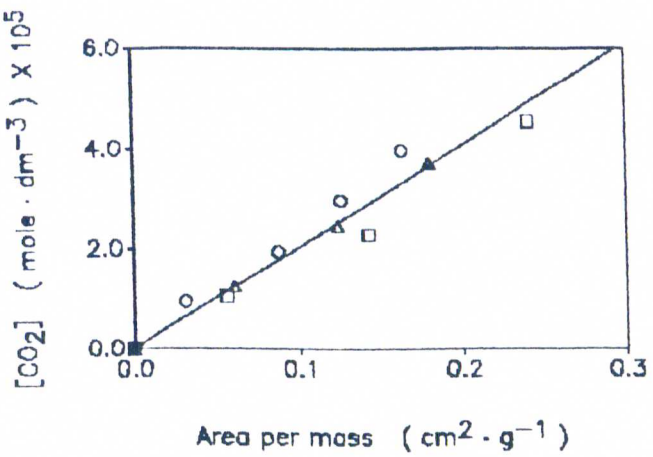

Figure 2.9. Calibration Curve for the Microdetermination of dissolved CO_2 in Irradiated Aqueous Solutions. Calibration systems: $5.0X10^{-4}$ mole dm^{-3} (O); and $2.5X10^{-4}$ mole dm^{-3} (△) sodium formate; and $7.5X10^{-4}$ mole dm^{-3} oxalic acid (□).

tion curves for H_2 and CO_2 obtained according the procedures described by Torres *et al*. (1982) and Castillo (1983).

2.6.2 Determination of ammonia

Ammonia was identified by mass spectrometry (section 2.6.1). Its quantitative determination was carried out using an ammonia selective electrode from Orion (model 95-12) connected to a model PHM84 pH meter from Radiometer. The electrode potentials of both an irradiated sample (P_{Sample}) and a reference solution ($P_{Reference}$), 0.1 mole dm^{-3} NH_4Cl were determined after adjusting the pH of the solutions to above 12 with a 5 mole dm^{-3} NaOH solution. The concentration of ammonia (C_{NH_3}) in the irradiated sample was determined according to the following equation:

$$C_{NH_3} = 10^{\left[\, 3.72 - 1.09X10^{-4}(P_{Reference}\ P_{Sample})\, \right]}$$

The calibration of the ammonia electrode was carried out in the concentration from 10^{-5} to 10^{-2} mole dm^{-3},

and the correlation coefficient for fitting the data to the derived equation was 0.998.

2.6.3 Determination of hydrogen cyanide

Gaseous HCN in the electric discharge experiments was dissolved in the aqueous phase by adjusting the pH of the solution to about 11 with a 1 mole dm^{-3} sodium hydroxide solution, and allowing the system to equilibrate for 1 hour at room temperature.

An aliquot of the liquid phase of the samples was injected directly into a Perkin Elmer model 990 gas chromatograph equipped with flame a ionization detector. The column used for the analysis was made of stainless steel (12 dm long, 0.03 dm external diameter), and was packed with Chromosorb 102 (80/100 mesh) from Varian Associates. The program temperature was from 60 to 200°C at a rate of 6°C min^{-1}. Nitrogen or helium (Air Products & Chemicals Inc.) were used as the carrier gases with a flow rate of 0.03 dm^3 min^{-1}. HCN was identified by its retention time (≈7.8 min), and by its coinjection with a standard HCN solution. A calibration equation was derived for the quantitative determination of HCN:

$$C_{HCN} = 1.69X10^{-7}\ Pa$$

where, C_{HCN} is the concentration of HCN in the sample; and Pa is peak area converted to attenuation factor 1. The calibration curve for HCN was carried out in the concentration from 10^{-5} to 10^{-2} mole dm^{-3}, and the correlation coefficient for fitting the data to the derived equation was 0.988.

Quantitative determination of HCN was also carried out by titrimetric analysis of the aqueous solutions using a 0.05 mole dm^{-3} $AgNO_3$ (Allied Chemical) aqueous solution (Bassett, 1978). In order to get a sharp end-point, iodide ion was used as the indicator according to the method of Dénigés (Bassett, 1978); the titration procedure consists of adding $AgNO_3$ to the HCN sample contained in an ammoniacal solution (0.2 mole dm^{-3}) in the presence of iodine ion (KI, 0.01 mole dm^{-3}) until the solution becomes turbid due to the precipitation of silver iodide.

HCN was also identified and quantified with a cyanide selective electrode (model: F1042CN) and a reference Calomel electrode (model: K401) connected to

a pH meter (model PHM84) from Radiometer. The electrode potential of the samples was obtained after adjusting the ionic strength (0.1) and the pH (11) of the sample with a $1.8X10^{-3}$ mole dm^{-3} $NaHCO_3$ and $3.2X10^{-3}$ mole dm^{-3} Na_2CO_3 aqueous solution. A calibration equation was derived for the quantitative analysis of HCN:

$$C_{HCN} = 10^{-\left[(1.72X10^{-2} P_{Sample} + 6.38) \right]}$$

where, C_{HCN} is the concentration of HCN; and P_{Sample} is the electrode potential of the sample. The calibration of the cyanide electrode was carried out in the concentration from 10^{-6} to 10^{-4} mole dm^{-3}, and the correlation coefficient for fitting the data to the derived equation was 0.999.

Calibration curves for the determination of HCN in solutions containing up to about 0.1 mole dm^{-3} chloride ion were also obtained; however, the calibration equations and factors did not change.

2.6.4 Determination of hexacyanoferrate(II) and (III)

Hexacyanoferrate(II) was determined by its quantitative oxidation by ceric sulfate (Day and Underwood, 1980): Few drops of indicator, diphenylamine (1% in H_2SO_4 c) were added to an aliquot of irradiated solution and titrated with a ceric sulfate solution (0.01 mole dm^{-3} $Ce(SO_4)_2.2(NH_4)_2SO_4.2H_2O$ in 0.2 mole dm^{-3} aqueous H_2SO_4) until a sharp color change to a deep blue-brown took place.

Hexacyanoferrate(III) was determined spectroscopically at its absorption maximum centered at 420 nm, where, its absorption coefficient was experimentally determined to be: 1020 dm^3 $mole^{-1}$ cm^{-1} at 25°C. Hexacyanoferrate(II) absorbed insignificantly under this conditions, $\varepsilon_{420\ nm} \leq 9$ dm^3 $mole^{-1}$ cm^{-1} at 25°C.

2.6.5 Determination of aldehydes and ketones

Aldehydes and ketones were analyzed by direct injection of the irradiated samples into a Perkin Elmer model 990 gas chromatograph equipped with a flame ionization detector. The chromatographic conditions are similar to those described in section 2.6.3 for the

gas-chromatography of HCN, and have been reported in detail elsewhere (Negrón-Mendoza *et al.*, 1983, 1984).

Aldehydes and ketones were converted via 2,4-dinitrophenyl-hydrazine (DNP) into 2,4-dinitrophenylhydrazones (DNPH), and were analyzed by paper chromatography (Navarro-González and Negrón-Mendoza, 1983a) or gas chromatography (Navarro-González and Negrón-Mendoza, 1983b) according to procedures already described. DNPH of aldehydes and ketones were also identified by mass spectrometry (VG Analytical, LTD model 7070E) using electron impact or chemical ionization (with isobutene) techniques at 70 eV. Their fragmentation pattern was compared with those of standard aldehyde derivatives and published MS spectra (Stanley *et al.*, 1975).

Calibration curves were obtained for DNPH derivatives of HCHO, CH_3CHO, CH_3CH_2CHO, and CH_3COCH_3 were carried out in the concentration range 10^{-3} to 10^{-2} mole dm^{-3}. A general calibration equation was derived:

$$C_{RCHO} = mP$$

where C_{RCHO} is the concentration of aldehydes; P is the peak height in cm at attenuation 1; and m is the slope of the calibration curve and were (mole dm^{-3} cm^{-1}): $2.83X10^{-6}$ (HCHO); $1.79X10^{-6}$ (CH_3CHO); and $1.10X10^{-6}$ (CH_3CH_2CHO and CH_3COCH_3). The R^2 values were equal or greater than 0.984.

2.6.6 Determination of polycarboxylic acids

Polycarboxylic acids were analyzed by gas-liquid chromatography as their methyl esters according to a procedure already described (Negrón-Mendoza and Navarro-González, 1982; Negrón-Mendoza *et al.*, 1983). The columns used for the analyses were packed with 10% Reoplex 400 (Anspec Co., Inc.) or 3% OV-17 (Supelco, Inc.) on Chromosorb W (A.W., DMCS, 80/100 mesh) from Supelco, Inc. The chromatographic conditions were as described previously (Negrón-Mendoza and Navarro-González, 1982; Negrón-Mendoza *et al.*, 1983). Dicarboxylic methyl esters were also analyzed with a Hewlett-Packard model HP5790 gas chromatograph coupled to a mass spectrometer (VG Analytical, LTD model 7070E) operated at 70 eV. A 25 m X 0.25 mm I.D. glass capillary column was used with bonded methyl 5% phenyl silicone from Perkin-Elmer. The carrier gas was

helium with a flow rate of 0.00042 dm^3 min^{-1}. The temperature was increased from 60°C to 200°C at 10°C min^{-1}.

Calibration curves were obtained in the concentration range from 10^{-2} to 10^{-4} mole dm^{-3}, and a general calibration equation was derived:

$$C_{RCO_2H} = mA$$

where C_{RCO_2H} is the concentration of carboxylic acids; A is the area of the peak; and m is the slopes of the calibration curves and are given in Table 2.2.

Table 2.2. Slopes (m) of calibration equations for polycarboxylic acids.

Acid	m[1]	R^2
Lactic, oxalic and pyruvic	2.44	0.992
Succinic	0.45	0.999
Glutaric	1.02	0.998
Pimelic	0.75	0.999
Aconitic	0.50	0.998

1. 10^{-5} mole dm^{-3} cm^{-2}.

2.6.7 Determination of oligomeric material

Oligomeric material, as referred in this study, is any non-volatile product that originates from solute molecules reactions initiated by irradiation.

Water insoluble oligomeric material produced by the sparking of a simulated atmosphere was filtered through a Millipore membrane (pore size 0.22 μm, type GS) and freeze-dried. Non-volatile radiolytic products from HCN/Fe mixtures were obtained by freeze-drying of the irradiated solution. The yield (g dm^{-3}) of oligomeric material was measured with a GRAM-ATIC balance from Mettler Instrument Co. Elemental analysis

of this material was obtained in order to determine its radiation chemical yield (*G*) in terms of carbon and/or nitrogen atoms converted into products. This analysis was performed by the staff members of the elemental analysis facility of the Department of Chemistry of the University of Maryland at College Park.

2.7 Radiation chemical yields: *G*

The radiation chemical yields of products and solutes were expressed as the number of molecules formed or destroyed per 100 eV of energy absorbed (Spinks and Woods, 1976), and were calculated from the slopes of concentration-dose plots (Ogura, 1968) according to the following expression: G=FS; where S is the slope of the curve in mole dm^{-3} kGy^{-1}, and F is $9.6485X10^{5}$ or $1.5292X10^{4}$ molecules $mole^{-1}$ cm^{-3} kGy for γ-irradiated or electric discharge systems, respectively.

2.8 Computer simulation of the chemical systems

Computer modeling is one of the most powerful tools for the quantitative understanding of highly complex chemical reaction systems (Braun *et al.*, 1988). Recently W. Braun and J.T. Herron from the Chemical Kinetics Division, and D. Kahaner from the Scientific Computing Division of the National Institute of Standards and Technology (Gaithersburg, Md.) have released an effective computer package named *ACUCHEM*, that is especially suitable for the numeric integration complex chemical rate equations. *ACUCHEM* is designed to operate on the IBM Personal Computer family and compatibles. It is a program for solving the system of differential equations describing the temporal behavior of spatially homogeneous, isothermal, multicomponent chemical reaction systems. Zeroth, first and second order reactions are allowed. Termolecular reactions are not handled explicitly; a two-step mechanism must be employed. There is no allowance for the input of equilibrium constants; reactions have to be entered separately in the forward and reverse reactions. The version used in this study is 1.4 (double precision), and handles up to 99 chemical species and 200 reactions (Braun *et al.*, 1988).

This program was used to perform computer simulations of electric discharge and γ-irradiated experiments. In the case of electric discharges, the chemical changes occurring are poorly understand (Wiener and Burton, 1953; Kobayashi and Ponnamperuma, 1985b). A possible chemical model and its computer-modeling to account for the observed chemical changes in electric discharge experiments will be described in Chapter 3.

In contrast to electric discharges, the radiation chemistry of liquid water is one of the best understood domains of radiation chemistry (Draganic and Draganic, 1971). The reactions occurring during the irradiation of water are well known, and their rates of reactions have been determined by a variety of techniques (Buxton *et al.*, 1988).

Tables 2.3 to 2.7 summarize the system of chemical reactions used in this study to model the γ-irradiation of liquid water and aqueous solutions. Unless otherwise stated, the rates of these reactions were taken from the comprehensive compilations of Anbar *et al.* (1971, 1975), Dorfman and Adams (1973), Ross (1975), Ross and Ross (1977), Buxton and Sellers (1978), Ross and Neta (1979, 1982), Hug (1981), Bielski *et al.* (1985), and Buxton *et al.* (1988). This set consists of

54 reactions. In section 2.8.1 two computer simulations are presented carried out with a well-understood irradiated system, the Fricke dosimeter, in order to demonstrate the validity of this set of reactions.

Table 2.3. Radiation and molecular product yields in irradiated liquid water by γ-rays and fast electrons with energies in the range 0.1 to 20 Mev[1].

No.	Species	*G*	
		pH 0.46	pH 3-13
1	$-H_2O$	4.45	4.10
2	H_2	0.40	0.45
3	H_2O_2	0.78	0.68
4	$H^{\cdot}$	3.65	0.55
5	$HO^{\cdot}$	2.90	2.72
6	H^+	0.00	2.65
7	e_{aq}^-	0.00	2.65

1. Draganic and Draganic, 1971; Spinks and Woods, 1976; Buxton *et al.*, 1988.

Table 2.4. Hydrogen atom reactions with transients from water.

No.	Reaction			k^1
8	$H\cdot + H\cdot$	$\xrightarrow[H_2O]{}$	H_2	7.8×10^{9}
9	$H\cdot + e_{aq}^-$	$\longrightarrow$	$H_2 + HO^-$	2.5×10^{10}
10	$H\cdot + \cdot O^-$	$\longrightarrow$	HO^-	2.0×10^{10}
11	$H\cdot + HO\cdot$	$\longrightarrow$	H_2O	7.0×10^{9}
12	$H\cdot + HO^-$	$\longrightarrow$	$e_{aq}^- + H_2O$	2.2×10^{7}
13	$H\cdot + H_2O$	$\longrightarrow$	$H_2 + HO\cdot$	1.0×10^{1}
14	$H\cdot + H_2O_2$	$\longrightarrow$	$H_2O + HO\cdot$	9.0×10^{7}
15	$H\cdot + O_2$	$\longrightarrow$	$HO_2\cdot$	2.1×10^{10}
16	$H\cdot + HO_2\cdot$	$\longrightarrow$	H_2O_2	1.0×10^{10}

1. The second order rate constant has units of dm^3 $mole^{-1}$ s^{-1}.

Table 2.5. Hydrated electron reactions with transients from water.

No.	Reaction			k^1
17	$e_{aq}^- + e_{aq}^-$	$\xrightarrow{2H_2O}$	$H_2 + 2HO^-$	$5.5X10^9$
18	$e_{aq}^- + H^+$	$\xrightarrow{H_2O}$	$H\cdot$	$2.3X10^{10}$
19	$e_{aq}^- + \cdot O^-$	$\xrightarrow{H_2O}$	$2HO^-$	$2.2X10^{10}$
20	$e_{aq}^- + HO\cdot$	$\xrightarrow{H_2O}$	HO^-	$3.0X10^{10}$
21	$e_{aq}^- + H_2O$	$\longrightarrow$	$H\cdot + HO^-$	$1.9X10^1$
22	$e_{aq}^- + O_2$	$\xrightarrow{H_2O}$	$\cdot O_2^-$	$1.9X10^{10}$
23	$e_{aq}^- + \cdot O_2^-$	$\xrightarrow{H_2O}$	$2HO^-$	$1.3X10^{10}$
24	$e_{aq}^- + HO_2^-$	$\xrightarrow{H_2O}$	$HO\cdot + 2HO^-$	$3.5X10^9$
25	$e_{aq}^- + H_2O_2$	$\longrightarrow$	$HO\cdot + HO^-$	$1.1X10^{10}$

1. The second order rate constant has units of dm^3 $mole^{-1}$ s^{-1}.

Table 2.6. Hydroxyl radical reactions with transients from water.

No.	Reaction	k^1
26	$HO\cdot + HO\cdot \longrightarrow H_2O_2$	$5.5X10^9$
27	$HO\cdot + \cdot O^- \longrightarrow HO_2^-$	$\leq 2.0X10^{10}$
28	$HO\cdot + HO^- \longrightarrow H_2O + \cdot O^-$	$1.3X10^{10}$
29	$HO\cdot + H_2 \longrightarrow H_2O + H\cdot$	$4.2X10^7$
30	$HO\cdot + HO_2\cdot \longrightarrow H_2O + O_2$	$6.0X10^9$
31	$HO\cdot + HO_2^- \longrightarrow HO^- + \cdot O_2^- + H^+$	$7.5X10^9$
32	$HO\cdot + H_2O_2 \longrightarrow H_2O + \cdot O_2^- + H^+$	$2.7X10^7$
33	$HO\cdot + H_2O_2\cdot^+ \longrightarrow H_2O + O2 + H^+$	$1.2X10^{10}$
34	$HO\cdot + \cdot O_2^- \longrightarrow HO^- + O_2$	$8.0X10^9$
35	$HO\cdot + \cdot O_3^- \longrightarrow \cdot O_2^- + HO_2\cdot$	$8.5X10^9$

1. The second order rate constant has units of dm^3 $mole^{-1}$ s^{-1}.

Table 2.7. Miscellaneous reactions with transients from water.

No.	Reaction	k^1
36	$\cdot O^- + \cdot O^- \xrightarrow{H_2O} HO_2^- + HO^-$	$8.3X10^9$
37	$\cdot O^- + H^+ \longrightarrow HO\cdot$	$1.0X10^{11}$
38	$\cdot O^- + H_2 \longrightarrow H\cdot + HO^-$	$8.0X10^7$
39	$\cdot O^- + H_2O \longrightarrow HO\cdot + HO^-$	$1.8X10^6$
40	$\cdot O^- + HO_2^- \longrightarrow HO^- + \cdot O_2^-$	$4.0X10^8$
41	$\cdot O^- + H_2O_2 \longrightarrow H_2O + \cdot O_2^-$	$\leq 5.0X10^8$

Table 2.7. Miscellaneous reactions with transients from water (Continue).

No.	Reaction	k^1
42	$\cdot O^- + O_2 \longrightarrow \cdot O_3^-$	$3.6X10^9$
	$\xrightarrow{H_2O}$	
43	$\cdot O^- + \cdot O_2^- \longrightarrow O_2 + 2HO^-$	$6.0X10^8$
44	$\cdot O^- + \cdot O_3^- \longrightarrow O_2 + O_2^{2-}$	$8.0X10^8$
45	$\cdot O_2^- + H^+ \longrightarrow HO_2\cdot$	$1.0X10^{11}$
46	$\cdot O_2^- + H_2O \longrightarrow HO_2\cdot + HO^-$	$1.0X10^9$
	$\xrightarrow{H_2O}$	
47	$\cdot O_2^- + HO_2^- \longrightarrow H_2O_2 + O_2 + 2HO^-$	2.0
48	$\cdot O_2^- + H_2O_2 \longrightarrow HO^- + HO\cdot + O_2$	$1.3X10^{-1}$
49	$HO_2\cdot + HO_2\cdot \longrightarrow H_2O_2 + O_2$	$3.4X10^6$
50	$HO_2\cdot + H_2O_2 \longrightarrow HO\cdot + O_2 + H_2O$	3.7
51	$HO_2^- + H_2O \longrightarrow H_2O_2 + HO^-$	$5.0X10^7$
52	$H_2O_2 + HO^- \longrightarrow HO_2^- + H_2O$	$1.0X10^{10}$
53	$H2O \longrightarrow H^+ + HO^-$	$2.5X10^{-5}$
54	$H^+ + HO^- \longrightarrow H_2O$	$1.4X10^{11}$

1. The first and second order rate constants have units of s^{-1}, and $dm^3\ mole^{-1}\ s^{-1}$, respectively.

2.8.1 Computer modeling of the Fricke dosimeter

The Fricke dosimeter is a chemical system that is widely used to determine the dose rate of ionizing radiation sources (Draganic and Draganic, 1971; Spinks and Woods, 1976). The dosimeter measures the oxidation of ferrous sulfate solutions induced by the interaction of ionizing radiations. This chemical system is the most thoroughly studied in radiation chemistry and is

the basis for the wide use of the Fricke dosimeter. The standard system is composed of 10^{-3} mole dm^{-3} $FeSO_4$ in air-saturated ($2.5X10^{-4}$ mole dm^{-3} O_2) 0.4 mole dm^{-3} H_2SO_4 (pH 0.46) (Spinks and Woods, 1976). The mechanism is well established, and the reactions involved are summarized in Table 2.8.

Table 2.8. Relevant reactions in the Fricke dosimeter.

No.	Reaction			k^1
F1	$H + Fe^{2+}$	$\longrightarrow$	HFe^{2+}	$7.5X10^6$
F2	$HFe^{2+} + H^+$	$\longrightarrow$	$H_2 + Fe^{3+}$	$1.0X10^5$
F3	$H + Fe^{3+}$	$\longrightarrow$	$Fe^{2+} + H^+$	$6.0X10^6$
F4	$HO + Fe^{2+}$	$\longrightarrow$	$Fe^{3+} + HO^-$	$1.7X10^7$
F5	$HO_2 + Fe^{2+}$	$\longrightarrow$	$Fe^{3+} + HO_2^-$	$2.5X10^6$
F6	$H_2O_2 + Fe^{2+}$	$\longrightarrow$	$Fe^{3+} + HO\cdot + HO^-$	$6.2X10^2$
F7	$Fe^{3+} + e_{aq}^-$	$\longrightarrow$	Fe^{2+}	$5.0X10^{10}$

1. The second order rate constant has units of dm^3 $mole^{-1}$ s^{-1}.

The computer modeling of this system consisted of the chemical equations summarized in Tables 2.4 to 2.8, and the radiation chemical yields of primary species from water at pH 0.46 (Table 2.3). Figures 2.10 and 2.11 show the computer modeling of the Fricke dosimeter

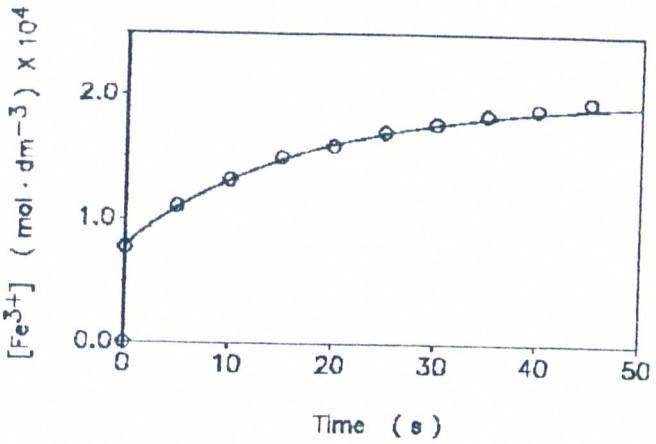

Figure 2.10. Computer Simulation (solid line) of the Fricke Dosimeter after a 155 Gy electron pulse. Conditions: 10^{-3} mole dm^{-3} $FeSO_4$ in aerated ($2.4X10^{-4}$ mole dm^{-3} O_2) 0.4 mole dm^{-3} H_2SO_4. Experimental data (O) was taken from Rasmussen and Bjergbakke, 1984.

under various conditions.

The excellent computer fitting with the experimental data shown in Figures 2.10 and 2.11 demonstrates that the chemical equations included in the data base (Tables 2.4 to 2.7) can effectively model the radiation chemistry of liquid water. Such a good agreement between experimental and computed trends is not surprising since the mechanism of water radiolysis has been thoroughly investigated and is one of the domains of radiation chemistry best understood (Draganic and Draganic, 1971). The development of pulse radiolysis techniques contributed significantly to the determina-

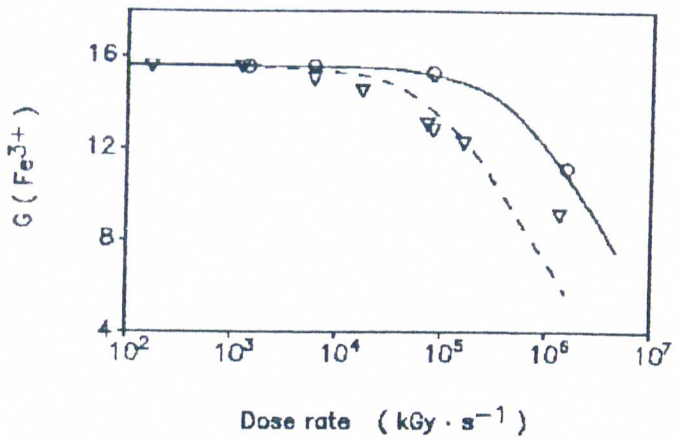

Figure 2.11. Computer Simulations (lines) of the Effect of G (Fe^{3+}) on Dose Rate after a 1 μsec electron pulse. Conditions: 10^{-3} mole dm^{-3} $FeSO_4$ in aerated ($2.4X10^{-4}$ mole dm^{-3} O_2) 0.4 mole dm^{-3} H_2SO_4 (▽, - - -); 10^{-2} mole dm^{-3} $FeSO_4$ in oxygenated ($1.2X10^{-3}$ mole dm^{-3} O_2) 0.4 mole dm^{-3} H_2SO_4 (O, ———). Experimental data (▽,O) were taken from Thomas and Hart, 1962.

tion of very accurate rate constants of unstable species produced in liquid water (Buxton *et al.*, 1988).

2.9 Presentation of data

The experimental data were fitted by polynomial regression analysis to show the trends of data points. No conclusions as regards to reaction mechanisms were drawn from the mathematical equations used in the curve fitting.

CHAPTER 3

ELECTROLYSIS OF A SIMULATED PRIMITIVE ATMOSPHERE: THE SYNTHESIS OF HYDROGEN CYANIDE

3.1. Introduction

The electric discharge driven production of HCN has been reported in numerous studies in prebiotic chemistry (Miller, 1957a; Sanchez *et al.*, 1966; Ponnamperuma *et al.*, 1969; Yuasa and Ishigami, 1975; Toupance *et al.*, 1975; Kobayashi and Ponnamperuma, 1985b; Stribling and Miller, 1987). However, little or no attention has been given to the measurement of the HCN yield. This is due in part to the apparent difficulty of determining the amount of energy transferred from the electric discharge to the absorbing systems. Consequently, the yields of HCN and other products typically have been expressed in terms of the percentage of the initial carbon atoms converted into products (carbon yields) (Miller, 1974; Kobayashi and

Ponnamperuma, 1985b, 1986; Stribling and Miller, 1987).

A method of directly determining the energy introduced (E_i) by electric discharges has long been recognized (Wiener and Burton, 1953), in which $E_i = IVt/n$, where I and V are the discharge current and voltage, respectively, t is the reaction time, and n is the number of moles of gas. The measurement of such variables have been reported in some prebiotic experiments carried out in this laboratory (Ponnamperuma *et al.*, 1969; Park *et al.*, 1975) and in others (Toupance *et al.*, 1975; Harada and Iwasaki, 1975; Harada *et al.*, 1978, 1984; Terasawa and Harada, 1980).

Measurement of the electric quantities (e.g. voltage, current) of prebiotic discharge experiments is difficult because they are most frequently done at high voltages (> 20,000 volt) at high frequencies (> 0.5 MHz). Voltage measurements in spark discharges were previously reported from this laboratory using a high voltage attenuator probe coupled to an oscilloscope (Park *et al.*, 1975). In a different approach, the energy input was estimated by measuring the input voltage and current supplied to a Tesla coil (Shimoyama *et al.*, 1978). The energy determined by this last method includes, however, the energy intro-

duced into the system not only as spark discharge but also the electricity converted into heat in the transformer.

A different method has been recently reported in which the energy introduced into the system was estimated by comparing the heat evolved during the sparking of an insulated discharge system with that produced by a known power input across a resistor (Stribling and Miller, 1986, 1987). However, the authors in that study did not take into account the energy converted into chemical form, light, or that not absorbed by the gaseous system. Navarro-González *et al.* (1986) have calculated that up to 24% of the energy introduced by the electric discharge can be converted into chemical form. In addition, gases have a low collisional mass stopping power when they are irradiated with low energy electrons (Spinks and Woods, 1976) such as are produced by electric discharges. As a consequence the method of Stribling and Miller underestimates the amount of energy introduced by electric discharges.

The purpose of this study is to develop dosimetric methods for high voltage, high frequency electric discharges, and to accurately determine the radiation chemical yield (G) of HCN in the electrolysis of a 4.2

dm^3 gaseous mixture at 60°C and 600 Torr composed of 0.0108 mole dm^3 of methane, 0.0108 mole dm^{-3} of nitrogen, and 0.00782 mole dm^{-3} of water vapor in equilibrium with a liquid phase of 0.1 dm^3 of 0.05 mole dm^{-3} aqueous ammonium chloride buffer at pH 8.7.

Three different methods were successfully applied to determine the dose supplied by electric discharges. The methodology is described in Chapter 2, section 2.4.1, and the results are reported here, in section 3.2. Once an accurate knowledge of the dose introduced into the electric discharges experiments was concluded, we could measure the initial chemical yields ($G°$) of HCN and other early products from the electrolysis of a CH_4-N_2-H_2O mixture. The results and a discussion are given in section 3.3.1. A mechanism to explain the electrolysis of the CH_4-N_2-H_2O mixture, and the formation of HCN is given in section 3.3.2. The implications of this study to chemical evolution are given in section 3.3.3 and the conclusions in section 3.4.

3.2. Dosimetry of high voltage electric discharges

The dosimetry of electric discharges was performed by chemical dosimetry, and electric and calorimetric

measurements of discharge voltage and current. The results from these measurements are given below.

3.2.1 Chemical dosimetry

The chemical dosimeter is an indirect method developed to estimate the power and dose rate supplied by alternating current electric discharges using the chemical system investigated by Wiener and Burton (1953): gaseous methane at 25°C and 760 Torr.

Analysis of the data reported by Wiener and Burton (1953) on the direct current electric discharge of methane at atmospheric pressure indicated that the power (P) of the electric discharge could be calculated according to the following equation (see Section 2.4.1, pages 65-68):

$$P = \frac{1.6022 \times 10^{-17}\ k(-CH_4)}{G^{\circ}\ (-CH_4)}$$

where, $k(-CH_4)$ is the rate of destruction of methane in

the electric discharge; and $G°\ (-CH_4)$ is the initial chemical yield of decomposition of methane. Calculating P required an accurate knowledge of $G°\ (-CH_4)$. $G°\ (-CH_4)$ was not determined by Wiener and Burton (1953), and therefore, was calculated from their data for this study (see pages 65-68, this dissertation); a value of 8.34 was derived for $G°\ (-CH_4)$ with an error of 20% (see Figure 2.3).

The rate of destruction of methane was determined in the alternating current electric discharge of methane at atmospheric pressure (Figure 3.1); $k(-CH_4)$

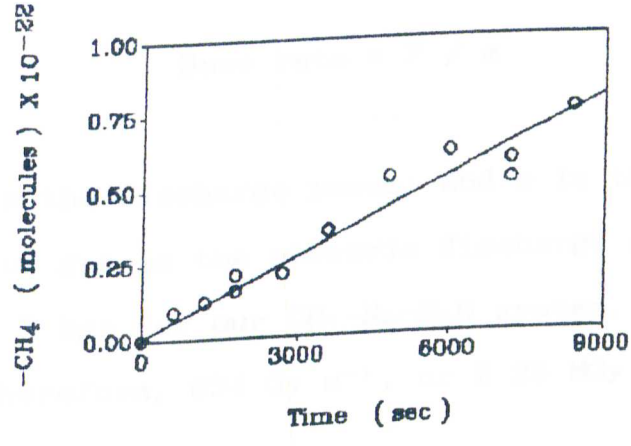

Figure 3.1. Time dependence of the destruction of methane in the alternating current electric discharge of methane at 25°C and 760 Torr.

was calculated from the slope of the curve shown figure 3.1 by linear regression analysis, and was determined to be: $8.73X10^{17}$ molecules sec^{-1} with a correlation coefficient of 0.986. The standard error of the data was calculated to be within 6%.

The power of the electric discharge was, therefore determined to be 1.68 W, with an estimated error of 20%. The error is mainly due to the deviation in G° ($-CH_4$).

The dose rate (Gy s^{-1}) of the electric discharge experiments was calculated from the equation,

$$\text{Dose rate} = P / m$$

where, P is the discharge power; and m is the number of kilograms of gas in the electric discharge system, and is $2.65X10^{-3}$ kgr for our CH_4-N_2-H_2O system. The dose rate is, therefore, 634 Gy s^{-1}, or 2.28 MGy hr^{-1}.

This method was the first dosimetric technique that was developed. Initially, the values of power and dose rate of the electric discharges were considered as estimates since we did not know if these parameters depended on the composition of the gas phase. Subse-

quently, two additional methods were developed (Sections 2.2.2 and 2.2.3), and it was found that these parameters do not depend on the chemical composition of the system. Furthermore, the dose rates determined independently by the different methods agreed to within a 15% deviation (Section 3.2.4).

The chemical dosimetric method described in this section was simple and reproducible. The determination of power and dose rate was obtained in a matter of hours for a single assay: this includes sample preparation, irradiation, and analysis. Several samples must be analyzed at various time intervals in order to obtain an accurate determination. The only precaution that must be taken into account is to measure the amount of methane decomposed when its rate of destruction is linearly related with irradiation time; this is usually at methane conversions $\leq$50% (Figure 3.1).

3.2.2 Electric measurements of voltage and current

Asymmetrical sinusoidal signals with a frequency of 0.3 MHz were produced for both discharge voltage and current (Figure 3.2). This frequency was independent of the chemical composition and conditions of the

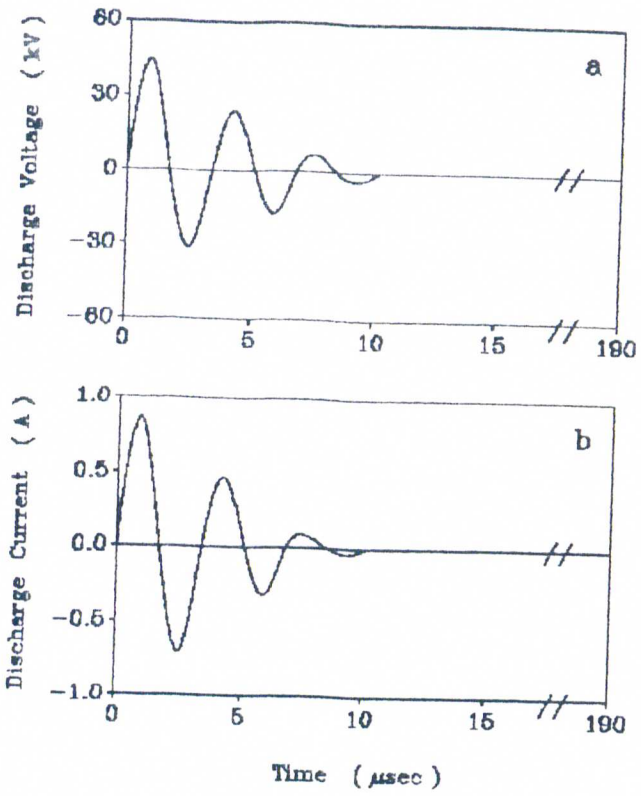

Figure 3.2. Peak-to-Peak and Zero-crossing Values taken from the Oscilloscope were plotted by smooth curve fitting to obtain the Voltage (a) and Current (b) Oscillations produced by an Electric Discharge in Air at room temperature and atmospheric pressure (1 cm gap).

system. The discharge voltage and current collapsed in about 10 μsec, and re-generated in about 190 μsec. A cluster of about 14 electric discharges were produced every 7.2 msec; the average frequency was calculated to

be 514 μsec per electric discharge.

The total voltage and current (Y) supplied by the electric discharge were calculated according to the following expression,

$$Y = \frac{A \left(\sum_{i=1}^{n} X_p i \right)}{F}$$

where, X_p is the absolute peak value of each positive and negative components during a transient discharge occurring in an interval of 10 μsec; A = 0.637, and is a conversion factor to calculate the area of a sinusoidal signal from its peak values (X_p) (Malmstadt *et al.*, 1981); and F = 514 μsec, and is the frequency of electric discharge.

The total voltage was found to depend under certain circumstances on the resistors (R) used to measure this quantity. Figure 3.3 shows the dependance of voltage on the total resistance of R_1 and R_2. At low

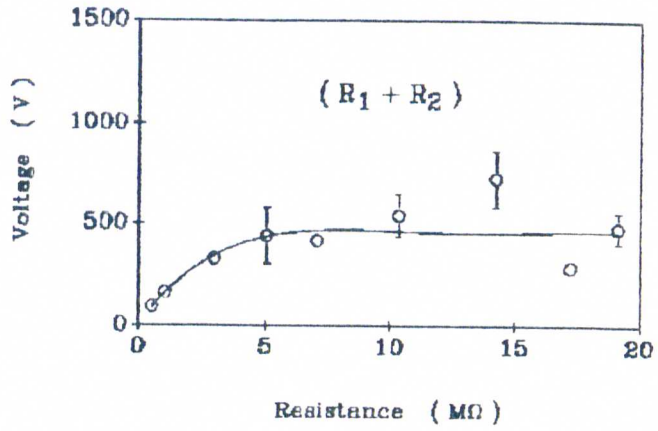

Figure 3.3. The Effect of Resistance of R_1 + R_2 on the Voltage of a 1 cm gap Electric Discharge in Air.

total resistance for R_1 and R_2, the voltage increased up to about 3 M Ω, where it reached a steady value of about 470 V (Figure 3.3). This effect was attributed to the facility by which electricity could flow more freely through the pathway containing R_1 and R_2 as the resistance on this pathway decreases (see Figure 3.4 for the electric circuit): When the resistance on such a pathway was zero, electric discharges were no longer produced.

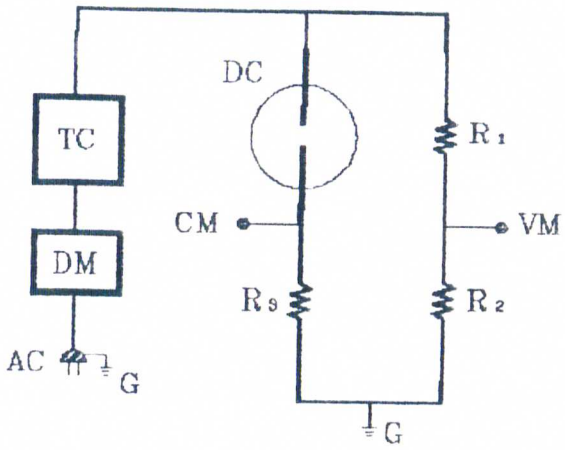

Figure 3.4. Schematic Representation of Electric Circuits for Measuring the Discharge Voltage and Current. AC: Alternating current power; CM: Current measurement; DC: Discharge chamber; DM: Digital multimeter; G: Ground; R: Resistors; TC: Tesla coil; VM: Voltage measurement. $20.0 \leq R_1 \geq 0.5$ M Ω; $10.0 \leq R_2 \geq 2.0$ k Ω; $1000 \leq R_3 \geq 50$ Ω.

The voltage measurements for dosimetry of the electric discharges were taken at high resistance for R_1 and R_2, usually above 5 M Ω, in order to minimize any interference on the electric discharge.

The current of the electric discharge was not altered by the resistance used for R_3. This is demonstrated in figure 3.5 where the current is plotted against a wide resistance range from 50 to 1000 Ω for R_3.

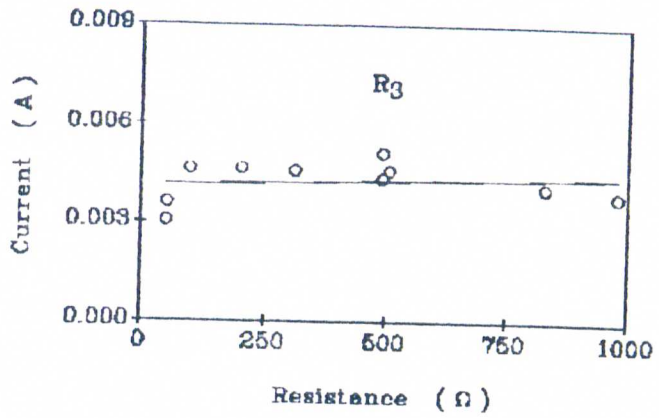

Figure 3.5. The Effect of Resistance of R_3 on the Current of a 1 cm gap Electric Discharge in Air.

Electric discharge experiments were performed at a 1 cm discharge gap; however, in order to gain insight on the effect of discharge gap size on voltage and current, we studied the electric quantities (e.g., voltage, current) as a function of discharge gap size. The total voltage increased linearly with the length of the discharge gap. Figure 3.6a shows this effect from 0 to 1 cm discharge gap; at high discharge gaps ($\geq$3 cm), electric discharges were no longer produced.

The total current of the electric discharge also increased linearly with the length of the discharge gap. This effect is shown in Figure 3.6b.

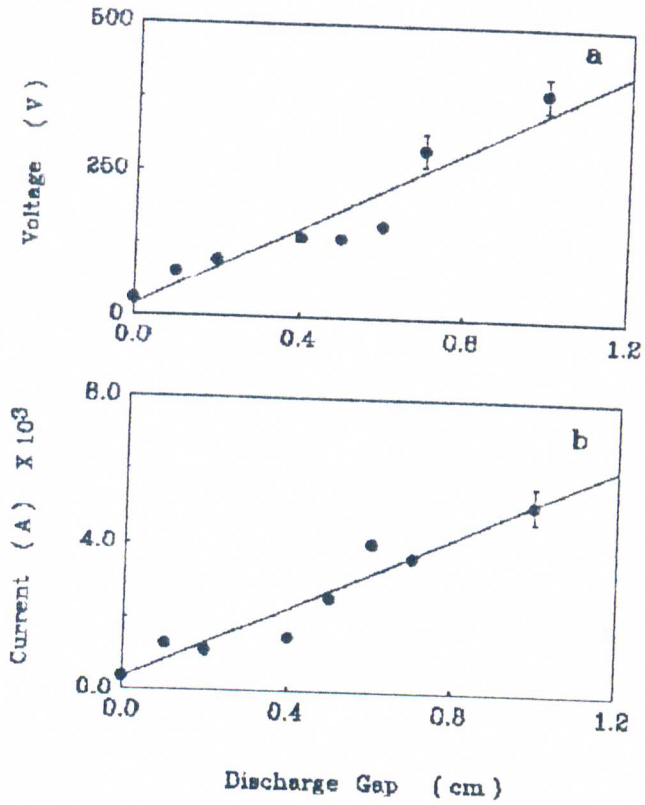

Figure 3.6. Dependence of the Voltage (a) and Current (b) with the Electric Discharge gap in a system composed of Air at Atmospheric Pressure.

The pressure dependence of voltage and current was studied in different gaseous systems: air, CH_4, and CH_4-N_2-H_2O. The electric discharges were produced with different Tesla coils and using different outputs. The experiments were performed at various discharge gaps from 0.1 to 1 cm. In order to normalize the data, the voltage and current per gap length were plotted

versus pressure (Figure 3.7). The voltage per gap length linearly increased with the total pressure of

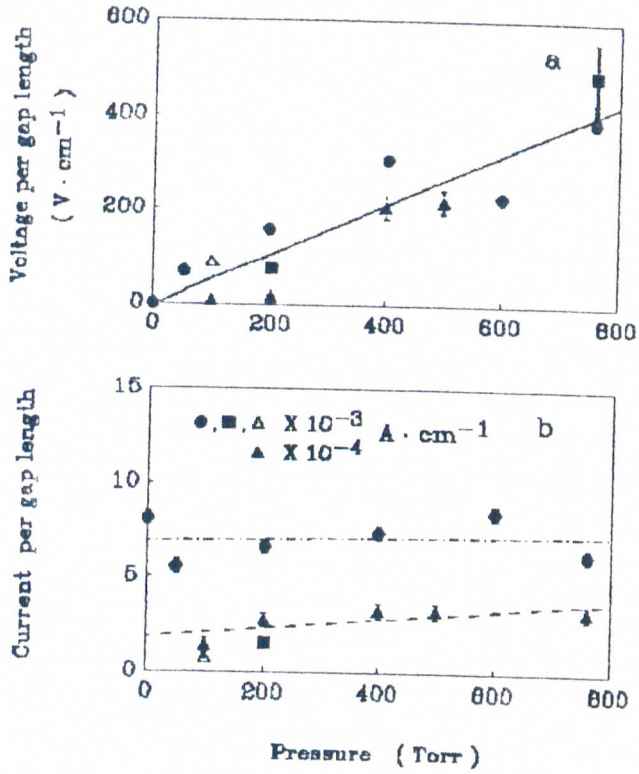

Figure 3.7. Pressure Dependence of Voltage (a) and Current (b) per Discharge Gap Length. N_2/O_2=3.7, Tesla coil (A) model BD-50, Output 8, discharge gap=0.7 cm, except at 760 Torr, where it varied from 0.1 to 1.0 cm (●); CH_4, Discharge Gap=0.7 cm, Tesla coil (B) model BD-50, output 4.5 (■); N_2/CH_4=1, Discharge gap=1 cm, Tesla coil model BD-50E, output 5.6 (▲) and Tesla coil (A) model BD-50, output 8 (△).

the system and did not depend neither on the chemical composition of the system nor on the instrument used to produce the electric discharge (Figure 3.7a). The current per gap did not depend strongly on the total pressure of the system but did depend on both the Tesla coil and the output used (Figure 3.7b). The minimum pressure plotted in Figure 3.7 corresponds to 1 Torr; however at lower pressures (≤50 mTorr), electric discharges were no longer produced.

The measurement of discharge currents and voltages was carried out in a matter of minutes and was performed routinely for each experiment. During low voltage and current measurements a noisy baseline was obtained on the oscilloscope due to reception of radio waves (around 5 MHz) produced by Tesla coils. These radio waves were visible on the oscilloscope even without direct connection to the electric circuit. In order to eliminate the effect of noisy baselines, the determinations of voltage and current were obtained with a number of resistances for Resistors 1 to 3. R_1 was usually varied from 3 to 20 M Ω; R_2 was changed from 2 to 10 k Ω; and R_3 was modified from 0.05 to 1 k Ω. The standard deviation from all of these different sets of measurements was determined to be 12%.

The power of the electric discharge was calculated by the equation, P=VI; where V and I are the total voltage and current of the electric discharge, respectively. Its value depended on the discharge gap length and the total pressure of the system and ranged from 0.01 to 2.29 W. The power of the electric discharge did not depend on the chemical composition of the system.

From the above studies, we conclude that the power of the electric discharge delivered in the electrolysis of the CH_4-N_2-H_2O mixture was 2.29 W with a deviation of 0.27 W at 60°C, 600-760 Torr, and at 1 cm discharge gap length. The dose rate was calculated to be 864 G s^{-1} or 3.11 MGy hr^{-1}. The standard deviation was determined to be within 12%.

3.2.3 Calorimetric measurements of voltage and current

The values of voltage and current were derived from the measurement of the heat dissipated from resistors 1 and 2 in an insulator box during the sparking of the electric discharge experiment (see Figure 2.5 for the experimental diagram). Figure 3.8 shows a typical experiment in which the rise of temperature was

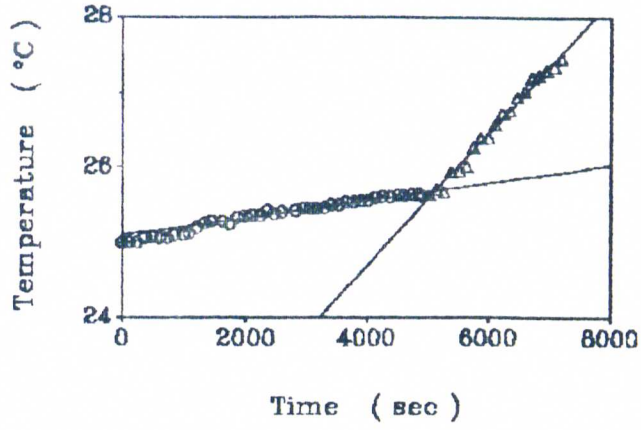

Figure 3.8. Temperature Increase as a Function of Time during the Calorimetric measurement of Voltage (O), and Voltage and Current (△) of the Electric Discharge of Air at 760 Torr and 1 cm discharge gap.
R_1 =0.5 M Ω; R_2=5 k Ω; (O) Q_1=1.16X10^{-4} °C sec^{-1}; (△) Q_{1+2}=8.87X10^{-4} °C sec^{-1}; C_p=1594.4 W sec °C^{-1}.

measured as a function of time for voltage and both voltage and current of the electric discharge. The heat (Q) dissipated from R_1 and R_1+R_2 was calculated from the slopes (m) of the curves (Figure 3.8) and from the heat capacity (Cp) of the calorimeter: Q = Cp m.

The heat released by R_1 was unmeasurable at resistances of $\geq$1 M Ω, and only resistances of $\leq$0.5 M Ω could be used to accurately determine the heat dissipated. The voltage of the electric discharge was

determined using resistors from 0.5 M Ω to 0.02 M Ω without affecting its value. In the previous section, it was shown that at low resistances for R_1 and R_2, the voltage of the electric discharge is diminished (Figure 3.3), and consequently less current flows through the electric discharge pathway and more through that containing R_1 and R_2. In spite of this alteration, the total amount of electricity that flows in both pathways was constant (see Figure 2.5 for the electric diagram). This conclusion was reached after determining that the total consumption of electricity by the Tesla coil was unaffected by connecting R_1 and R_2 to the electric discharge. Because of this effect, the voltage and current were simultaneously determined by measuring the heat dissipated by R_1 and R_2 in order to quantify the total amount of electricity that flow in both pathways. Independently, the voltage was also measured to be able to solve for the value of current from the previous determination. The resistance of R_2 was adjusted to 5 k Ω and was not varied since the current of the electric discharge was not interfered by the value used for R_2 (see Figure 3.5).

The power of the electric discharge experiments was determined to be 2.07 W at 60°C, 600-760 Torr, and an 1 cm discharge gap length. It was found to indepen-

dent of the chemical composition of the system used. The dose rate was determined to be 781 Gy s^{-1} or 2.81 MGy hr^{-1}. The standard deviation was calculated to be 26%.

The dosimetry of an electric discharge experiment by this method was simple and could be accomplished in a relatively short period of time, about 6 hrs. The only inconvenience was to determine the appropriate resistance of R_1 in order to obtain a measurable heat dissipation rate; this was about $\leq$0.5 M Ω at 1 cm discharge gap and 760 Torr of total pressure for the system.

3.2.4 Comparison of the different methods

The three methods described above (sections 3.2.1 to 3.2.3) were effective in determining the dose rates of the electric discharge experiments. The dose rate vary from 2.28 MGy hr^{-1} (using the chemical dosimeter) to 2.81 MGy hr^{-1} (calorimetric measurements of V and I) or 3.11 MGy hr^{-1} (electric measurements of V and I), and in all cases was independent of the chemical composition of the system. The average dose rate was determined to be 2.73 MGy hr^{-1}. The standard deviation

among the three different methods was reasonable, 15%. This value is to be contrasted to a 50% deviation obtained by Stribling and Miller (1987) using a different approach to determine the energy introduced by electric discharges.

The method suggested by Stribling and Miller (1987) consists of determining the power of the electric discharge by measuring the heat evolved during the sparking of the electric discharge sample (Stribling and Miller, 1987). We have already discussed that this approach underestimates the amount of energy supplied by the electric discharge since it does not taken into account the energy converted into chemical form, light and that not absorbed (see section 1.2.3). In order to experimentally demonstrate the weakness of such a method, we also determined the power in our electric discharge experiments according to their method (see page 72 for experimental conditions).

Figure 3.9 shows the temperature increase as a function of time during the sparking of an electric discharge experiment. The power (P) of the electric discharge was calculated from the slope of the curve (m) and the heat capacity of the calorimeter (Cp): $P = Cp\ m$. The average value of P was 0.37 W with a

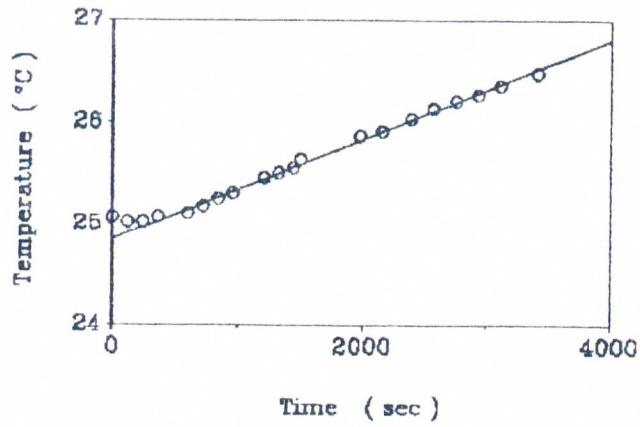

Figure 3.9. Temperature Increase as a Function of Time during the Measurement of Power of a 1 cm Electric Discharge in air at 760 Torr. $m=4.89X10^{-4}$ °C sec^{-1}; $C_p=1594.4$ W sec $°C^{-1}$.

standard deviation of 10%. The dose rate was determined to be 140 Gy s^{-1} or 0.50 MGy hr^{-1}. Therefore, the method of Stribling and Miller underestimates the dose rate by about a factor of 5.

3.3.4 Evaluation of the dosimetry of electric discharges

Electric discharges have been extensively used to induce abiotic syntheses in the last forty years (see for instance, Fox and Dose, 1977). The measurement of the amount of energy supplied from the electric dis-

charges has been usually neglected mainly because of the difficulty of determining such a parameter, and only recently have there been attempts to estimate this quantity by Navarro-González *et al.* (1986) and Stribling and Miller (1986, 1987). However, this is the first study in which the dose rate of abiotic discharge experiments is comprehensively investigated.

The average dose rate of our electric discharge experiments was determined to be 2.73 MGy hr^{-1} at a 1 cm gap electric discharge and 600 Torr of pressure. This value depends on the discharge gap length and the total pressure but does not depend on the chemical composition of the system.

Knowledge of the dose rate of electric discharge experiments is important because it allows to determine the dose absorbed in the experiments and to calculate the chemical yields of the products. Furthermore, it permits direct comparison with other energy sources in order to contrast the relative contributions that they may have played in the syntheses of organic compounds in the primitive Earth. The next sections on this chapter demonstrate the accomplishments that are obtained by knowing the dose rate of electric discharge experiments.

3.3 Electrolysis of gas mixture

The electrolysis of a 4.2 dm^3 gaseous mixture at 60°C and 600 Torr composed of 0.0108 mole dm^{-3} of methane, 0.0108 mole dm^{-3} of nitrogen, and 0.00782 mole dm^{-3} of water vapor in equilibrium with a liquid phase of 0.1 dm^3 of 0.5 mole dm^{-3} aqueous ammonium chloride buffer at pH 8.7, was investigated in the dose range from 0.38 to 152.30 MGy.

3.3.1 General

Decomposition of initial gases. Methane and nitrogen were identified and quantified in the electrolyzed samples and blanks by mass spectrometry. Figure 3.10 shows the decomposition of methane as a function of dose. The concentration[1] of methane linearly decreased with dose up to about 20 MGy and then decreased steadily up to about 150 MGy; less than 6% of the initial methane remained in the dose range from 80 to 150

---

[1] The concentrations of solutes and/or products are given in terms of moles per dm^{-3} of gas phase.

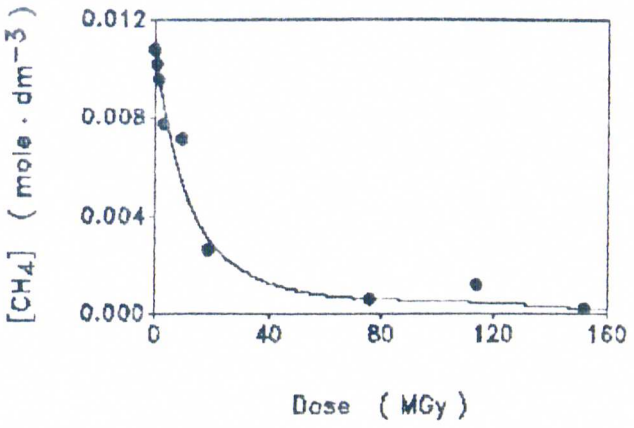

Figure 3.10. Dose Dependance of the Decomposition of Methane in the High Voltage Electric Discharge of CH_4-N_2-H_2O.

MGy. The initial chemical yield[2] ($G°$) of the decomposition of methane was determined to be:

$G°$ ($-CH_4$)=6.54.

The decomposition of nitrogen as a function of dose is shown in Figure 3.11. The concentration of nitrogen linearly decreased with increasing dose up to about 40 MGy, where it reached a steady value of about 0.0081 mole dm^{-3} in the dose range from 40 to 150 MGy. The chemical yield of decomposition of nitrogen was

---

[2]The chemical yield ($G°$), number of molecules formed or destroyed per 100 eV absorbed, is calculated from the slope of a dose versus dose curve , e.g. as Figure 3.10.

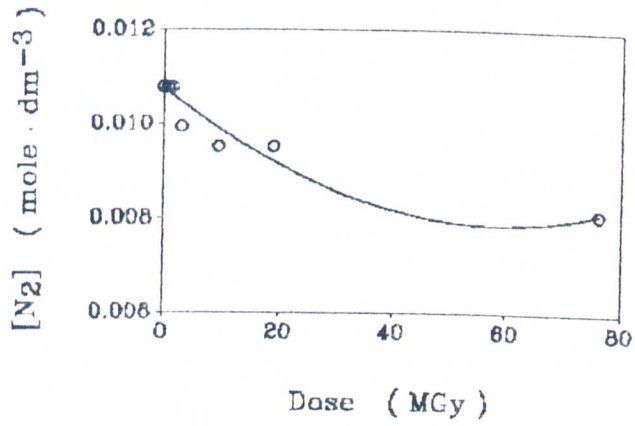

Figure 3.11. Dose Dependance of the Decomposition of Nitrogen in the High Voltage Electric Discharge of $CH_4-N_2-H_2O$.

determined to be: $G^{\circ}(-N_2) = 1.26$.

Nitrogen was quite stable to electrolysis; its decomposition occurred only in the dose range where a significant amount of the original methane remained in the system down to about 20% of CH_4. This suggests that the channel of decomposition of nitrogen depends on methane and/or a transient chemical species formed in the decomposition of methane during the bombardment of electrons into the system.

Formation of hydrogen cyanide. HCN was identified and quantified by its titration with silver nitrate and

with a selective cyanide electrode. Its concentration increased linearly at low dose and then steadily above 30 MGy (Figure 3.12); its chemical yield of formation was determined to be: G° (HCN)=0.26. About 10% of the initial methane or nitrogen was converted into HCN at 150 KGy.

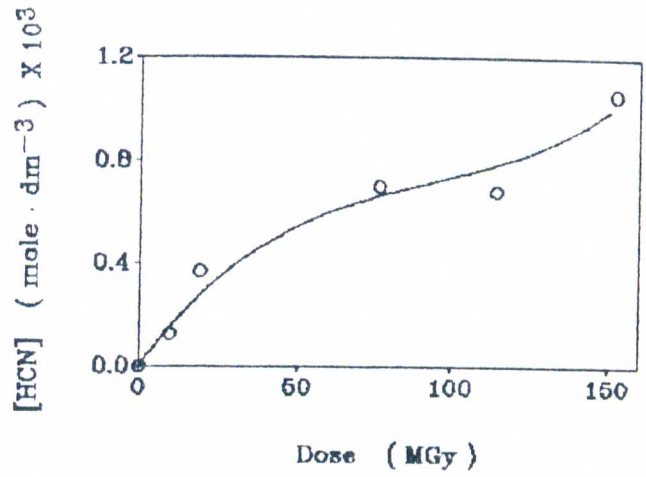

Figure 3.12. The Effect of Dose on the Synthesis of Hydrogen Cyanide in the Electric Discharge of CH_4-N_2-H_2O.

In order to get a better insight into the chemical mechanism of formation of HCN during the electrolysis of the simulated atmosphere, other initial products

such as hydrocarbons and aldehydes were also investigated.

Formation of hydrocarbons. C_2H_2 and C_2H_6 were identified and quantified in the experiments by mass spectrometry; however, C_2H_4 could not be quantified because its molecular ion ($C_2H_4^+$, 28) and the predominant fragment ($C_2H_3^+$, 27) formed in the mass spectrometry analysis overlapped with those of ethane and also nitrogen (N_2^+, 28); the latter were extremely abundant.

Figure 3.13 shows the formation of C_2H_2 and C_2H_6 as a function of dose. At low doses, their concentrations linearly increased with dose up to a maximum located at about 30 MGy; these maxima also coincided with the maximum decomposition of methane (Figure 3.10). C_2H_2 was the most abundant hydrocarbon, and its chemical yield of formation was determined to be: G° (C_2H_2)=2.14. C_2H_6 was formed with a smaller chemical yield: G° (C_2H_6)= 0.57. The concentrations of C_2H_2 and C_2H_6 decreased rapidly with increasing dose starting after about 50 MGy.

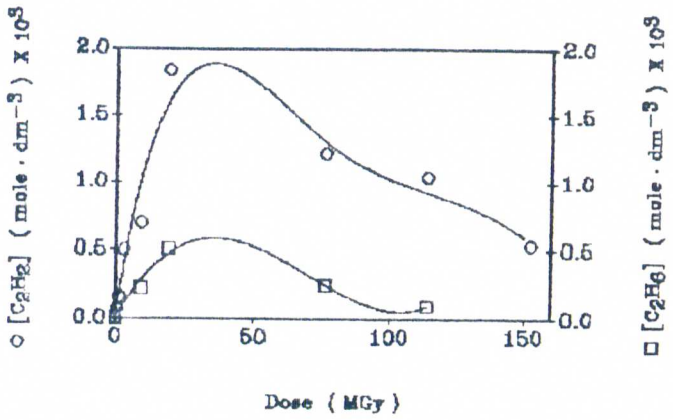

Figure 3.13. The Effect of Dose on the Formation of C_2H_2 and C_2H_6 in the High Voltage Electric Discharge of $CH_4-N_2-H_2O$.

Formation of aldehydes. Figures 3.14 and 3.15 show a gas-chromatogram and mass spectra, respectively, of aldehyde products that were derivatized *via* 2,4-dinitrophenyl-hydrazine (DNP) into 2,4-dinitrophenyl-hydrazones (DNPH) derivatives. Acetaldehyde, propionaldehyde and butyraldehyde were identified by gas chromatography based on their retention times and coinjections with standard DNPH derivatives; additional evidence was provided by detection of the mass ions and the mass ions plus one in the electron impact and chemical ionization mass spectrometric analyses, respectively (see Figure 3.15).

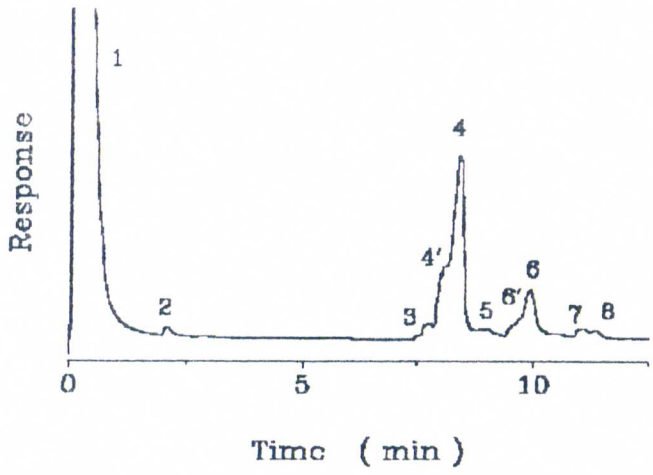

Figure 3.14. Gas Chromatogram of DNPH Derivatives of Aldehydes Formed at 6.35 MGy. 1. Solvent (CH_2Cl_2); 2. DNP; 3. Formaldehyde; 4. Acetaldehyde; 5. Propionaldehyde; 6. butyraldehyde; 7 and 8. Unknowns. 4' and 6' are syn isomers.

A peak (3) in the gas chromatographic analysis of DNPH derivatives at high doses, $\geq$1.59 MGy, (Figure 3.14) was resolved with a retention time corresponding to that of formaldehyde; coinjection of the electric discharge sample with a standard solution of formaldehyde-DNPH resulted in an increment of the area under peak 3. The electron impact mass spectrum of this fraction (Figure 3.15a) demonstrated the presence of a low abundance, $\approx$1%, mass fragment, 210 m/e, that could originate from formaldehyde-DNPH (M.W. 210); however, the mass ion plus one was not produced by chemical ionization mass spectrometry under similar conditions

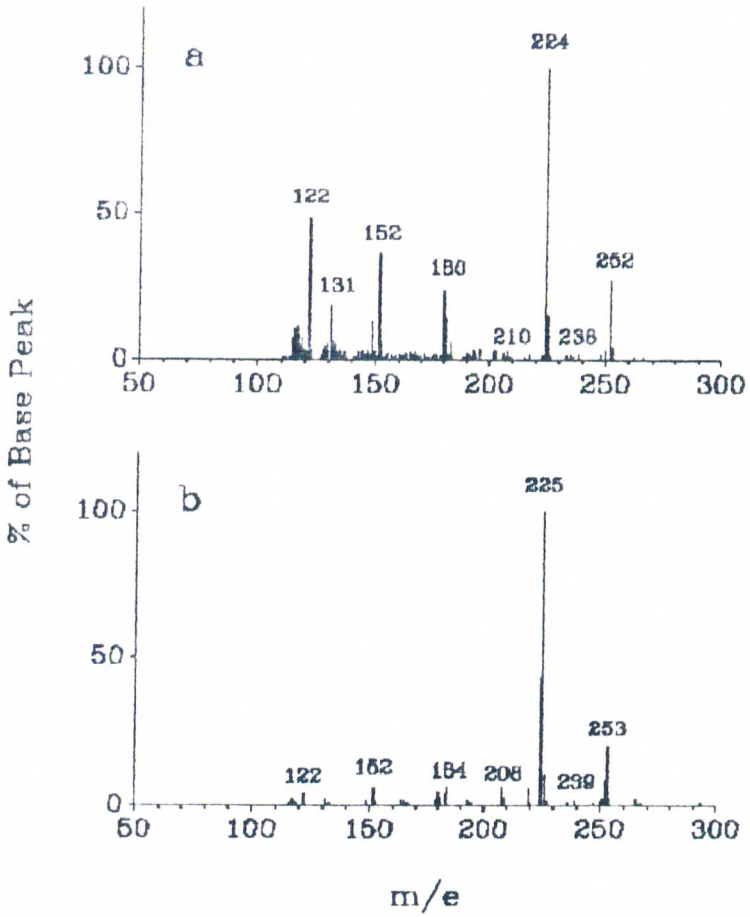

Figure 3.15. Mass Spectra of DNPH Derivatives Formed at 1.59 MGy. Electron impact mass spectrum (a). Mass ions: Acetaldehyde (224); propionaldehyde (238), and butyraldehyde (252). Chemical ionization mass spectrum (b). Mass ions plus one: Acetaldehyde (225), propionaldehyde (239), and butyraldehyde (253).

(Figure 3.15b). The identification of formaldehyde is, therefore tentative at the present time; further work needs to be done at high doses in order to obtain a higher amount of sample for its analysis and subsequent

identification. The concentration of formaldehyde was estimated to be $\leq 1.05X10^{-6}$ mole dm^{-3} at 6.35 MGy; the derived chemical yield was calculated to be: G° (HCHO)$\leq$ 0.00264.

Other peaks (7, and 8) in the gas chromatographic analysis of DNPH derivatives were not identified (Figure 3.14). They were only present at the highest dose (6.35 MGy) analyzed for this type of compounds.

Figure 3.16 shows the formation of acetaldehyde, propionaldehyde, and butyraldehyde as a function of dose. Their concentrations increased linearly with dose up to about 1.6 MGy, and then reached a steady value (for propionaldehyde) or decreased (for acetaldehyde and butyraldehyde). Their chemical yields were determined to be: G° (CH_3CHO)=0.13; G° (CH_3CH_2CHO)= 0.011; and G° ($CH_3CH_2CH_2CHO$)=0.016.

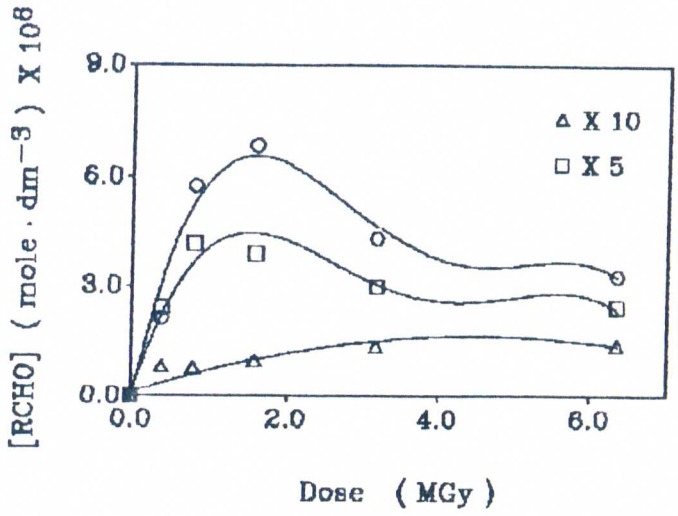

Figure 3.16. Dose Dependance of the Formation of Aldehydes in the Electric Discharge of CH_4-N_2-H_2O: Acetaldehyde (O); Propionaldehyde (△); and butyraldehyde (□).

Formation of oligomeric material. A water-insoluble material deposited on the walls of the flask during the electrolysis of the gas sample. The material was analyzed for H, C, and N content in order to evaluate its yield of formation and to perform a material balance of major products from the electric discharge experiments. Figure 3.17 shows the formation of such a material as a function of dose. Its abundance linearly increased with dose; its rate of formation was calculated to be $2.72X10^{-2}$ gr dm^{-3} MGy^{-1}, and was

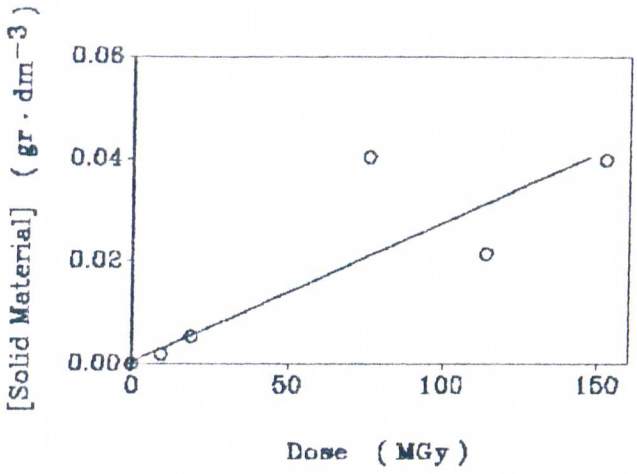

Figure 3.17. Effect of Dose on the Formation of Solid Material in the Electric Discharge of CH_4-N_2-H_2O.

calculated from the slope of the curve given in Figure 3.17.

Figure 3.18 shows the chemical yields of this water-insoluble material in terms of carbon, hydrogen, nitrogen, oxygen, and chloride as calculated from elemental analysis obtained at various doses. The chemical yields for this material were calculated from extrapolation to infinitesimal conversion and were

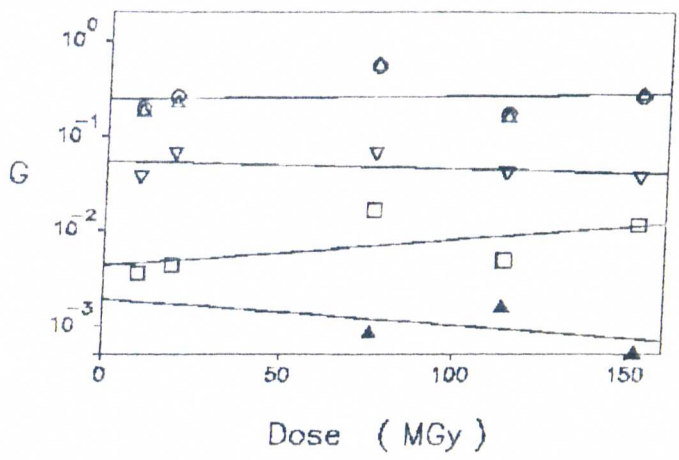

Figure 3.18. Dose Dependance of the Chemical Yield of Solid Material in terms Carbon (O), Hydrogen (△), Nitrogen (□), Oxygen (▽) and Chloride (▲).

determined to be: G° (H, C)=0.25; G° (N)=0.042; G° (O)=0.054; and G° (Cl)=0.0019.

The functional groupings of the oligomeric material were not investigated. The empirical formula was calculated to be: $C_{128}H_{128}O_{28}N_2Cl$. The main atomic constituents were carbon and hydrogen at one to one ratio. The primary interest in the quantitative analysis of this material was exclusively to obtain a balance for the products as completely as possible.

Material balance. Table 3.1 summarizes the initial chemical yields ($G°$) for the analyzed products in the electric discharge experiments. Acetylene and ethylene were the most abundant products, followed by the oligomeric material, acetaldehyde, hydrogen cyanide, butyraldehyde, and finally propionaldehyde. In order to maintain a material balance, the chemical yield(s) of decomposition of solute(s) must equal to the chemical yields of identified and unknown products. For the

Table 3.1. Initial chemical yields ($G°$) in the electrolysis of gaseous CH_4–N_2–H_2O.

Compound	$G°$
$-CH_4$	6.54
$-N_2$	1.26
C_2H_2	2.14
C_2H_6	0.57
HCN	0.26
CH_3CHO	0.13
CH_3CH_2CHO	0.011
$CH_3(CH_2)_2CHO$	0.016
Solid Material:	
C	0.25
H	0.25
O	0.054
N	0.0042
Cl	0.0019

*gr dm^{-3} MGy^{-1}.

case of carbon, the following expression is derived:

$$G^{\circ}(-CH_4) = 2G^{\circ}(C_2H_2) + 2G^{\circ}(C_2H_6) + G^{\circ}(HCN) + 2G^{\circ}(CH_3CHO) + 3G^{\circ}(CH_3CH_2CHO) + 4G^{\circ}(CH_3(CH_2)_2CHO) + G^{\circ}(\text{Solid material}) + G^{\circ}(\text{Unknown products});$$

where, $6.54 \approx 6.29 + G^{\circ}$ (Unknown products); G° (Unknown carbon containing products) ≈ 0.25. The identified products represent approximately 96% of the initial carbon-containing products in the electrolysis of the CH_4-N_2-H_2O mixture.

For case of nitrogen, HCN and the oligomeric material were the only nitrogen-products identified, and the following expression is obtained:

$$2G^{\circ}(-N_2) = G^{\circ}(HCN) + G^{\circ}(\text{Solid material}) + G^{\circ}(\text{Unknown products});$$

where, $2.52 = 0.26 + G^{\circ}$ (Unknown products); therefore, G° (Unknown products) = 2.26.

These calculations indicate that about 96% of the total methane and 10% of the total nitrogen were converted into the identified products in the early stages of electrolysis of the gas mixture. A number of other

products are also formed in the experiments such as amino acids (Kobayashi and Ponnamperuma, 1985); however, they are formed through secondary reactions involving the primary products, e.g., C_2H_2, C_2H_6, CH_3CHO, HCN, etc.

The results presented in this section enable us to infer possible reaction schemes that may operate in the electrolysis of a CH_4-N_2-H_2O mixture. The next section deals with this topic.

3.3.2. Reaction mechanism

A possible reaction mechanism was developed to account for the observed chemical changes described in the previous section. The reaction mechanism was tested by computer simulation using *ACUCHEM* (see Chapter 2, section 2.8) to evaluate its potential to explain the early stages of electrolysis of a CH_4-N_2-H_2O mixture.

During the irradiation of the gas mixture, the electrons from the electric discharge interact with gas molecules producing excited gas molecules (Reactions 3.1 to 3.3) (Bossard *et al.*, 1983). The probabilities

of interaction depend on the concentration of each gas in the mixture, and are 37.5% for either methane and nitrogen, and 25% for water vapor (denoted by H_2O).

$$CH_4 \xrightarrow{e} CH_4^* \qquad (3.1)$$

$$N2 \xrightarrow{e} N_2^* \qquad (3.2)$$

$$H_2O \xrightarrow{e} H_2O^* \qquad (3.3)$$

The excited molecules produced in reactions 3.1 to 3.3 may undergo dissociation producing free radicals. Excited water molecules (H_2O^*) dissociate producing hydrogen atoms ($H\cdot$) and hydroxyl radicals ($HO\cdot$) (Reaction 3.4) (Spinks and Woods, 1976; Mourey *et al.*, 1981). Excited methane could dissociate producing $CH_3\cdot$, $:CH_2$ and $:CH\cdot$ radicals, reaction 3.5 (Slager and Black, 1982; Bossard *et al.*, 1983). Computer fitting of the experimental data suggests that channel 3.5a is the major dissociation reaction accounting for 87.5%; whereas channel 3.5b and c were less important.

$$H_2O^* \longrightarrow H\cdot + HO\cdot \qquad (3.4)$$

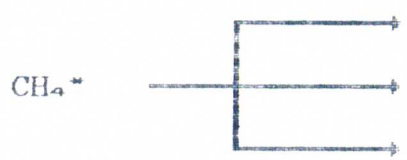

$$CH_4^{*} \longrightarrow CH_3\cdot + H\cdot \quad (87.5\%) \quad (3.5a)$$

$$CH_4^{*} \longrightarrow :CH_2 + 2H\cdot \quad (11.0\%) \quad (3.5b)$$

$$CH_4^{*} \longrightarrow :CH\cdot + 3H\cdot \quad (1.5\%) \quad (3.5c)$$

Nitrogen molecules were found to be stable to electrolysis in a CH_4-N_2-H_2O mixture, and only a small percentage of the nitrogen decomposed in the early stages of electrolysis, reaction 3.6a. Computer simulation suggests that channels 3.6a and b represent 0.25% and 99.75%, respectively.

$$N_2^{*} \longrightarrow \cdot N: + \cdot N: \quad (0.25\%) \quad (3.6a)$$

$$N_2^{*} \longrightarrow N_2 + h\nu \quad (99.75\%) \quad (3.6b)$$

Computer fitting of the reaction mechanism (reactions 3.1 to 3.30) with the experimental results of decomposition of CH_4 and formation of C_2H_2, C_2H_6, HCN, and C_2H_4, indicate that the rate of production of electrons (e) in the electric discharge was $7.95X10^{-3}$ electrons MGy^{-1}, and its yield was calculated to be G° (e)= 121.5. Table 3.2 summarizes the predicted radical and molecular yields of primary species obtained by

Table 3.2. Predicted radical (R) and molecular (M) yields ($G_{R/M}$) in the electrolysis of CH_4-N_2-H_2O.

Species	$G_{R/M}$
CH_3·	26.42
:CH_2	3.32
:CH·	0.45
H·	70.76
HO·	36.34
·N:	0.27
$-CH_4$	30.20
$-N_2$	0.14
$-H_2O$	36.34

simulation of the electrolysis of CH_4-N_2-H_2O. CH_3·, H·, and HO· are the major radicals, and :CH_2, :CH· and ·N: are produced in low yield. Supporting evidence for the formation of CH_3·, :CH_2, :CH·, H_2 and H· is provided by their spectroscopic identification in the electric discharge of gaseous methane (Peters and Wagner, 1931; Harkins and Jackson, 1933; Willey, 1934).

Water vapor was constantly produced during the experiments by maintaining the aqueous phase at 60°C. The vapor pressure of water was 149.38 Torr at 60°C (Weast *et al.*, 1985). The equilibrium reaction of

liquid water (denoted by H_2O (l)) going into water vapor is given by reaction 3.7; the equilibrium constant was calculated to be $1.3X10^{-4}$, taking into account the concentration of water vapor and liquid water.

$$H_2O\ (l) \rightleftharpoons H_2O \qquad (3.7)$$

An additional source of water vapor was its reformation from the reactions of hydroxyl radicals with hydrogen atoms (reactions 3.8 and 3.9). The rate constant for reaction 3.8 is $2.2X10^{16}\ T^{-2}\ dm^6\ mole^{-2}\ s^{-1}$ (Tsang and Hampson, 1986), while that for reaction 3.9 is $1.5X10^{19}\ T^{-2.6}\ dm^6\ mole^{-2}\ s^{-1}$ (Wilson, 1972).

$$H\cdot + HO\cdot + N_2 \longrightarrow H_2O + N_2 \qquad (3.8)$$

$$H\cdot + HO\cdot + H_2O \longrightarrow H_2O + H_2O \qquad (3.9)$$

In addition to the formation of water molecules, hydroxyl radicals could dimerize producing hydrogen peroxide (reaction 3.10); the rate constant for such a reaction is $2.4X10^{11}\ (T/300)^{-0.7}\ dm^6\ mole^{-2}\ s^{-1}$ (Baulch, *et al.*, 1982).

$$HO\cdot + HO\cdot + N_2 \longrightarrow H_2O_2 + N_2 \qquad (3.10)$$

Molecular hydrogen was not examined in this work, but supporting evidence for its formation was provided by the studies of Wiener and Burton (1953), Toupance *et al.* (1975), and Bossard *et al.* (1983) on the electrolysis of methane and/or methane-nitrogen mixtures. Formation of molecular hydrogen is predicted by dimerization of hydrogen atoms, reactions 3.11 to 3.12; the rate constants are $5.4X10^{12}\ T^{-1.3}\ dm^6\ mole^{-2}\ s^{-1}$ (Cohen and Westberg, 1983; Tsang and Hampson, 1986), and $1.0X10^{13}\ T^{-1}\ dm^6\ mole^{-2}\ s^{-1}$ (Cohen and Westberg, 1983), respectively.

$$H\cdot + H\cdot + N_2 \longrightarrow H_2 + N_2 \qquad (3.11)$$

$$H\cdot + H\cdot + H_2O \longrightarrow H_2 + H_2O \qquad (3.12)$$

Methane molecules were re-formed in the electric discharge according to reaction 3.13; the rate constant for such a reaction is $1.2X10^{12}\ T^{-0.4}\ dm^3\ mole^{-1}\ s^{-1}$ (Tsang and Hampson, 1986).

$$CH_3\cdot + H\cdot \longrightarrow CH_4 \qquad (3.13)$$

Methyl radicals may also dimerize leading to the formation of ethane, reaction 3.14; the rate constant

for this reaction is $1.0X10^{12}\ T^{-0.64}$ $dm^3\ mole^{-1}\ s^{-1}$ (Tsang and Hampson, 1986). A minor loss of methyl radicals may be attributed to its reaction with methylene radicals which could lead to the formation of ethylene, reaction 3.15; the rate constant of such a reaction is $4.2X10^{10}$ $dm^3\ mole^{-1}\ s^{-1}$ (Tsang and Hampson, 1986).

$$CH_3\cdot + CH_3\cdot \longrightarrow C_2H_6 \qquad (3.14)$$

$$CH_3\cdot + :CH_2 \longrightarrow C_2H_4 + H\cdot \qquad (3.15)$$

Acetylene may be formed by collision of two CH_2 radicals, reaction 3.16 (Weiner and Burton, 1953); this reaction has a rate constant of $3.2X10^{10}$ $dm^3\ mole^{-1}\ s^{-1}$ (Tsang and Hampson, 1986). Acetylene may also be formed by dimerization of two CH radicals, reaction 3.17 (Braun *et al.*, 1967). The rate constant for such a reaction is $1.2X10^{11}$ $dm^3\ mole^{-1}\ s^{-1}$ (Braun *et al.*, 1967). An additional source for CH radicals could be attributed to the reaction of hydrogen atoms with methylene radicals, reaction 3.18; the rate constant for this reaction is $1.6X10^{11}$ $dm^3\ mole^{-1}\ s^{-1}$ (Tsang and Hampson, 1986).

$$:CH_2 + :CH_2 \longrightarrow C_2H_2 + H_2 \quad (3.16)$$

$$:CH^{\cdot} + :CH^{\cdot} \longrightarrow C_2H_2 \quad (3.17)$$

$$:CH_2 + H^{\cdot} \longrightarrow :CH^{\cdot} + H_2 \quad (3.18)$$

Formation of hydrogen cyanide may be explained by the reaction of CH_3 and CH_2 radicals with atomic nitrogen, reactions 3.19 and 3.20, respectively (Bossard *et al.*, 1983). The rate constants for these reactions have been estimated by Yung *et al.* (1984) to be $3.0X10^{10}$ exp(-250/T) dm^3 $mole^{-1}$ s^{-1} (13).

$$CH_3^{\cdot} + {\cdot}N: \longrightarrow HCN + H_2 \quad (3.19)$$

$$:CH_2 + {\cdot}N: \longrightarrow HCN + H^{\cdot} \quad (3.20)$$

Nitrogen atoms may also dimerize to form molecular nitrogen, reaction 3.21; the rate constant for such a reaction has not yet been determined; however, it can be estimated by analogy to the dimerization of atomic oxygen (reaction 3.22), for which a rate constant has been determined to be: $1.9X10^7$ exp(900/T) dm^6 $mole^{-2}$ s^{-1} (Tsang and Hampson, 1986).

$$2\ {\cdot}N: + N_2 \longrightarrow N_2 + N_2 \quad (3.21)$$

$$2\ {\cdot}O^{\cdot} + N_2 \longrightarrow O_2 + N_2 \quad (3.22)$$

Reactions 3.1 to 3.22 were used to model the electrolysis of a CH_4-N_2-H_2O mixture. Figure 3.19 shows the computed trends of decomposition of CH_4 and N_2, and the formation of H_2, C_2H_2, C_2H_6, C_2H_4 and HCN in the electrolysis of the CH_4-N_2-H_2O mixture. The behavior predicted by computer simulation is essentially similar to that found experimentally (see Figure 3.19). At doses above 30 MGy the computed tendencies deviate from the experimental trends mainly because the accumulation products and decomposition of the initial products complicates the reaction mechanism, and computer simulations cannot be done with existing experimental data for doses larger than 30 MGy.

Computer simulation enable us to predict the chemical yield of formation of HCN under a variety of conditions that were not experimentally examined. Figure 3.20a shows the computer trend (solid line) for G° (HCN) as a function of the molar ratio for nitrogen, $nN_2 / (nCH_4 + nN_2)$. G° (HCN) increases linearly with increasing nitrogen content in the mixture, up to a maximum, and then sharply decreases down to zero when

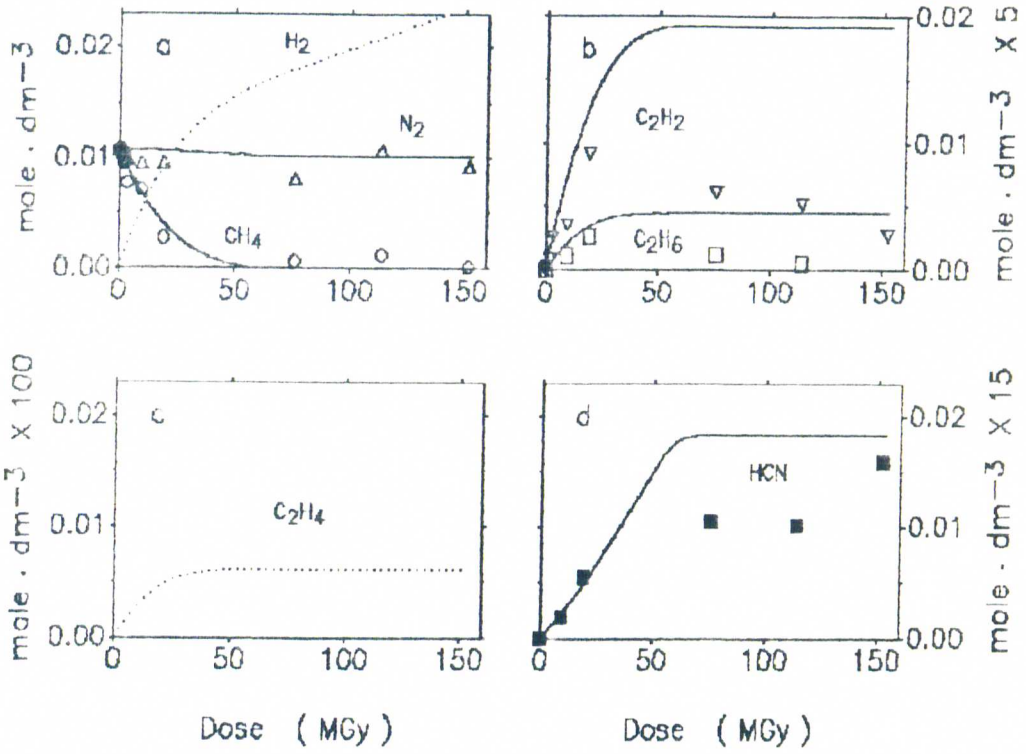

Figure 3.19. Computer Simulations of the Electrolysis of a CH_4-N_2-H_2O Mixture. Solid lines were obtained by *ACUCHEM* using reactions 3.1 to 3.22, and were plotted with experimental values (symbols) for comparison. Dotted lines are simulations of un-analyzed products.

no methane is present. Experimental support for such a trend was obtained by Raulin *et al.* (1982) who investigated the effect of initial nitrogen on the electrosynthesis of HCN. Their data (symbols) has been plotted in Figure 3.20a for comparison, and as can be seen, there is a very good correlation between computed trends and experimental results.

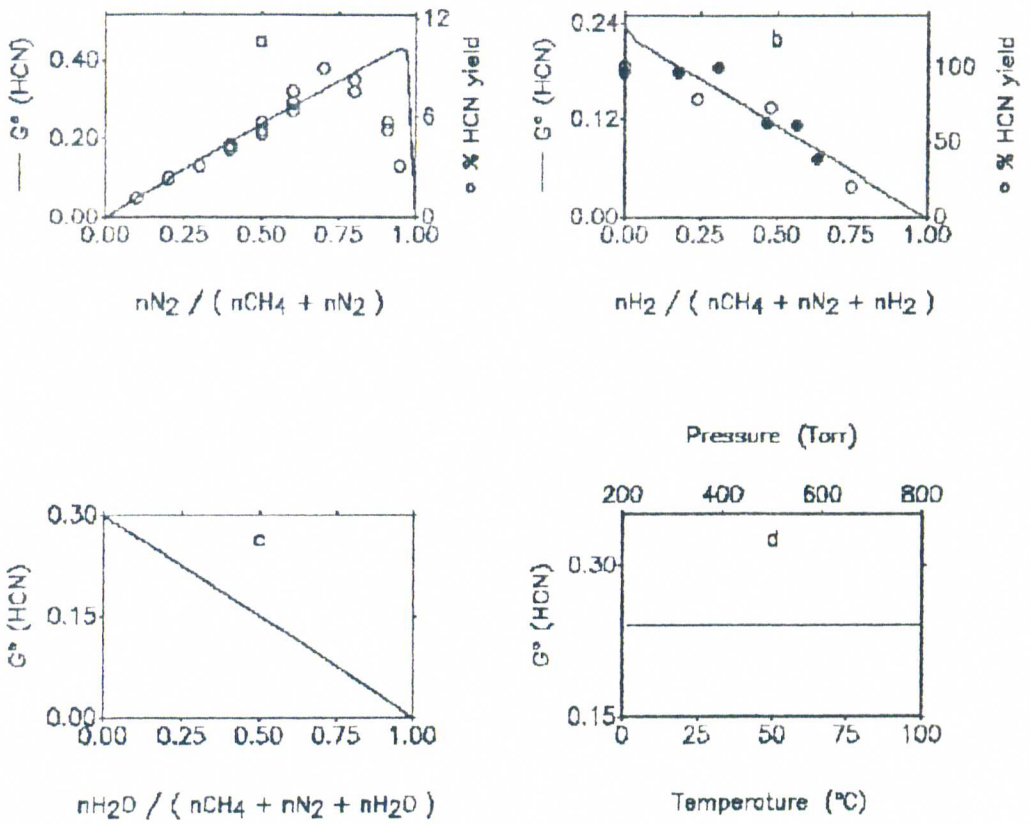

Figure 3.20. Computer Simulations of the Effect of $G°$ (HCN) on the molar ratio of Nitrogen (a), Hydrogen (b), Water vapor (c), and also as a function of Pressure and Temperature (d) during the Electrolysis of a CH_4-N_2-H_2O mixture. Lines were obtained by *ACUCHEM* using reactions 3.1 to 3.22 (a, c, d) or to 3.23 (b) and were plotted with published values for comparison: (O) Raulin *et al.* (1982); and (●) Stribling and Miller (1987). The total concentration of gas phase molecules was $2.879X10^{-2}$ mole dm^{-3} except in (d) where it was changed accordingly to the pressure change. The concentration of water vapor was kept constant in all cases ($7.19X10^{-3}$ mole dm^{-3}) except in (c) where it was varied from 0 to $2.879X10^{-2}$ mole dm^{-3}. CH_4 and N_2 were present in one-to-one ratio, except in (a) where it varied from 0 to 1.

Raulin *et al*. (1982) and Stribling and Miller (1987) have investigated the effect of added hydrogen on the synthesis of HCN. Computer simulations can also predict the trend of G° HCN as a function of the molar ratio for H_2, but it is necessary to include reaction 3.23 to account for the electric discharge dissociation of molecular hydrogen into atomic hydrogen. Figure 3.20b shows the computer trend (solid line) and experimental behavior (symbols) as a function of the molar ratio for hydrogen. G° (HCN) is maximum in the absence of hydrogen; the yield decreases linearly with increasing hydrogen content, down to zero in the absence of either CH_4 and N_2. A similar behavior as for hydrogen, is also predicted as a function of water vapor in the mixture (see Figure 3.20c).

$$H_2 \xrightarrow{e} H_2^* \longrightarrow H^- + H^- \qquad (3.23)$$

The total pressure and/or the temperature of the gas phase does not have any effect on the yield of HCN as predicted by computer simulation (see Figure 3.20d). Therefore, G° (HCN) depends only on the composition of the gas mixture.

The results presented in this section may be used to predict the possible production of HCN by electric discharges in the primitive atmosphere; this is considered in the next section.

3.3.3. HCN synthesis in primitive atmospheres

Atmospheric electricity is a poorly understood subject, and no estimates of the energy available from this source on the primitive Earth have been made (Fox and Dose, 1977). Cloud electrification is a common phenomenon in the atmosphere (Weast, et al., 1986). The processes by which the charges in a cloud are formed and separated are still controversial (Bar-Nun, 1981). The most common forms of neutralization of the charges are by intracloud and cloud-to-ground discharges; the former is more abundant by a factor of about 5 than the latter (Bar-Nun, 1981).

It has been calculated that the flux of lightning energy in the tropics is about $1.5X10^{19}$ J cm^{-2} y^{-1} (Bar-Nun, 1981). In mid-latitudes, the number of lightning strokes is much smaller and in high latitudes thunderstorms are rare (Bar-Nun, 1981). The globally

averaged energy input by electrical discharges projected per square-centimeter surface area of the Earth is about 16.74 J cm^{-2} y^{-1} (Fox and Dose, 1977). This value includes 3.77 J cm^{-2} y^{-1} due to lightning and about 12.55 J cm^{-2} y^{-1} due to corona discharges from pointed objects (Miller and Orgel, 1974). The quantity of electric discharges that occurred on the primitive Earth is unknown (Fox and Dose, 1977); however, it is generally accepted that electric discharges were as abundant in the primitive atmosphere as are today; and therefore, an energy flux of 16.74 J cm^{-2} y^{-1} has been extensively used to estimate the electrosynthesis of organic compounds in the primitive Earth (Miller and Orgel, 1974; Stribling and Miller, 1987). A dose rate of $1.04X10^{20}$ eV cm^{-3} y^{-1} or 13.9 MGy y^{-1} is derived for electric discharges.

The composition of the primitive atmosphere is not known precisely (Fox and Dose, 1977); although it is usually accepted that an atmosphere composed mainly of methane, nitrogen and water could be reasonable for the initial stages of development of the Earth (Ferris and Chen, 1975; Bossard *et al.*, 1982); however, there is

no estimate on the relative proportions of CH_4, N_2 and H_2O in the primitive atmosphere.

In this study we carried out an extensive investigation to determine the chemical yield of formation of HCN from the electrolysis of a gas mixture composed of CH_4 (36.7%), N_2 (36.7%), and H_2O (26.6%); and a G° (HCN)=0.26 was experimentally determined. Computer simulations predict that G° (HCN) could vary from a factor of 2 to 4 depending on the composition of water vapor or nitrogen in the gas mixture, respectively. If we consider these effects, G° (HCN) could have varied from 0.1 to 0.4 depending on the initial nitrogen and water vapor content of the primitive atmosphere. If we take into account the dose rate of electric discharges in the atmosphere, and consider that G° (HCN) could have varied from 0.1 to 0.4 depending on the atmospheric conditions, an estimate for the rate of electrosynthesis of HCN in the primitive atmosphere would vary from 10^{-4} to 10^{-3} mole cm^{-3} y^{-1}.

Table 3.3 summarizes the chemical yields of HCN synthesis and estimated HCN production in the primitive atmosphere triggered by various energy sources. Shock waves are the most efficient energy source for the synthesis of HCN, followed by ionizing radiations and

Table 3.3. Estimated productions of HCN in the primitive atmosphere by different energy sources.

Energy source	G° (HCN)	HCN production (mole dm^{-3} y^{-1})
UV light	negligible[1]	negligible
Ionizing radiation:	0.01-0.9[2]	
Upper atmosphere		10^{-6}-10^{-4}
Lower atmosphere		10^{-5}-10^{-1}
Electric Discharges	0.1-0.4[3]	10^{-4}-10^{-3}
Shock waves	3.2[4]	10^{-2}
Total		10^{-2}-10^{-1}

1. Raulin *et al.*, 1982; 2. Zhdamirov *et al.*, 1970; 3. This study; 4. Bar-Nun and Shaviv, 1975.

electric discharges. Ultraviolet light has been found to contribute negligibly to the HCN synthesis (Raulin *et al.*, 1982). The estimated total production of HCN in the primitive atmosphere would be about 10^{18}-10^{19} molecules cm^{-3} y^{-1}. Fegly *et al.*, (1986) have derived a HCN rainout rate of (3-14)X10^{11} mole y^{-1}; this indicates that HCN synthesized in the primitive atmosphere would be efficiently transported into the oceans by precipitation processes.

The physical conditions of the primitive Earth are not known but it is believed that they did not change significantly during the history of the Earth (Ferris and Hagan, 1984). If we assume that the volumes of the atmosphere and hydrosphere have not changed, and if all HCN synthesized in the atmosphere would be dissolved in the hydrosphere without any loss due to HCN hydrolysis and/or oligomerization, the concentration of HCN in the hydrosphere would vary from 10^{-3} to 10^{-2} mole dm^{-3} y^{-1}. These figures represent only the upper limits since HCN would be hydrolyzed and/or oligomerized in hydrosphere; however, as it was discussed in Chapter 1 (section 1.3), these values could be increased by concentrating mechanisms such as the eutectic freezing of water volumes (Sanchez *et al.*, 1967) and by the formation of stable cyanocomplexes as ferro and/or ferricyanide (Navarro-González, 1983; Navarro-González *et al.*, 1989).

3.4. Conclusions

This study describes and characterizes three new methods to determine the dose rate supplied by high frequency, high voltage electric discharges. The dose

rate was calculated to be 2.73 0.042 MGy hr^{-1}, and was found to be independent of the chemical composition of the system. Knowledge of the dose rate of electric discharge experiments was essential to study the electrolysis of a simulated primitive atmosphere, and to accurately determine the chemical yields of solutes and products.

The electrolysis of a gas mixture composed of 0.0108 mole dm^{-3} of methane, 0.0108 mole dm^{-3} of nitrogen, and 0.00782 mole dm^{-3} of water vapor in equilibrium with a liquid phase of 0.05 mole dm^{-3} aqueous ammonium chloride buffer at pH 8.7, was investigated at 60°C and 600 Torr in the dose range from 0.38 to 152.30 MGy. The initial chemical yields of decomposition of methane and nitrogen were determined to be 6.54 and 1.26, respectively. About 96% of the initial methane and 10% of the initial nitrogen were converted into: C_2H_2 ($G°=2.14$), C_2H_6 ($G°=0.57$); HCN ($G°=0.26$); CH_3CHO ($G°= 0.13$); CH_3CH_2CHO ($G°=0.011$); $CH_3(CH_2)_2CHO$ ($G°=0.016$); and unidentified water-insoluble oligomeric material ($G°=0.25$ for carbon).

A free radical chemical mechanism was developed to account for the chemical changes produced by electric

discharges. Computer simulations of this mechanism can effectively model the early stages of electrolysis of the gas mixture; the following radical yields are predicted: G° (CH_3)=26.42; G° (CH_2)=3.32; G° (CH)=0.45; G° (H)=70.76; G° (HO)=36.34; G° (N)=0.27.

Computer simulations of the electrosynthesis of HCN under a variety of conditions (e.g., chemical composition, pressure, temperature) were carried out in order to establish the effect on G° for HCN. These studies indicate that the chemical yield of HCN does not depend on the gas pressure and/or temperature, but does depend on the chemical composition of gas mixture, varying by a factor of 2 or 4 depending on the relative abundance of nitrogen and water or hydrogen in the gas mixture.

The possible rate of electrosynthesis of HCN in the primitive atmosphere was estimated to vary from 10^{-4} to 10^{-3} mole cm^{-3} y^{-1} depending on the atmospheric conditions, and for which G° (HCN) was considered to change from 0.1 to 0.4. In addition, the possible contributions of other energy sources to trigger the synthesis of HCN in the primitive atmosphere

were considered, and a possible total rate of HCN synthesis was estimated to be: 10^{-2}-10^{-1} mole cm^{-3} y^{-1}. From such a value, it can be estimated that the possible upper limit for the concentration of HCN in the hydrosphere would have varied from 10^{-3} to 10^{-2} mole dm^{-3} y^{-1}.

The concentration of HCN in the primitive hydrosphere may have been increased by mechanisms such as the eutectic freezing of water volumes (Sanchez *et al.*, 1967) and by the formation of stable cyanocomplexes as hexacyanoferrate(II) and/or (III) (Navarro-González, 1983; Navarro-González *et al.*, 1989), as already discussed in section 1.3 (Chapter 1). The presence of cyanocomplexes of metal ions such as hexacyanoferrate(II) and/or (III) in the primitive hydrosphere could have been important to promote abiotic organic syntheses (Beck, 1978; Kobayashi and Ponnamperuma, 1985). Chapter 4 describes the potential of such species in promoting the free-radical oligomerization of HCN in aqueous solution.

CHAPTER 4

THE EFFECT OF CYANOCOMPLEXES ON THE FREE-RADICAL OLIGOMERIZATION OF HYDROGEN CYANIDE

4.1. Introduction

Transition metal ions are generally believed to have played a role in the process of chemical evolution because of their wide distribution on the Earth crust and also because they are ubiquitous among living systems (Kobayashi and Ponnamperuma, 1985a). Beck (1978) has suggested that the transition metal ion content of the primordial and contemporary sea water could differ by several orders of magnitude based on the dissolving capacity of cyanide: A dilute cyanide solution (10^{-2} mole dm^{-3}) readily dissolves transition metal ions from igneous rocks (Beck, 1978). The author has further suggested that the rate of hydrolysis of HCN in the primitive hydrosphere might have also been

small on account of its coordination with metal ions leading to the formation of cyanocomplexes of transition elements (Beck, 1978).

Cyanocomplexes of iron are characterized by their high solubilities (Weast *et al.*, 1985) and high stability constants (Smith and Martell, 1976). They have been postulated as probable candidates for playing crucial roles in promoting the synthesis of prebiotic compounds in the primitive Earth (Beck, 1978, and references therein); however, only a limited number of studies has been devoted to examine the effects of metal ions in catalyzing reactions of abiotic significance (Kobayashi and Ponnamperuma, 1985a,b). Furthermore, hexacyanoferrate(II) has been found to possess enzyme-like activity, and has been suggested as an intermediate in the evolution of iron-containing enzymes (Kammaludin, *et al.*, 1986).

The purpose of this study was to provide experimental evidence of the possible role of cyanocomplexes of iron on the free-radical oligomerization of HCN. Hexacyanoferrate(II) or (III) readily reduces or oxidizes a variety of free radicals (Ross and Neta, 1982; Buxton *et al.*, 1988). Therefore it was

considered important to study the effect of hexacyanoferrate(II) and (III) on the fate of the free-radical oligomerization of HCN.

An extensive investigation was carried out to study the free radical reactions initiated by the radiolysis of liquid water (H., HO., e_{aq}^-) with hexacyanoferrate(II) and with mixtures of HCN and hexacyanoferrate(II) or (III). The results and discussions of this study are given below.

4.2 The γ-irradiation of aqueous hexacyanoferrate(II)

The radiation chemistry of hexacyanoferrate(II) and (III) is fairly well understood in pulse radiolysis experiments carried out at high dose rates in the 10^{-6}-10^{-3} s time scale (Rabani and Matheson, 1966; Rabani and Meyerstein, 1968; Zehavi and Rabani, 1972, 1974); however, the data presently available are not sufficient to explain the radiolytic behavior of hexacyanoferrate(II) at low dose rate experiments (as those usually done with ^{60}Co-γ-sources), in particular, in anoxic solutions (Masri and Haissinsky, 1963;

Haissinsky *et al.*, 1966). We were prompted to investigate this system in order to determine if the cyano group coordinated to the metal ion could contribute to the formation of organic compounds.

Aqueous, oxygen-free, 0.02 mole dm^{-3} $K_4Fe(CN)_6$ aqueous solutions (pH 6.6) were irradiated with ^{60}Co-γ-rays in a wide dose range from 0.1 to 690 kGy. Figure 4.1 shows the decomposition of hexacyanoferrate(II) as a function of dose; its concentration decreased linearly with increasing dose during the early stages of γ-irradiation (Figure 4.1a), but as the dose increased above 200 kGy, it approached a steady value of about 0.0145 mole dm^{-3} (Figure 4.1b). The initial radiation chemical yield (G°) of decomposition of hexacyanoferrate(II) was calculated from the slope of the curve in Figure 4.1a, and was determined to be 1.15.

The dotted line shown in Figure 4.1 was obtained by computer simulation of the reaction mechanism using *ACUCHEM* (see Chapter 2, section 2.8). The reactions included in the simulations consist of those produced during the irradiation of liquid water: Reactions 1 to 54 given in Tables 2.3 to 2.7 in Chapter 2, section

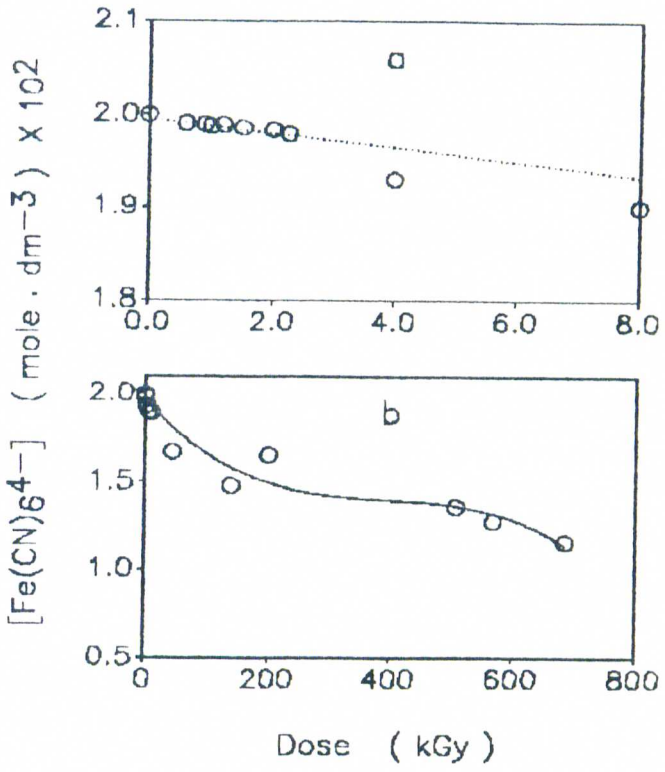

Figure 4.1. Decomposition of hexacyanoferrate(II) at low (a) and high dose (b) of γ-irradiation of a 0.02 mole dm^{-3} $K_4Fe(CN)_6$ aqueous solution. Dotted line was obtained by computer simulation of the reaction mechanism (see text for details).

2.8. The overall process of water radiolysis may be summarized by reaction 4.1:

$$H_2O \longrightarrow HO\cdot + H\cdot + e_{aq}^- + H^+ + H_2 + H_2O_2 \qquad (4.1)$$

In addition to such reactions, computer modeling of the irradiation of aqueous solutions of hexacyanoferrate (II) included reactions 4.2 to 4.22 that are described below.

Hexacyanoferrate(II) reacts with hydroxyl radicals according to reaction 4.2 leading to the formation of hexacyanoferrate(III) and hydroxide ion:

$$HO\cdot + Fe(CN)_6^{4-} \longrightarrow Fe(CN)_6^{3-} + HO^- \qquad (4.2)$$

The rate constant of this reaction has been determined in pulse radiolysis experiments by Zehavi and Rabani (1972) to be $1.25X10^{10}$ dm^3 $mole^{-1}$ s^{-1}. As the concentration of hydroxide ion, $G^{\circ}=0.59$, starts to increase with dose (Figure 4.2), the pH of the irradiated solutions increases from 6.6 to about 11 (Figure 4.3). Under these conditions, hydroxyl radicals dissociates, reaction 4.3 (Draganic and Draganic, 1971), and the radical-anion ($\cdot O^-$) reacts with hexacyanoferrate(II) (reaction 4.4) with a smaller rate constant, $1.5X10^9$ dm^3 $mole^{-1}$ s^{-1} (Ross and Ross, 1977).

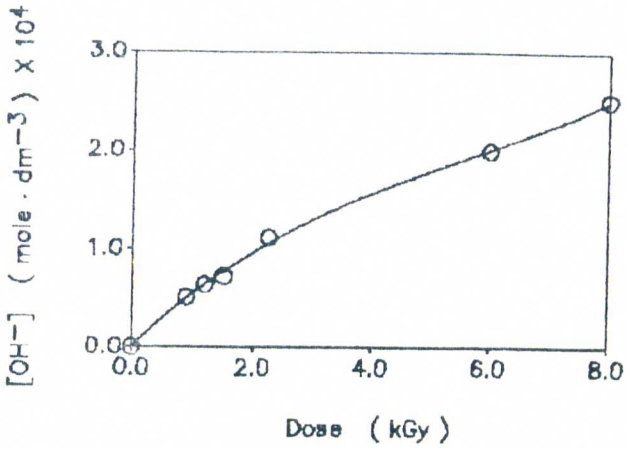

Figure 4.2. Dose dependance of the concentration of hydroxide ion.

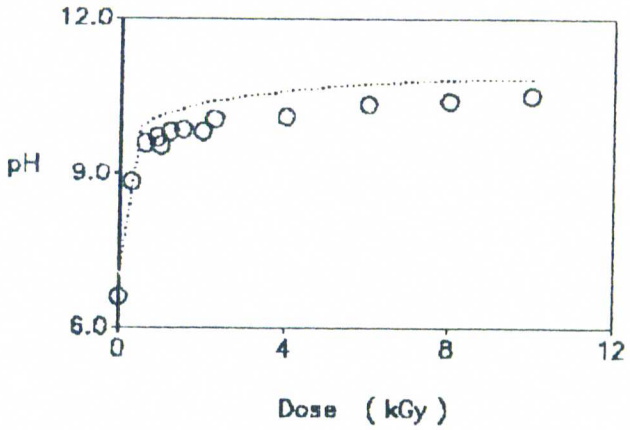

Figure 4.3. Variation of pH with irradiation dose of an aqueous solution of $K_4Fe(CN)_6$. Dotted line was obtained by computer simulation (see text for details).

$$HO\cdot \rightleftharpoons \cdot O^- \qquad pK=11.7 \qquad (4.3)$$

$$\cdot O^- + Fe(CN)_6^{4-} \xrightarrow{H_2O} Fe(CN)_6^{3-} + 2HO^- \qquad (4.4)$$

Hexacyanoferrate(III) was identified in the irradiated solutions by spectroscopy. Figure 4.4 shows the spectra of an irradiated solution (dashed line) and of standard solutions hexacyanoferrate(II) (dotted line) and hexacyanoferrate(III) (Solid line). The

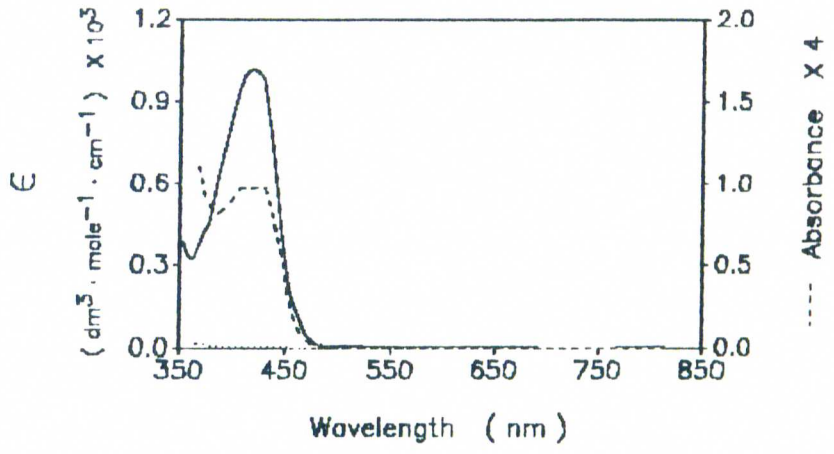

Figure 4.4. Extinction coefficient of hexacyanoferrate (II) (dotted line) and hexacyanoferrate(III) (solid line) as a function of wavelength, and absorbance (dashed line) of an aqueous solution of 0.02 mole dm^{-3} $K_4Fe(CN)6$ at 200 kGy.

formation of hexacyanoferrate(III) was attributed mainly to reactions 4.2 and 4.4; a minor source was ascribed to the reaction of hydroperoxyl radicals, $HO_2\cdot$ (reaction 4.5) with hexacyanoferrate(II), reaction 4.6. The rate constant for reaction 4.6 was determined be $3X10^4$ dm^3 $mole^{-1}$ s^{-1} in pulse radiolysis experiments carried out by Zehavi and Rabani (1972).

$$H_2O_2 + HO\cdot \longrightarrow H_2O + HO_2\cdot \qquad (4.5)$$

$$HO_2\cdot + Fe(CN)_6^{4-} \longrightarrow HO_2^- + Fe(CN)_6^{3-} \qquad (4.6)$$

Figure 4.5 shows the formation of hexacyanoferrate(III) as a function of dose; its concentration linearly increases with dose, G°=1.08, and then steadily increases at higher doses reaching a steady concentration of about 0.004-0.005 mole dm^{-3}. The experimental results agree quite well with the trend predicted by computer simulation at low doses of irradiation (Figure 4.5a); however, at higher doses the reaction mechanism complicates due to unknown reactions involving the initial products. Computer simulations cannot be done at higher doses with existing experimental data.

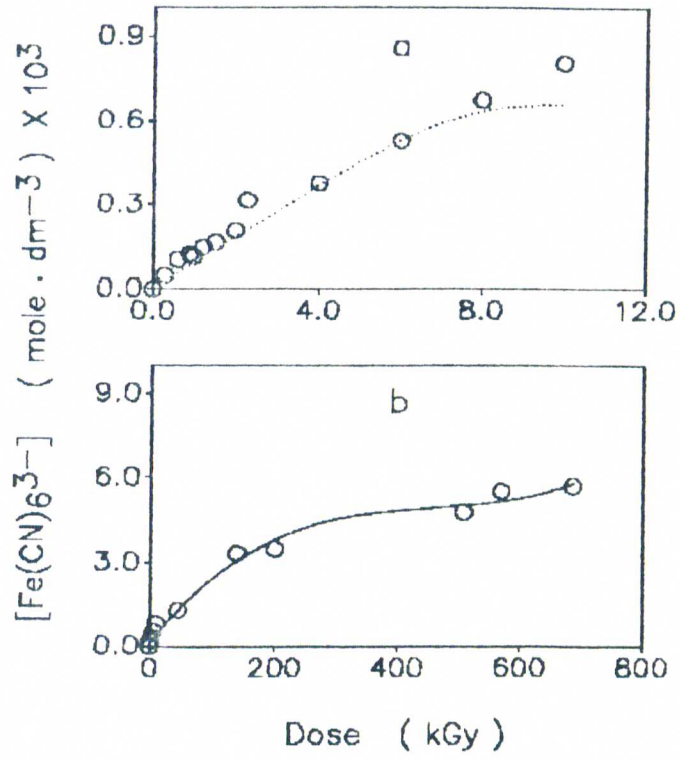

Figure 4.5. Dose dependance of the concentration of hexacyanoferrate (III) at low (a) and high dose of γ-irradiation of a 0.02 mole dm^{-3} $K_4Fe(CN)_6$ aqueous solution. Dotted line was obtained by computer simulation of the reaction mechanism.

Hexacyanoferrate(II) may also react with hydrated electrons leading to the formation of hexacyanoferrate (I), reaction 4.7. The rate constant for this reaction has been determined to be $\leq 7X10^{4}$ dm^{3} $mole^{-1}$ s^{-1} in pulse radiolysis experiments carried out by Zehavi and Rabani (1974).

$$e_{aq}^- + Fe(CN)_6^{4-} \longrightarrow Fe(CN)_6^{5-} \qquad (4.7)$$

Hydrogen atoms react with hexacyanoferrate(II) leading to the addition of hydrogen in the triple carbon-nitrogen bond of the ligand (reaction 4.8); the rate constant was determined by Zehavi and Rabani (1974) in pulse radiolysis experiments, and was found to be $3.9X10^7$ dm^3 $mole^{-1}$ s^{-1} (Zehavi and Rabani, 1974).

$$H + Fe(CN)_6^{4-} \longrightarrow Fe(CN)_6H^{4-} \qquad (4.8)$$

Reaction 4.8 is followed by two consecutive processes, of which the first one is first order (reaction 4.9), while the second one is a reaction of the intermediate with hexacyanoferrate(III) (reaction 4.10) (Zehavi and Rabani, 1974).

$$Fe(CN)_6H^{4-} \longrightarrow Fe(CN)_5^{4-} + HCN \qquad (4.9)$$

$$Fe(CN)_6H^{4-} + Fe(CN)_6^{3-} \longrightarrow Fe(CN)_5^{3-} + Fe(CN)_6^{4-} + HCN \qquad (4.10)$$

The rate constant of reaction 4.9 was found to decrease with pH from 10^5 to 10^3 s^{-1} at pH 0-4 (Zehavi and Rabani, 1974), and the lowest value was used in computer simulation experiments, while the rate of

reaction 4.10 was set to $2X10^{7}$ dm^{3} $mole^{-1}$ s^{-1} (Zehavi and Rabani, 1974).

Zehavi and Rabani (1974) have suggested that pentacyanoferrate(I) may react with hexacyanoferrate(II) and (III), reactions 4.11 and 4.12, respectively. The authors found that the rate constants of these reactions are pH dependent, and a value of $1X10^{8}$ dm^{3} $mole^{-1}$ s^{-1} (Zehavi and Rabani, 1974) was used in computer modeling.

$$Fe(CN)_5^{4-} + Fe(CN)_6^{3-} \longrightarrow Fe(CN)_5^{3-} + Fe(CN)_6^{4-} \quad (4.11)$$

$$Fe(CN)_5^{4-} + Fe(CN)_6^{4-} \longrightarrow Fe(CN)_5^{3-} + Fe(CN)_6^{5-} \quad (4.12)$$

Pentacyanoferrate(II) formed in reactions 4.10 to 4.12, may react with hydrogen peroxide (reaction 4.13) or its anion (reaction 4.14) leading to the formation of pentacyanoferrate(III). The rate constants for these reactions were determined by Davies and Garafalo (1976) to be: 107 and 3 dm^{3} $mole^{-1}$ s^{-1}, respectively.

$$Fe(CN)_5^{3-} + H_2O_2 \longrightarrow Fe(CN)_5^{2-} + HO^{-} + HO\cdot \quad (4.13)$$

$$Fe(CN)_5^{3-} + HO_2^- \longrightarrow Fe(CN)_5^{2-} + HO^- + \cdot O^- \quad (4.14)$$

Figure 4.6 shows the predicted dose dependance for the formation of pentacyanoferrate(II) and (III) in the irradiated solutions. Their concentration is predicted to increase to a maximum at low doses (≤2 kGy), and then rapidly decrease on account of their reactions with H_2O_2 (reactions 4.13 and 4.14) or with $^-CN/HCN$ (reactions 4.15 and 4.16), respectively. The equilibrium constant for reaction 4.15 has been determined to be $5X10^8$ (James and Murray, 1975) while the rate constant for the reverse reaction has been found to be

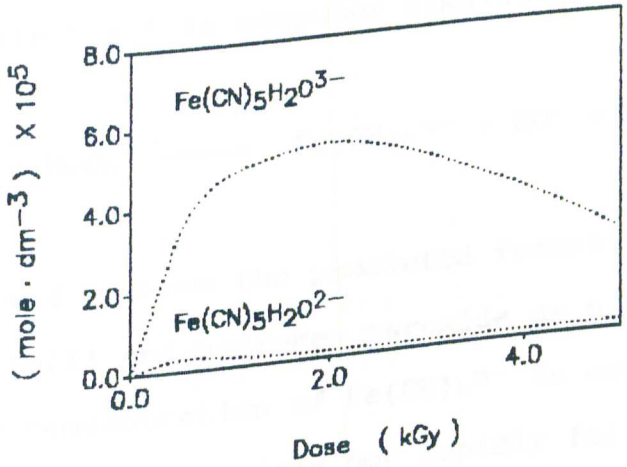

Figure 4.6. Computed trends for the formation of pentacyanoferrate(II) and (III) in the γ-irradiation of aqueous solutions of hexacyanoferrate(II).

$6X10^{-7}$ s^{-1} (Sharpe, 1976). The equilibrium constant for reaction 4.16 is 50 (James and Murray, 1975).

$$Fe(CN)_5^{2-} + {}^-CN \rightleftharpoons Fe(CN)_6^{3-} \qquad (4.15)$$

$$Fe(CN)_5^{2-} + HCN \rightleftharpoons Fe(CN)_6^{3-} + H^+ \qquad (4.16)$$

The fate of hexacyanoferrate(I) which is predicted to be formed according to reactions 4.7 and 4.12, is not known but it is possible that it may react with hydrogen peroxide (reaction 4.17) leading to the formation of hexacyanoferrate(II). Its rate of reaction was assumed to be greater than that of hexacyanoferrate (II), which is a more stable species, and was set to 10^3 dm^3 $mole^{-1}$ s^{-1} in computer simulation experiments.

$$Fe(CN)_6^{5-} + H_2O_2 \longrightarrow Fe(CN)_6^{4-} + HO^- + HO^{\cdot} \qquad (4.17)$$

Figure 4.7 shows the predicted formation of hexacyanoferrate(I) and hydrogen peroxide as a function of dose. The concentration of $Fe(CN)_6^{5-}$ is estimated to reach a maximum at low dose but rapidly falls off due to reactions 4.17 and 4.18; the latter becoming dominant at doses above 0.2 kGy.

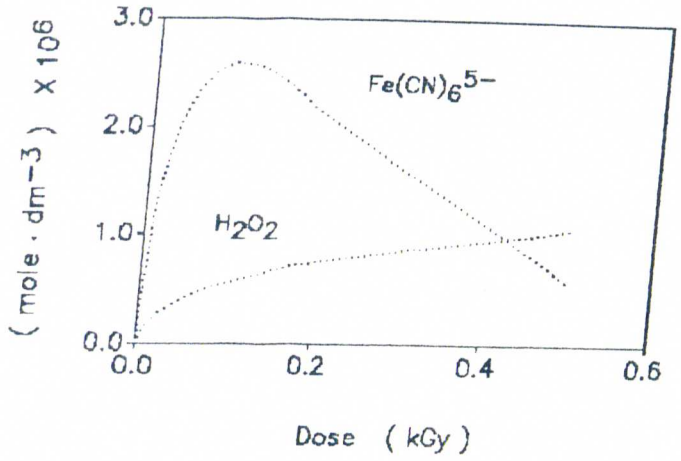

Figure 4.7. Computed trends for the formation of hexacyanoferrate(I) and hydrogen peroxide in the γ-irradiation of aqueous solutions of 0.02 mole dm^{-3} $K_4Fe(CN)_6$.

$$e_{aq}^- + Fe(CN)_6^{3-} \rightarrow Fe(CN)_6^{4-} \quad (4.18a)$$

$$e_{aq}^- + Fe(CN)_6^{3-} \rightarrow Fe(CN)_5^{3-} + {}^-CN \quad (4.18b)$$

Reaction 4.18 has been studied by Zehavi and Rabani (1974) in pulse radiolysis experiments and a rate constant of $2.4X10^9$ dm^3 $mole^{-1}$ s^{-1} was derived; channels 4.18a and 4.18b represent 88% and 12%, respectively (Zehavi and Rabani, 1974).

The hydrogen atom may also react with hexacyanoferrate(III) as its concentration starts to build up in solution. The rate constant for this reaction is

$5.8X10^{9}$ dm^{3} $mole^{-1}$ s^{-1}, and channels 4.19a and 4.19b represent 90% and 10%, respectively (Zehavi and Rabani, 1974). Reaction 4.19 competes with reaction 4.8 and becomes dominant at high dose.

$$H^{\cdot} + Fe(CN)_6^{3-} \longrightarrow \begin{cases} Fe(CN)_6^{4-} + H^{+} & (4.19a) \\ Fe(CN)_5^{3-} + HCN & (4.19b) \end{cases}$$

Another source of disappearance of hexacyanoferrate(III) was reaction 4.20; however, its contribution is predicted to be minor as compared to reactions 4.18 and 4.19. The rate constant for such a reaction is relatively small, $2.7X10^{2}$ dm^{3} $mole^{-1}$ s^{-1} (Zehavi and Rabani, 1972).

$$\cdot O_2^{-} + Fe(CN)_6^{3-} \longrightarrow O_2 + Fe(CN)_6^{4-} \qquad (4.20)$$

As the pH of the solutions increases with dose, hydrogen peroxide dissociates according to reaction 4.21, pK=11.6 (Eaton and Pankratz, 1985), and the anion reacts with hexacyanoferrate(III) with a rate constant of 99 dm^{3} $mole^{-1}$ s^{-1}, reaction 4.22 (Eaton and Pankratz, 1985).

$$H_2O_2 \longrightarrow HO_2^- + H^+ \qquad (4.21)$$

$$HO_2^- + Fe(CN)_6^{3-} \longrightarrow Fe(CN)_6^{4-} + HO_2\cdot \qquad (4.22)$$

Computer simulation experiments cannot predict the actual trends of products at doses above 10 kGy. This may be due to secondary reactions that involved the pentacyanoferrates, $Fe(CN)_5^{3-}$ and $Fe(CN)_5^{2-}$, with hydrogen atoms, hydrated electrons and hydroxyl radicals. It may also involved complexation reactions with stable molecules such as molecular hydrogen, which is formed in the irradiated solutions (G°=0.30), but in a lower yield than predicted by computer simulations (Figure 4.8).

The irradiated solutions of hexacyanoferrate(II) were also analyzed for the formation of carbon containing products. Search for carbon dioxide, aldehydes and carboxylic acids gave negative results in the dose range studied (up to 690 kGy) with techniques having detection limits $\leq 10^{-6}$ mole dm^{-3}. Therefore, the cyano group coordinated to the iron complex does not decompose.

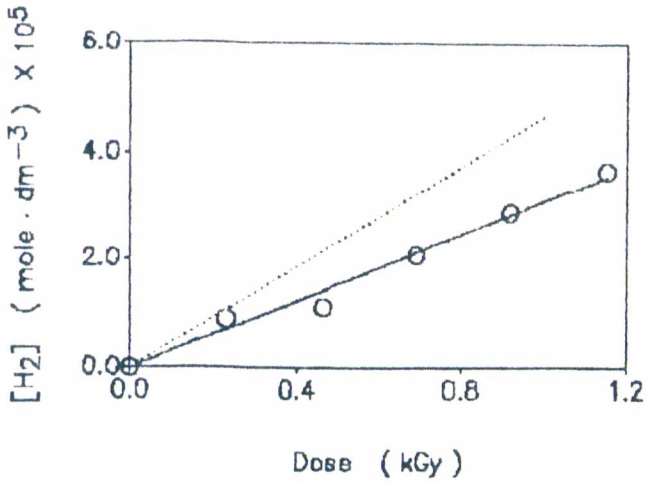

Figure 4.8. Dose dependance of the concentration of molecular hydrogen in the irradiation of aqueous solutions of hexacyanoferrate(II). Dotted line was obtained by computer simulation.

The results presented in this section clearly demonstrate that hexacyanoferrate(II) is very reactive toward free radical reactions. However, the cyano groups coordinated to the metal ion do not participate in the formation of organic compounds as does when it is not coordinated. Therefore, it seems likely that HCN might have not played a significant role on the synthesis of organic compounds in the primitive Earth if it was mainly present as a ligand coordinated to metal ions such as iron.

The effects of hexacyanoferrate(II) in aqueous mixtures containing free HCN and hexacyanoferrate(II) are discussed in the next section.

4.3 The γ-irradiation of aqueous hexacyanoferrate(II)-HCN mixtures

Aqueous, oxygen-free solutions (pH ≈6) of 0.1 mole dm^{-3} HCN and 0.001 mole dm^{-3} $K_4Fe(CN)_6$ were irradiated with ^{60}Co-γ-rays in a wide dose range up to about 100 kGy.

Hydrogen cyanide is initially present in solution in its non-dissociated form; however during the irradiation of the aqueous solution, the pH increases from 6 to about 7.5 (Figure 4.9). Under these conditions, hydrogen cyanide is reversibly converted into cyanide ion according to reaction 4.23; the rate constants of both forward and reverse reactions are known, and are: $5.2X10^4$ dm^3 $mole^{-1}$ s^{-1}, and $3.7X10^7$ dm^3 $mole^{-1}$ s^{-1}, respectively (Wilson, 1972a).

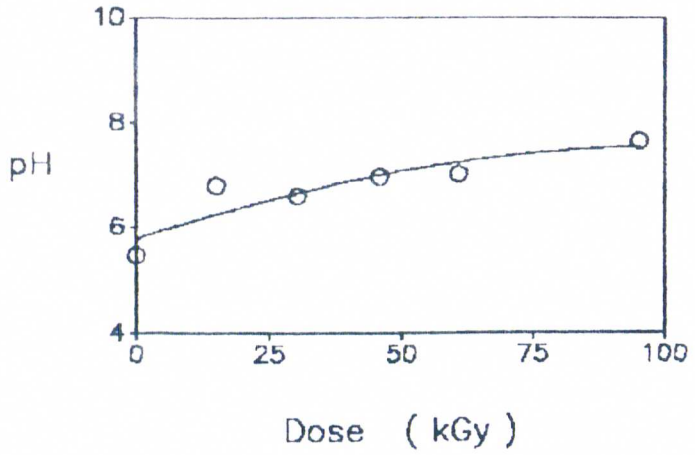

Figure 4.9. Variation of pH as a function of dose during the γ-irradiation of an aqueous solution of 0.1 mole dm^{-3} HCN and 0.001 mole dm^{-3} $K_4Fe(CN)_6$.

$$^{-}CN + H_2O \rightleftharpoons HCN + HO^{-} \qquad (4.23)$$

The reaction scheme for the radiation-induced decomposition of HCN has been examined in detail in Chapter 1, section 1.4.2. Hydrogen atoms react with hydrogen cyanide (reaction 4.24) with a rate constant of $3.3X10^{7}$ dm^{3} $mole^{-1}$ s^{-1}, (Ogura, 1968; Draganic *et al.*, 1973), while cyanide ion reacts at a higher rate constant (reaction 4.25): $2.6X10^{9}$ dm^{3} $mole^{-1}$ s^{-1} (Anbar and Neta, 1967).

$$HCN + H^{\cdot} \longrightarrow H_2C{=}N^{\cdot} \qquad (4.24)$$

$$^{-}CN + H^{\cdot} \xrightarrow{H_2O} H_2C{=}N^{\cdot} + HO^{-} \qquad (4.25)$$

Hydrated electrons react with HCN and ^{-}CN according to reactions 4.26 and 4.27, respectively. The rate constants for these reactions are $6.6X10^{9}$ dm^{3} $mole^{-1}$ s^{-1} (Draganic *et al.*, 1973), and $5X10^{5}$ dm^{3} $mole^{-1}$ s^{-1} (Bielski and Allen, 1977), consecutively.

$$HCN + e_{aq}^{-} \xrightarrow{H_2O} H_2C{=}N^{\cdot} + HO^{-} \qquad (4.26)$$

$$^{-}CN + e_{aq}^{-} \xrightarrow{2H_2O} H_2C{=}N^{\cdot} + 2HO^{-} \qquad (4.27)$$

Hydroxyl radical and its anion reacts with HCN and ^{-}CN according to reactions 4.28 to 4.30. The rate constant of reaction 4.28 is $6X10^{9}$ dm^{3} $mole^{-1}$ s^{-1} (Buchler *et al.*, 1976) while that of reaction 4.29 is $6.5X10^{9}$ dm^{3} $mole^{-1}$ s^{-1} (Kraljic and Trumbore, 1965; Behar, 1974; Buchler *et al.*, 1976; Bielski and Allen, 1977). The rate constant of reaction of the radical-anion with cyanide ion (reaction 4.30), is smaller: $2.6X10^{8}$ dm^{3} $mole^{-1}$ s^{-1} (Behar, 1974; Buchler *et al.*, 1976).

$$HCN + HO^{\cdot} \longrightarrow HO-CH=N^{\cdot} \qquad (4.28)$$

$$^{-}CN + HO^{\cdot} \longrightarrow HO-\dot{C}=N^{-} \qquad (4.29)$$

$$^{-}CN + {}^{\cdot}O^{-} \longrightarrow {}^{-}O-\dot{C}=N^{-} \qquad (4.30)$$

The radicals produced by reactions 4.24 to 4.27 undergo disproportionation reaction (4.31) leading to the re-formation of HCN and formation of $H_2C=NH$. The rate of this reaction is $1.3X10^{9}$ dm^{3} $mole^{-1}$ s^{-1} (Buchler *et al.*, 1976).

$$2H_2C=N^{\cdot} \longrightarrow HCN + H_2C=NH \qquad (4.31)$$

Figure 4.10 shows the decomposition of HCN as a function of dose. The initial radiation chemical yield of decomposition of HCN was determined to be 2.00; this value is considerably smaller than that obtained in pure aqueous HCN solutions (G°=7.60). Reactions 4.24 to 4.31 are not sufficient to account for the decomposition of HCN in the presence of $K_4Fe(CN)_6$. Analysis of data indicates that hexacyanoferrate(II) reacts with $HO-CH=N^{\cdot}$ leading to the re-formation of HCN, reaction 4.32. The rate constant of reaction 4.32 was derived by computer simulations and was determined to be

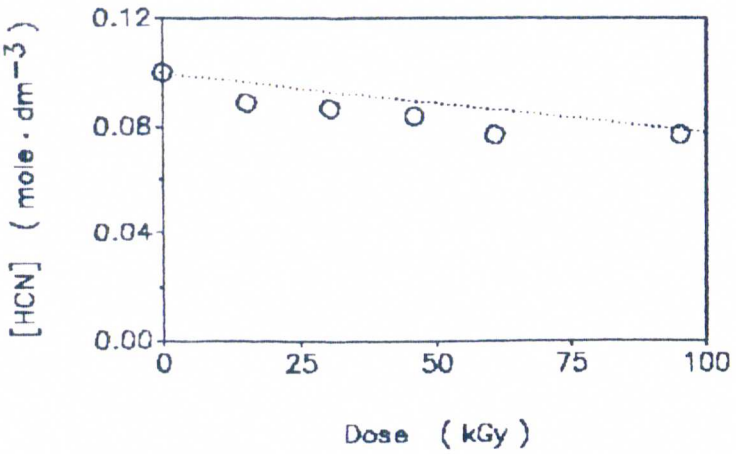

Figure 4.10. Decomposition of HCN during the γ-irradiation of an aqueous 0.1 mole dm^{-3} solution of HCN and 0.001 mole dm^{-3} of $K_4Fe(CN)_6$. Dotted line was obtained by computer simulation (see text for details).

$5.0X10^{-3}$ dm^3 $mole^{-1}$ s^{-1} with an estimated error of about 10%. As the pH of the solution increases with dose, HO-CH=N· dissociates with a pK=5, reaction 4.33 (Behar, 1974; Buchler *et al.*, 1976); the radical-anion formed also reacts with hexacyanoferrate(II) according to reaction 4.34. The reactions 4.32 and 4.34 were undistinguishable in computer simulations.

$$HO-CH=N\cdot + Fe(CN)_6^{4-} \longrightarrow Fe(CN)_6^{3-} + HCN + HO^- \quad (4.32)$$

$$HO-CH=N\cdot \rightleftharpoons {}^-O-CH=N\cdot + H^+ \quad (4.33)$$

$$^{-}O\text{-}CH{=}N^{\cdot} + Fe(CN)_6^{4-} \longrightarrow Fe(CN)_6^{3-} + HO^{-} + {}^{-}CN \quad (4.34)$$

Computer simulation experiments were carried out taking into account reactions 1 to 54 which were given in Tables 2.3 to 2.7 (Chapter 2, section 2.8) as well as reactions 4.2 to 4.54.

Figure 4.11 shows the formation of hexacyanoferrate(III) in the aqueous mixture; its radiation chemical yield of formation was determined to be 4.10. The origin of $Fe(CN)_6^{3-}$ was mainly attributed to

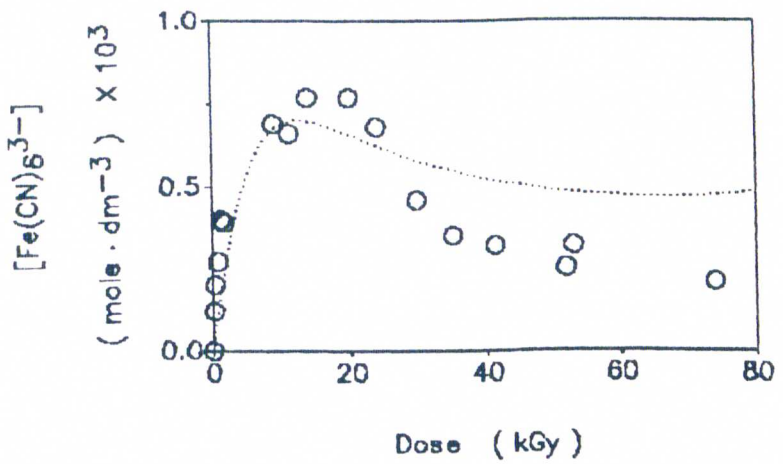

Figure 4.11. Formation of hexacyanoferrate(III) during the γ-irradiation of an aqueous, oxygen-free solution of HCN and hexacyanoferrate(II). Dotted line was obtained by computer simulation (see text for details).

reactions 4.32 and 4.34, and to a much lesser extent to reactions 4.2, 4.4, 4.6, and reactions 4.13 and 4.14 followed by 4.15 and 4.16. At doses above 10 kGy, it disappears according to reactions 4.18 and 4.19. However, as in the case of the $K_4Fe(CN)_6$ system (section 4.2), computer simulations failed at high doses mainly because of the lack of knowledge on the fate of the pentacyanoferrates in the mechanism of radiolysis.

Figure 4.12 shows the experimental and predicted dose dependance of formation of hydrogen ($G°$=0.45) while figure 4.13 presents the predicted formation of

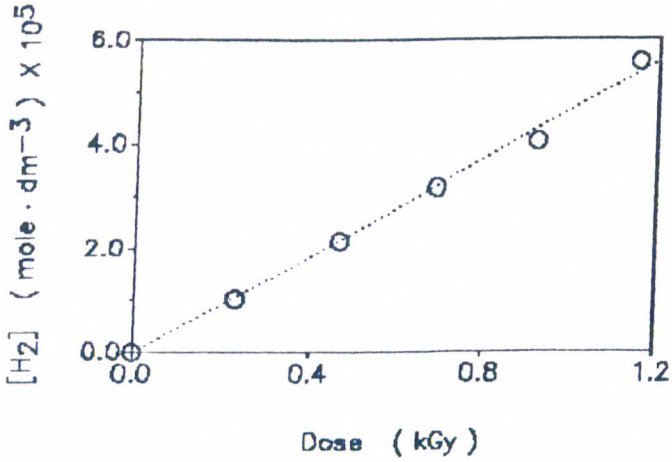

Figure 4.12. Formation of molecular hydrogen during the irradiation of HCN and hexacyanoferrate(II) solutions. Dotted line was obtained by computer simulation.

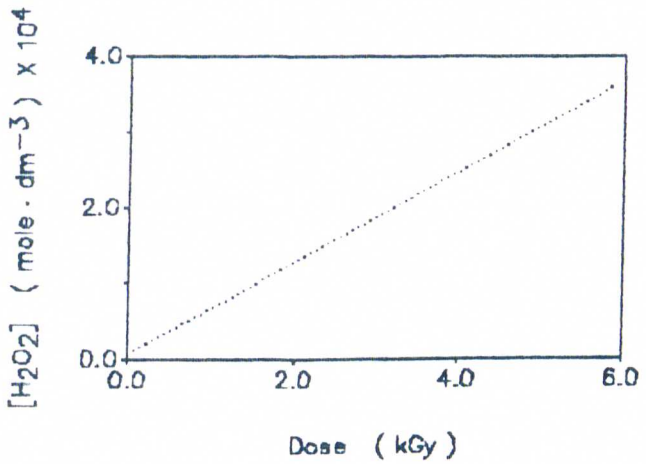

Figure 4.13. Computer simulation for the formation of hydrogen peroxide during the irradiation of HCN and $K_4Fe(CN)6$ solutions.

hydrogen peroxide ($G°$=0.59). The mechanism of formation of both H_2 and H_2O_2 was considered in detail in Chapter 2, section 2.8, and is summarized by reaction 4.1.

CO_2 (Figure 4.14) and NH_3 (Figure 4.15) are the main products formed directly from HCN in the presence of hexacyanoferrate(II); their initial radiation chemical yields of formation were determined to be 0.60 and 1.01, respectively. The origin of both compounds may be explained as follows. Disproportionation of

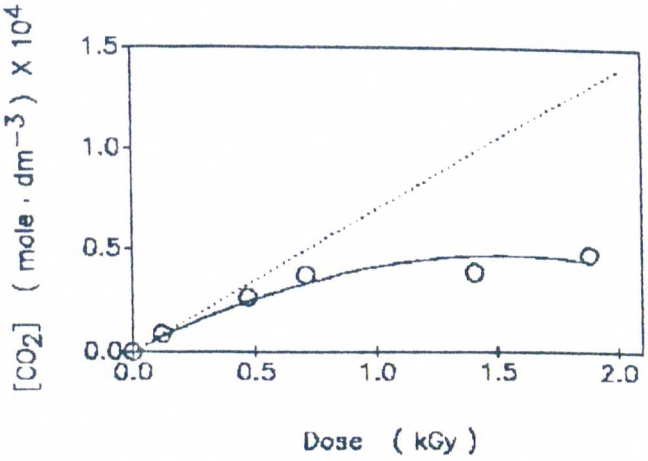

Figure 4.14. Formation of CO_2 during the γ-irradiation of a solution of 0.1 mole dm^{-3} HCN and 0.001 mole dm^{-3} $K_4Fe(CN)6$. Dotted line was obtained by computer simulation (see text for details).

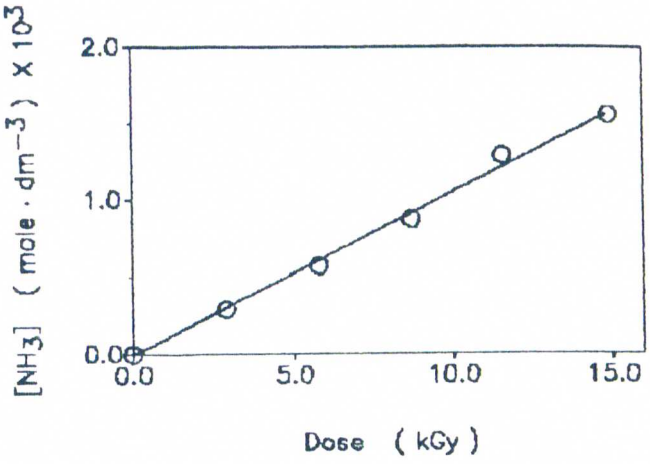

Figure 4.15. Formation of NH_3 during the irradiation of a solution of 0.1 mole dm^{-3} HCN and 0.001 mole dm^{-3} $K_4Fe(CN)_6$.

$HO-CH=N^{\cdot}$ or $^{-}O-CH=N^{\cdot}$ leads to the formation of cyanic acid or cyanate with rate constants of $1.1X10^{9}$ dm^{3} $mole^{-1}$ s^{-1} (reaction 4.35) (Behar, 1974; Buchler *et al.*, 1976) or $6.5X10^{8}$ dm^{3} $mole^{-1}$ s^{-1} (reaction 4.36) (Behar, 1974), respectively. Cyanic acid or cyanate undergo hydrolysis and/or ammonolysis leading to the formation of CO_2, NH_3 and urea (reactions 4.37 to 4.43). The second order rate constants (k) given in these reactions have units of dm^{3} $mole^{-1}$ s^{-1} and were taken from Wilson, 1972a. In addition, the acid-base equilibrium reactions for ammonia, reactions 4.44 and 4.45 (Castellan, 1983), and for carbon dioxide, reactions 4.46 and 4.47 (Weast *et al.*, 1985) were taken into account in computer simulations.

$$2HO-CH=N^{\cdot} \longrightarrow HO-CH=NH + HO-CN \qquad (4.35)$$

$$2\,^{-}O-CH=N^{\cdot} \longrightarrow HCN + HO^{-} + {}^{-}O-CN \qquad (4.36)$$

$$HO-CN \rightleftharpoons {}^{-}O-CN + H^{+} \quad pKa=3.46 \qquad (4.37)$$

$$HO-CN + H^{+} \xrightarrow{H_2O} NH_4^{+} + CO_2 \quad (k=6.0X10^{-2}) \qquad (4.38)$$

$$HO-CN + H_2O \longrightarrow NH_3 + CO_2 \quad (k=7.8X10^{-4}) \qquad (4.39)$$

$$^{-}O-CN + H_2O \xrightarrow{H_2O} NH_3 + HCO_3^{-} \quad (k=8.3X10^{7}) \qquad (4.40)$$

$$^{-}O\text{-}CN + H^{+} \xrightarrow{H_2O} NH_3 + CO_2 \quad (k=43) \quad (4.41)$$

$$HO\text{-}CN + NH_3 \longrightarrow NH_2CONH_2 \quad (k=17.8) \quad (4.42)$$

$$^{-}O\text{-}CN + NH_4^{+} \longrightarrow NH_2CONH_2 \quad (k=9.6X10^{-6}) \quad (4.43)$$

$$NH_3 + H_2O \longrightarrow NH_4^{+} + HO^{-} \quad (k=6.0X10^{5}) \quad (4.44)$$

$$NH_4^{+} + HO^{-} \longrightarrow NH_3 + H_2O \quad (k=3.4X10^{10}) \quad (4.45)$$

$$CO_2 + H_2O \rightleftharpoons HCO_3^{-} + H^{+} \quad pKa=6.37 \quad (4.46)$$

$$HCO_3^{-} \rightleftharpoons CO_3^{2-} + H^{+} \quad pKa=10.25 \quad (4.47)$$

Another source for the formation of NH_3 was attributed to hydrolysis of $H_2C{=}NH$ and HO-CH=NH, reactions 4.48 and 4.49. Their rates of hydrolysis are not known but were assumed to be: 10^{3} dm^{3} $mole^{-1}$ s^{-1}.

$$H_2C{=}NH + H_2O \longrightarrow H_2C{=}O + NH_3 \quad (4.48)$$

$$HO\text{-}CH{=}NH + H_2O \longrightarrow HCO_2H + NH_3 \quad (4.49)$$

The formation of formaldehyde is predicted by reaction 4.48. Figures 4.16 and 4.17 show gas chromatograms and mass spectra of aldehydes products that were derivatized by 2,4-dinitrophenyl-hydrazine (DNP) into 2,4-dinitrophenyl-hydrazone (DNPH) derivatives. Formaldehyde, acetaldehyde, propionaldehyde and

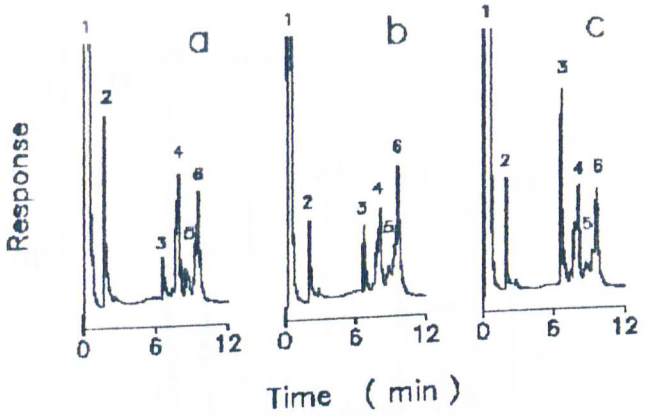

Figure 4.16. Gas chromatograms of DNPH derivatives of aldehydes formed at 30 (a), 61 (b) and 95 (c) kGy in aqueous solutions of 0.1 mole dm^{-3} HCN and 0.001 mole dm^{-3} $K_4Fe(CN)_6$. Legend: 1. Solvent; 2. DPH; 3. Formaldehyde; 4. Acetaldehyde; 5. Propionaldehyde; 6. Butyraldehyde.

butyraldehyde were identified by gas chromatography and mass spectrometry. Figure 4.18 shows the dose dependence of the formation of formaldehyde. The radiation chemical yields of formation were calculated to be: G° $(HCHO)=9.10X10^{-3}$; G° $(CH_3CHO)=2.70X10^{-2}$; G° $(CH_3CH_2CHO)=2.09X10^{-3}$; G° $(CH_2(CH_2)_2CHO)=7.26X10^{-3}$.

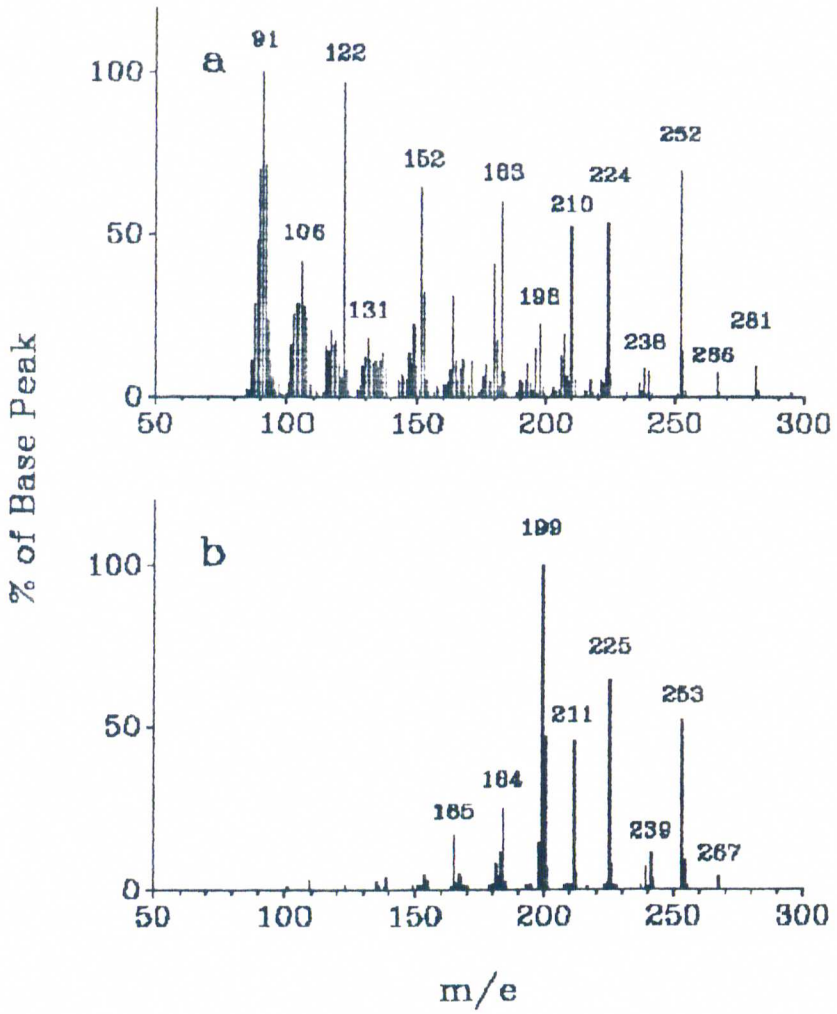

Figure 4.17. Electron impact (a) and chemical ionization (b) mass spectra of the DNPH fraction formed at 95 kGy. Molecular weights of DNPH derivatives: Formaldehyde 210; acetaldehyde: 224; propionaldehyde: 238; butyraldehyde:252; valeraldehyde: 266.

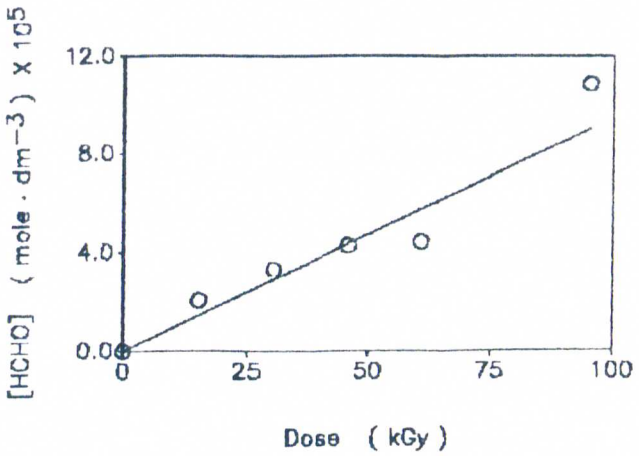

Figure 4.18. Formation of formaldehyde as a function of dose in aqueous solutions of 0.1 mole dm^{-3} HCN and 0.001 mole dm^{-3} $K_4Fe(CN)6$.

A variety of polycarboxylic acids are formed in irradiated HCN solutions. Figure 4.19 shows gas chromatograms obtained at different doses. Except for oxalic acid (peak 1 in Figure 4.19), their concentrations exponentially increased with dose. Figure 4.20 shows the variation of concentration of oxalic and malonic acids with dose. The identifications of polycarboxylic acids were confirmed by mass spectrometry using electron impact and chemical ionization techniques (Figure 4.21). Table 4.1 summarizes the identification type for each carboxylic acid as well as their initial radiation chemical yield.

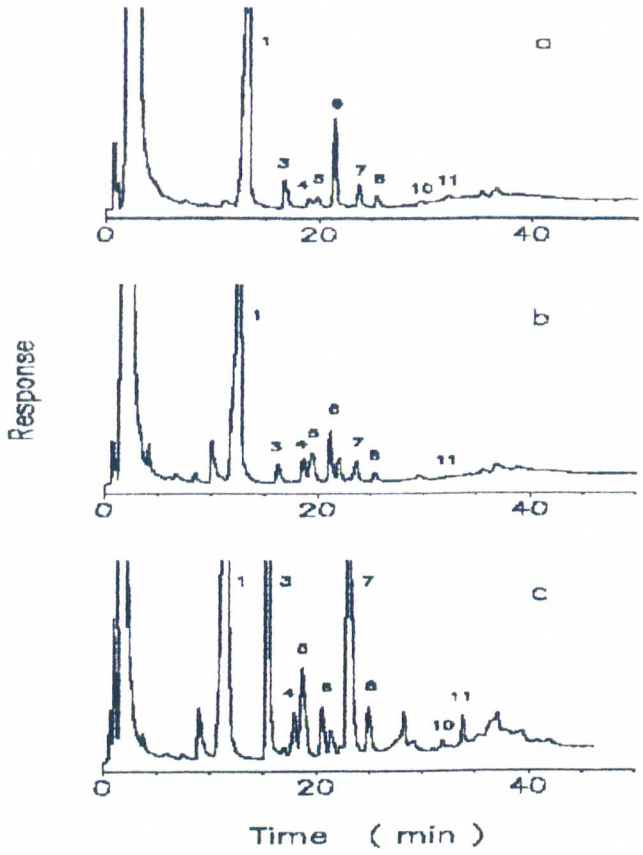

Figure 4.19. Gas chromatograms of polycarboxylic acids methyl esters from HCN-$K_4Fe(CN)_6$ mixtures at 30 (a), 46 (b) and 95 (c) kGy. 1. Oxalic; 3. Malonic; 4. Fumaric; 5. Succinic; 6. 1,2 Dimethyl succinic; 7. Maleic; 8. Glutaric; 10. Malic; 11. Carboxysuccinic.

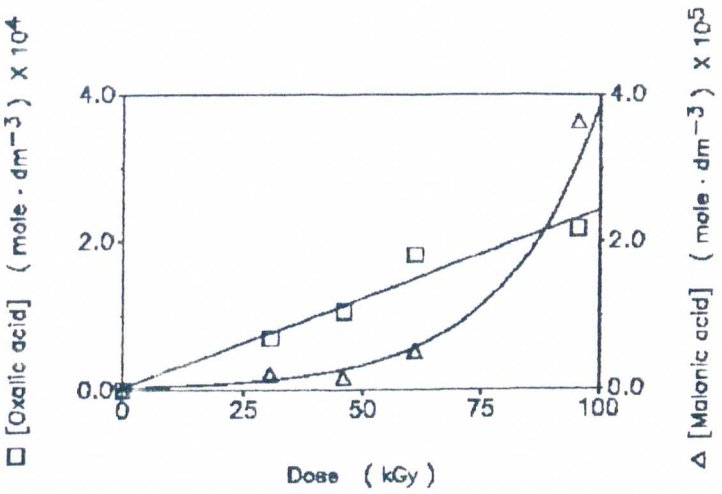

Figure 4.20. Dose dependance of the formation of oxalic and malonic acids in HCN-$K_4Fe(CN)_6$ mixtures.

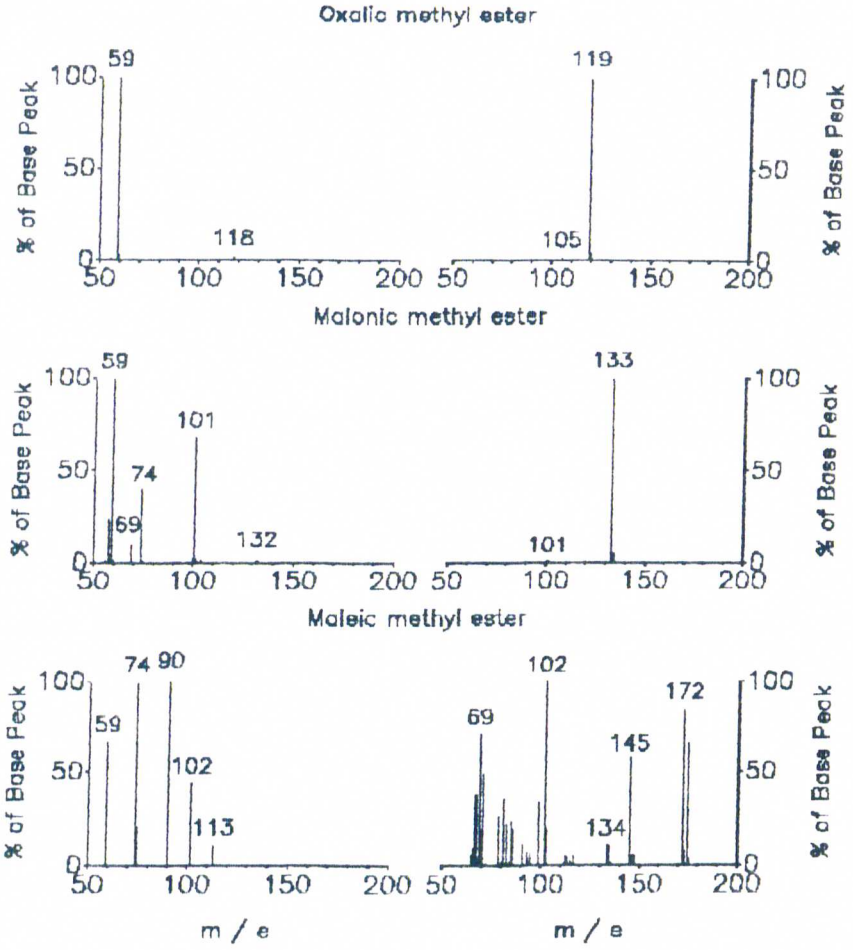

Figure 4.21. Electron impact (left) and chemical ionization (right) mass spectra of polycarboxylic acids formed at 95 kGy.

Table 4.1. Initial chemical yields ($G°$) of formation of polycarboxylic acids.

Acid	Identification type*	$G°$
Oxalic	△ □ ▲ ■	$2.34X10^{-2}$
Malonic	△ □ ▲ ■	$2.24X10^{-4}$
Fumaric	△ □ ▲ ■	$3.39X10^{-5}$
Succinic	△ □ ▲ ■	$6.61X10^{-5}$
1,2-Dimethyl succinic	△ □ ▲ ■	$<X10^{-6}$
Maleic	△ □ ▲ ■	$5.36X10^{-5}$
Glutaric	△ □ ■	$8.44X10^{-5}$
Adipic	△ □	$3.57X10^{-6}$
Malic	△ □ ▲	$4.99X10^{-6}$
Pimelic	△ □	$<X10^{-6}$
Carboxysuccinic	△ □ ▲	$4.56X10^{-6}$

* Retention time (△); coinjection with standard (□); electron impact mass spectrometry (▲); and chemical ionization mass spectrometry (■).

The existing data is not sufficient for modeling the formation of polycarboxylic acids in HCN solutions exposed to irradiation; however, reactions 4.50 to 4.54 were included in the simulation to account for the formation of oxamide and/or oxalic acid. The kinetic data were taken from Behar (1974) and/or Buchler *et al.* (1976).

$$HO\text{-}\dot{C}{=}N^- + H^+ \rightleftharpoons HO\text{-}\dot{C}{=}NH \quad pK=10.2 \qquad (4.50)$$

$$HO\text{-}\dot{C}{=}NH \longrightarrow \cdot CONH_2 \quad k=4X10^7\ s^{-1} \qquad (4.51)$$

$$2\cdot CONH_2 \longrightarrow (CONH_2)_2 \quad k=3.1X10^9\ dm^3\ mole^{-1}\ s^{-1} \qquad (4.52)$$

$$^-O\text{-}\dot{C}{=}N^- \underset{}{\overset{H^+}{\rightleftharpoons}} {}^-O\text{-}\dot{C}{=}NH \longleftrightarrow O{=}\dot{C}\text{-}NH^- \qquad (4.53)$$

$$2\ O{=}\dot{C}\text{-}NH^- \xrightarrow{2H_2O} (CONH_2)_2 + 2HO^-$$

$$k=1.1X10^9\ dm^3\ mole^{-1}\ s^{-1} \qquad (4.54)$$

Oligomeric material was formed in low yield in HCN mixtures containing $K_4Fe(CN)_6$. Figure 4.22 shows the formation of this material as a function of dose. Its yield increases exponentially as a function of dose; the initial chemical yields of formation for this material were determined to be: G° (C)=1.22; G° (N)=1.06; G° (H)=1.85; and G° (O)=0.84. Its origin may be explained by successive oligomerization reactions of the radicals previously described (generically refereed as X·) with HCN molecules, reaction 4.55.

$$X\cdot + nHCN \xrightarrow{X\cdot} \text{Oligomeric material} \qquad (4.55)$$

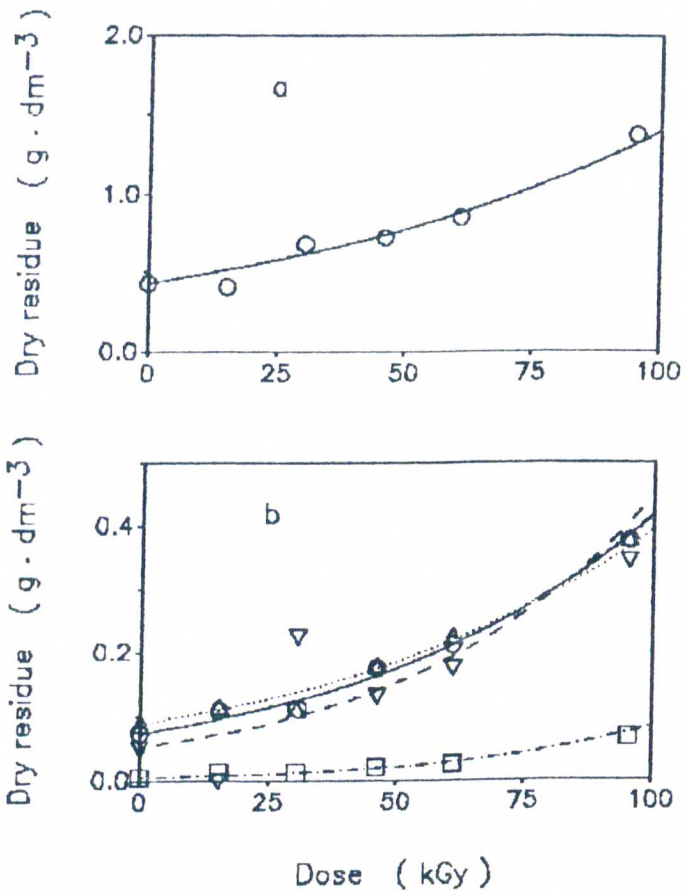

Figure 4.22. Dose dependance for the formation of oligomeric material measured as total dry residue (a) and as specific elemental composition in the residue (b). Legend for b: Carbon (O); nitrogen (△); hydrogen (□); and oxygen (▽).

Figure 4.23 shows the effect of the concentration of hexacyanoferrate(II) on the free radical oligomerization of HCN. The amount of HCN decomposed is only

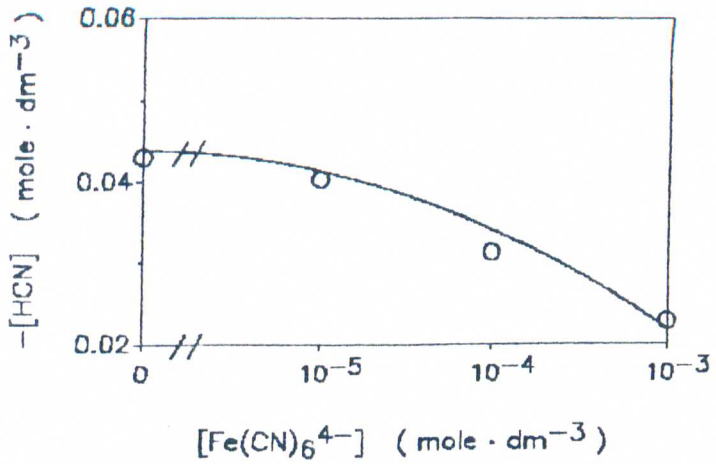

Figure 4.23. Dependance of the decomposition of HCN as a function of the concentration of $K_4Fe(CN)_6$ in aqueous solutions of 0.1 mole dm^{-3} HCN that have been exposed to a dose of 61 kGy.

markedly decreased at high concentrations of $Fe(CN)_6^{4-}$ above $>10^{-4}$ mole dm^{-3}. Figure 4.24 shows gas chromatograms of a variety of polycarboxylic acids that are synthesized. Their yields are only markedly decreased at high concentrations (10^{-3} mole dm^{-3}) of $Fe(CN)_6^{4-}$ but are not significantly affected at concentrations $\geq 10^{-4}$ mole dm^{-3} (Figure 4.24).

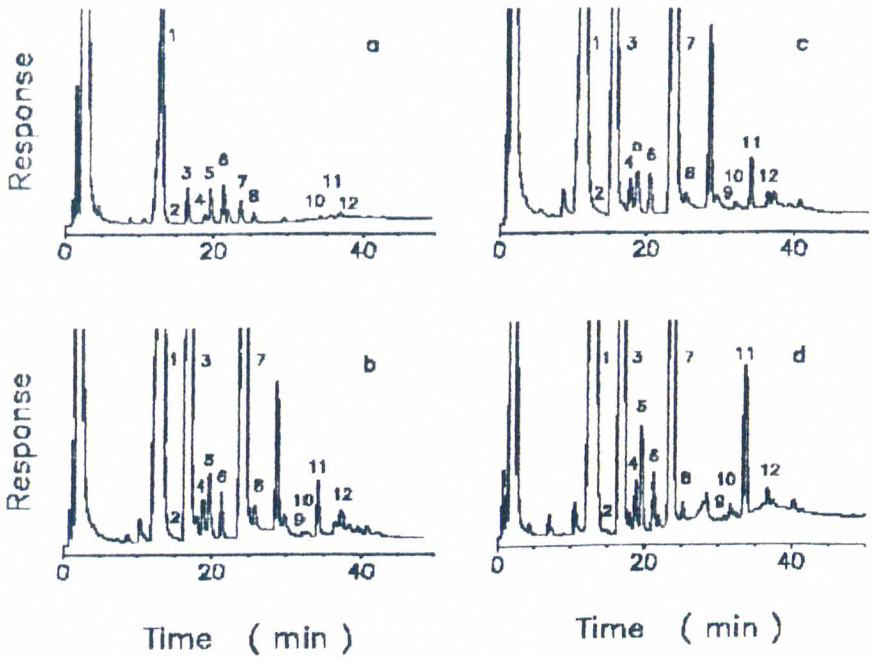

Figure 4.24. Gas chromatograms of polycarboxylic acids formed in the γ-irradiation of an aqueous solution of 0.1 mole dm^{-3} HCN and $K_4Fe(CN)_6$ that have been exposed 61 kGy. The concentration of $K_4Fe(CN)_6$ was set to (mole dm^{-3}): $1X10^{-3}$ (a); $1X10^{-4}$ (b); $1X10^{-5}$ (c); and no additive (d).

Based on the previous discussion it is evident that the effect of hexacyanoferrate(II) on the free-radical oligomerization of HCN was only its inhibition. No new synthetic pathways nor enhancement in products yields was influenced by the reactions of hexacyanoferrate(II) with the free-radicals produced from HCN. On the contrary, hexacyanoferrate(II) only led to the re-formation of HCN by its reaction with the radicals:

$HO-CH=N^{\cdot}$ and $^{-}O-CH=N^{\cdot}$ (reactions 4.32 and 4.34). Therefore, in contradiction to the general ideas of the possible catalytic role of cyanocomplexes in chemical evolution (Beck, 1978), it seems reasonable to conclude that hexacyanoferrate(II) did not play a role in the oligomerization of HCN *via* free-radicals.

The next section examines the effect of hexacyanoferrate(III) on the free-radical oligomerization of HCN.

4.4 The γ-irradiation of aqueous hexacyanoferrate(III)-HCN mixtures

Aqueous, oxygen-free solutions (pH≈6) of 0.1 mole dm^{-3} HCN and 0.001 mole dm^{-3} $K_3Fe(CN)_6$ were irradiated with ^{60}Co-γ-rays in a wide dose range up to about 100 kGy.

Figure 4.25 shows the decomposition of HCN as function of dose. The initial radiation chemical yield of decomposition of HCN was determined to be 2.00. This value is considerably smaller than that obtained

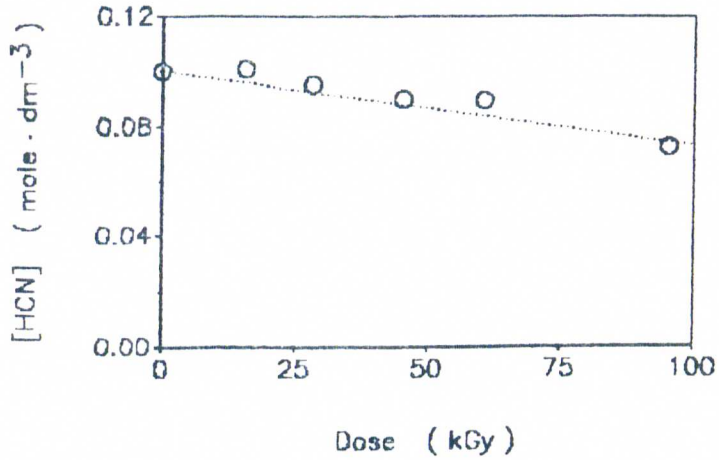

Figure 4.25. Decomposition of HCN in solutions of HCN and $K_3Fe(CN)6$. Dotted line was obtained by computer simulation (see text for details).

in pure aqueous HCN solutions ($G°$=7.60).

The predicted rate decomposition of HCN (dotted line in figure 4.25) is consistent with experimental results. Modeling of this system was carried out taken into account reactions 1 to 54 given in Tables 2.3 to 2.7 (Chapter 2, section 2.7) as well as reactions 4.2 to 4.54 considered in sections 4.2 and 4.3 in this chapter.

The decomposition of HCN was attributed to reactions 4.24 to 4.31. A possible reaction (4.56) of

hexacyanoferrate(III) with $H_2C{=}N^{\cdot}$ radicals could account for the marked decreased of G° (-HCN) in this system:

$$H_2C{=}N^{\cdot} + Fe(CN)_6^{3-} \longrightarrow Fe(CN)_6^{4-} + H^{+} + HCN \qquad (4.56)$$

This reaction was included in computer modeling in order to derive its rate constant; however, computer simulations indicated that such a reaction does not participate in the overall reaction mechanism of decomposition of HCN, and therefore, was ruled out.

The marked decrease in G° (-HCN) is due to a scavenging effect of the species, $H^{\cdot}$ by hexacyanoferrate(III): About 64% of hydrogen atoms react with hexacyanoferrate(II) according to reaction 4.18, and 36% react with hydrogen cyanide according to reaction 4.24.

Figure 4.26 shows the decomposition of hexacyanoferrate(III) as a function of dose. The radiation chemical yield of decomposition of hexacyanoferrate(III) was determined to be 0.18. Computed and experimental trends agree quite well at low doses (<5kGy). Hexacyanoferrate(III) mainly disappears by

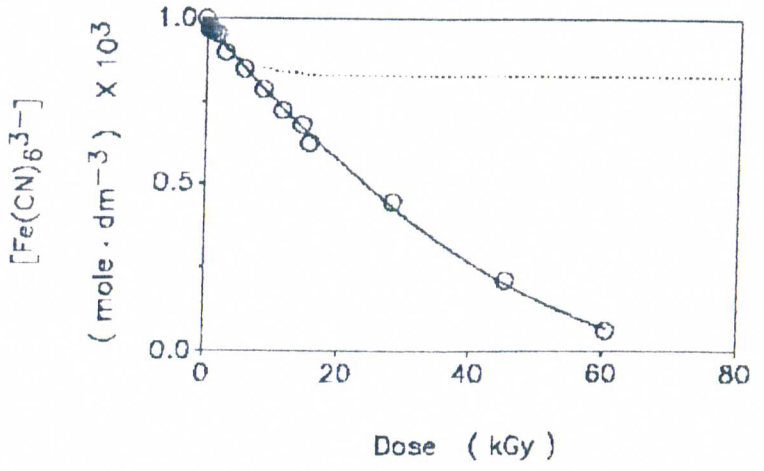

Figure 4.26. Decomposition of hexacyanoferrate(III) in solutions of HCN and $K_3Fe(CN)_6$. Dotted line was obtained by computer simulation (see text for details.

reactions 4.18 and 4.19. At higher doses, the computed and experimental trends deviate. This might be due to reactions of pentacyanoferrate(II) with the free radicals from water radiolysis.

Figure 4.27 and 4.28 show the experimental dose dependence for the formation of hydrogen (G°=0.45) and predicted formation of hydrogen peroxide (G°=0.57), respectively. Their mechanism of formation was given in detail in Chapter 2, section 2.7, and is summarized by reaction 4.1.

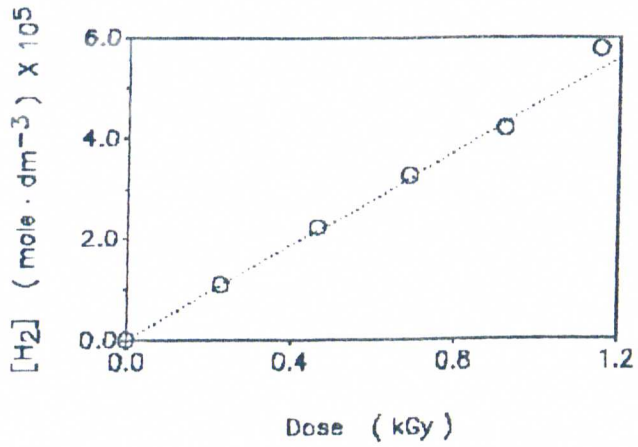

Figure 4.27. Formation of molecular hydrogen during the γ-irradiation of an oxygen-free, aqueous solution of 0.1 mole dm^{-3} HCN and 0.001 mole dm^{-3} $K_3Fe(CN)_6$. Dotted line was obtained by computer simulation (see text for details).

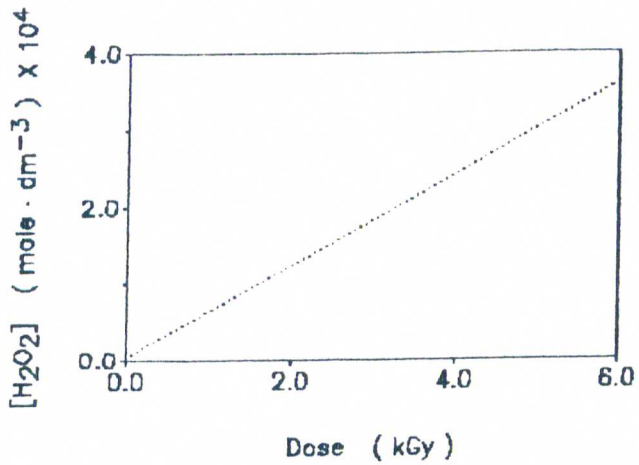

Figure 4.28. Computer simulation for the formation of hydrogen peroxide during the γ-irradiation of an oxygen-free, aqueous solution of 0.1 mole dm^{-3} HCN and 0.001 mole dm^{-3} $K_3Fe(CN)_6$.

Carbon dioxide (Figure 4.29) and ammonia (Figure 4.30) are the major products formed from HCN-$K_4Fe(CN)_6$ mixtures. Their initial radiation chemical yields of formation are 1.00 and 1.10, respectively. Their mechanism of formation may be explained by reactions 4.35 and 4.36, followed by reactions 4.37 to 4.43. In addition, ammonia may also formed by hydrolysis of $H_2C=NH$ (reaction 4.48) and HO-CH=NH (reaction 4.49).

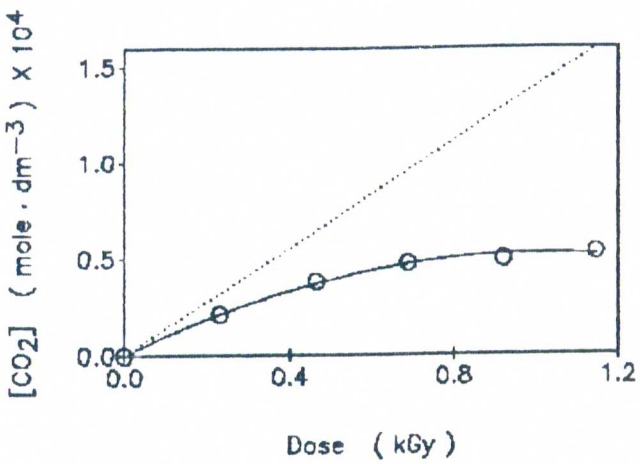

Figure 4.29. Formation of carbon dioxide during the γ-irradiation of an oxygen-free, aqueous solution of 0.1 mole dm^{-3} HCN and 0.001 mole dm^{-3} $K_4Fe(CN)_6$. Dotted line was obtained by computer simulation.

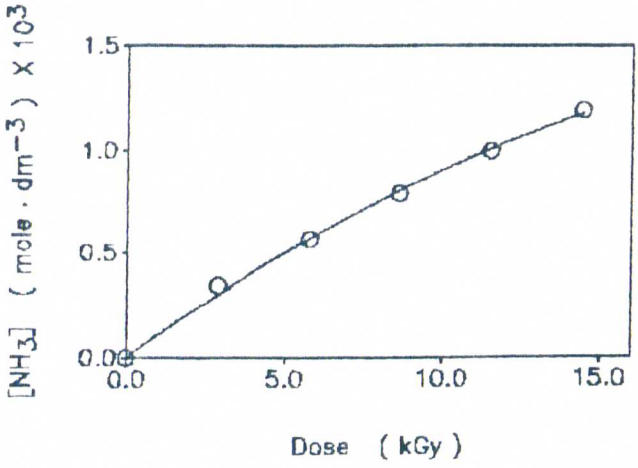

Figure 4.30. Effect of dose on the concentration of ammonia formed radiolytically in 0.1 mole dm^{-3} HCN and 0.001 mole dm^{-3} $K_3Fe(CN)_6$ aqueous solutions.

Figure 4.31 shows gas chromatograms of aldehydes formed in the radiolysis of HCN-$K_3Fe(CN)_6$ mixtures. Formaldehyde ($G°=9.10X10^{-3}$), acetaldehyde ($G°=3.41X10^{-2}$); propionaldehyde ($G°=7.19X10^{-3}$), and butyraldehyde ($G°=1.75X10^{-2}$) were all identified by their retention times and coinjection of standards in gas chromatography, and also by their fragmentation pattern by electron impact and chemical ionization mass spectrometry (Figure 4.32). Their radiation chemical yields were calculated from the slope of concentration *vs* dose plots as that shown in Figure 4.33. The concentration of formaldehyde linearly increase with

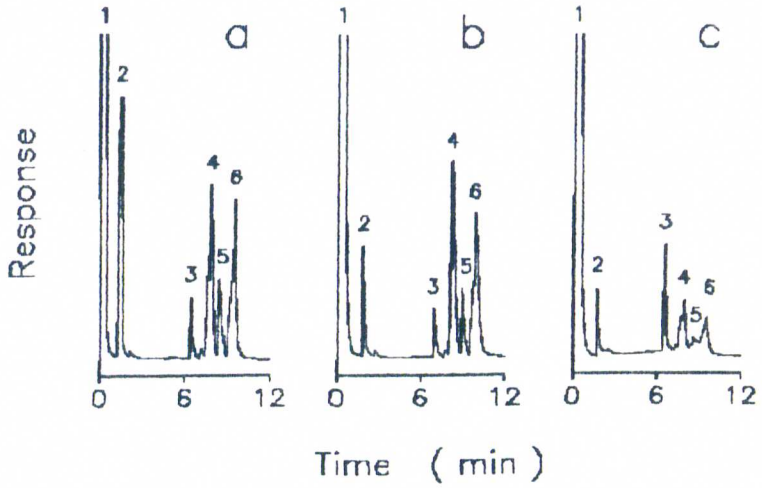

Figure 4.31. Gas chromatogram of 2,4-dinitrophenyl-hydrazone derivatives of aldehydes formed at 27 (a), 61 (b) and 95 (b) kGy of ^{60}Co-irradiation of an oxygen-free, aqueous solution of 0.1 mole dm^{-3} HCN and 0.001 mole dm^{-3} $K_3Fe(CN)6$. See legend in Figure 4.16 for peak assignment.

irradiation dose. Its mechanism of formation may be explained by reaction 4.48.

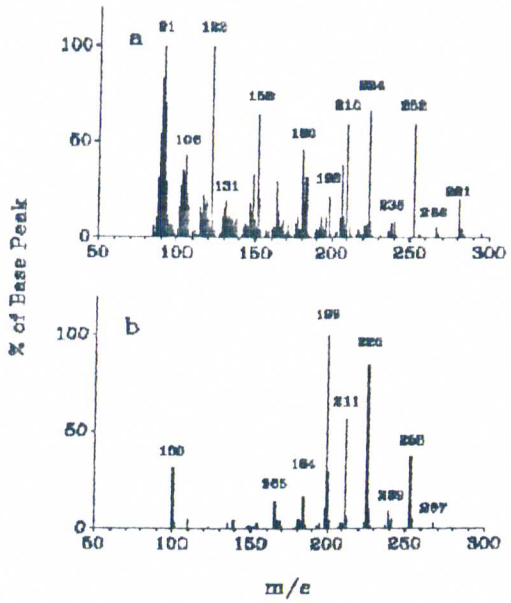

Figure 4.32. Electron impact (a) and chemical ionization (b) mass spectra of the 2,4-dinitrophenyl-hydrazone fraction formed at 95 kGy in the HCN-$K_3Fe(CN)_6$ system.

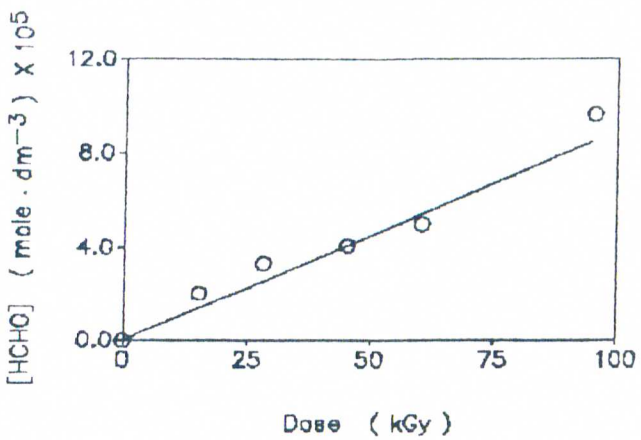

Figure 4.33. Dose dependence for the formation of formaldehyde in the HCN-$K_3Fe(CN)_6$ system.

Oxalic acid was identified as the major polycarboxylic acid formed in irradiated HCN-$K_3Fe(CN)_6$ solutions (Figure 4.34). A variety of other acids were

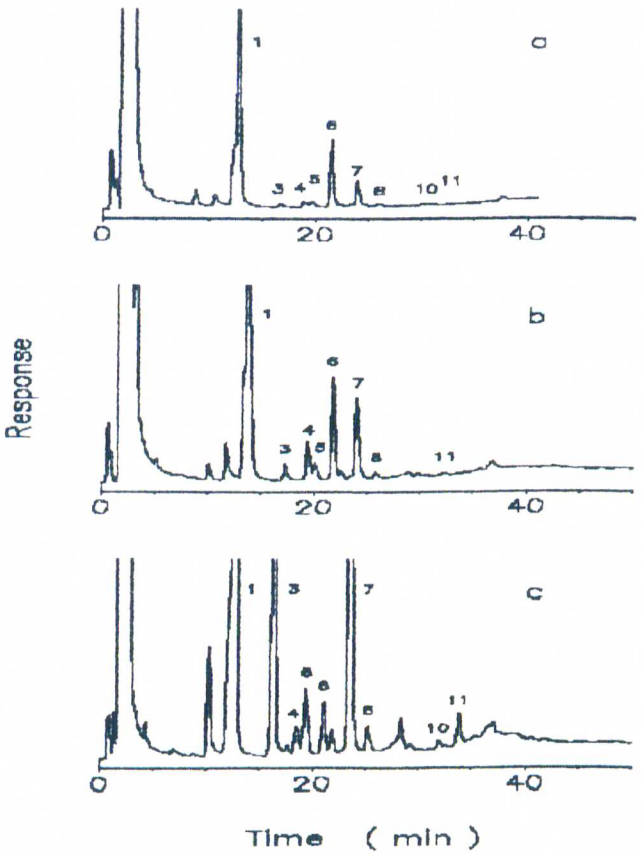

Figure 4.34. Gas chromatograms of polycarboxylic acids methyl esters formed at 27 (a), 46 (b) and 95 (c) kGy in the HCN-$K_3Fe(CN)_6$ system. See Figure 4.19 for peak assignment.

also formed but in low yield. Their identification was based on retention times and coinjections with standards in gas chromatography. Supporting evidence was based on the GC-MS analysis carried out for the HCN-$K_4Fe(CN)_6$ system (Section 4.3).

Table 4.2 summarizes the initial radiation chemical yields of formation of polycarboxylic acids.

Table 4.2. Initial chemical yields ($G°$) of formation of polycarboxylic acids.

Compound	$G°$
Oxalic	1.60×10^{-2}
Malonic	1.15×10^{-4}
Fumaric	3.90×10^{-5}
Succinic	2.57×10^{-5}
1,2-Dimethyl succinic	9.95×10^{-6}
Maleic	1.14×10^{-4}
Glutaric	2.83×10^{-5}
Adipic	5.12×10^{-6}
Malic	5.87×10^{-6}

The concentration of polycarboxylic acids exponentially increases with dose with the exception of oxalic acid. Figure 4.35 shows these behavior for oxalic and maleic acids.

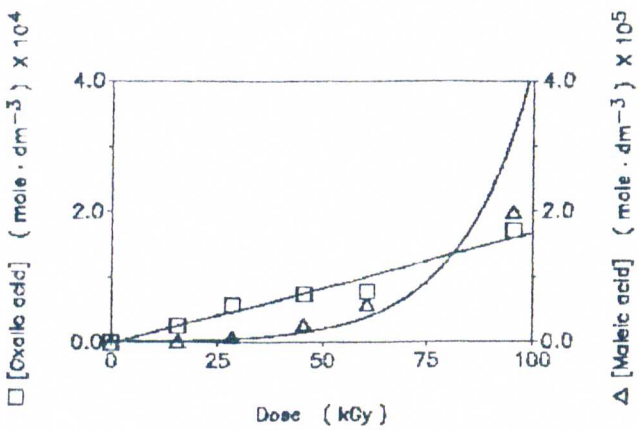

Figure 4.35. Dose dependance of the formation of oxalic and maleic acids in the HCN-$K_3Fe(CN)_6$ system.

Oligomeric material was formed in low yield in HCN-$K_3Fe(CN)_6$ mixtures (Figure 4.36). At low doses its is very low but exponentially increases with irradiation dose. The initial radiation chemical yields of

formation for this material were determined to be: G° (C)=0.87; G° (N)=0.82; G° (H)=0.88; and G° (O)=0.09.

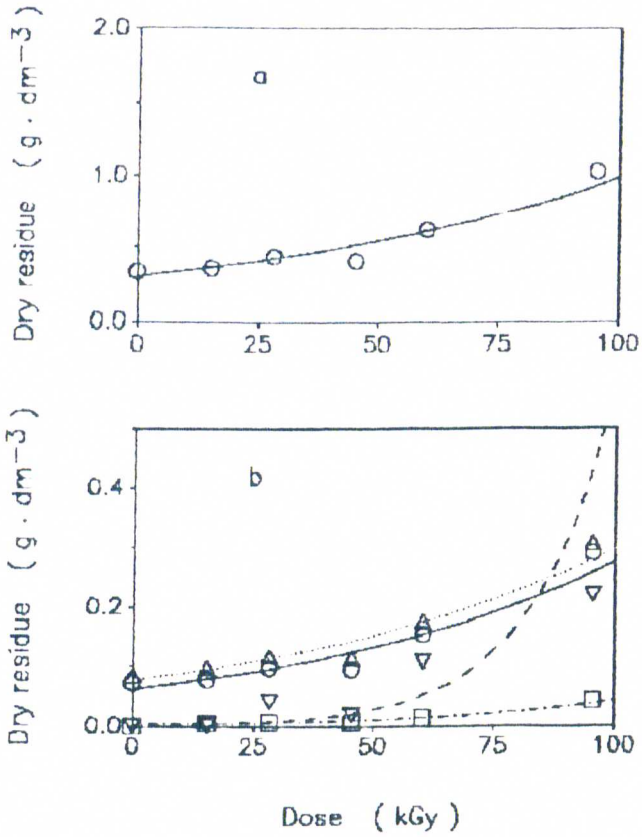

Figure 4.36. Dose dependance of the formation of oligomeric material measured as total dry residue (a) and as specific elemental composition in the residue (b): Carbon (O); nitrogen (△); hydrogen (□); and oxygen (▽).

The results given in this section indicate that hexacyanoferrate(III) does not lead to an enhancement of products yields nor contribute to new synthetic pathways. Hexacyanoferrate(III) markedly inhibits the decomposition and oligomerization of hydrogen cyanide. The mechanism responsible for such an effect is due to the scavenging of $H^{\cdot}$ and e_{aq}^{-} by hexacyanoferrate(III), reactions 4.18 and 4.19. Therefore, it seems reasonable to conclude that hexacyanoferrate(II) did not play a role in the oligomerization of HCN *via* free-radicals.

A comparison of the results obtained in the radiolysis of hydrogen cyanide in the presence or absence of hexacyanoferrate(II) or (III) is given in section 4.4.

4.5 The effect of cyanocomplexes in the free-radical oligomerization of HCN: Implications to chemical evolution

Table 4.3 summarizes the initial radiation chemical yields of major products obtained in the radiolysis of aqueous solutions of 0.1 mole dm^{-3} HCN in the

Table 4.3. Initial radiation chemical yields ($G°$).

Compound	$G°$		
	HCN		
	No additive	$K_4Fe(CN)_6$	$K_3Fe(CN)_6$
-HCN	7.60	2.00	2.00
$Fe(CN)_6^{3-}$	----	4.10	-0.18
H_2	0.38*	0.45	0.45
CO_2	0.80*	0.60	1.00
NH_3	2.46*	1.01	1.10
HCHO	0.18	0.009	0.009
(CO_2H)	0.22	0.022	0.016
Oligomeric material: (-HCN)	5.80	1.22	0.87

*Draganic *et al.*, 1973.

absence or presence of 0.001 mole dm^{-3} of $K_4Fe(CN)_6$ or $K_3Fe(CN)_6$.

The decomposition of hydrogen cyanide is markedly decrease from 7.60 to 2.00 in the presence of hexacyanoferrates. Carbon dioxide and ammonia were the major products in the presence of cyanocomplexes. The yields of other products such as formaldehyde and oxalic acid were decreased at least by an order of magnitude. About 76% of decomposed HCN molecules are built up into larger molecules in pure HCN solutions. The yield of this oligomeric material decreases to about 61% or 44% in the presence of hexacyanoferrate(II) or (III), respectively.

The effect of hexacyanoferrate(II) or (III) on the radiolysis of aqueous solutions of HCN was the marked decrease in the yield of decomposition of HCN. In the case of hexacyanoferrate(II), this effect was attributed to the re-formation of HCN by the reactions of $Fe(CN)_6^{4-}$ with HO-CH=N· and $^-$O-CH=N· , reactions 4.32 and 4.34:

$$HO\text{-}CH{=}N^{\cdot} + Fe(CN)_6^{4-} \longrightarrow Fe(CN)_6^{3-} + HCN + HO^{-} \quad (4.32)$$

$$^{-}O\text{-}CH{=}N^{\cdot} + Fe(CN)_6^{4-} \longrightarrow Fe(CN)_6^{3-} + HO^{-} + {}^{-}CN \quad (4.34)$$

Whereas in the case of hexacyanoferrate(III), the marked decrease in G° (-HCN) was attributed to a scavenging effect of $H^{\cdot}$ by hexacyanoferrate(III): 64% of hydrogen atoms react with hexacyanoferrate(II) according to reaction 4.18, and 36% react with hydrogen cyanide according to reaction 4.24.

$$H^{\cdot} + Fe(CN)_6^{3-} \longrightarrow Fe(CN)_6^{4-} + H^{+} \quad (4.19a)$$

$$H^{\cdot} + Fe(CN)_6^{3-} \longrightarrow Fe(CN)_5^{3-} + HCN \quad (4.19b)$$

$$H^{\cdot} + HCN \longrightarrow H_2C{=}N^{\cdot} \quad (4.24)$$

In spite of the differences in mechanisms between hexacyanoferrate(II) and (III), the overall effect is the same, a marked decrease in G° (-HCN). Furthermore, the initial yields of certain products such as H_2, NH_3 and HCHO are almost similar, and at higher doses of irradiations the differences in product yields becomes less apparent between the two systems (see for instance GC profiles for carboxylic acids, Figures 4.19 and 4.34). The lack of a significant difference between the two systems, particularly at high doses, is due to

the fast interconversion of hexacyanoferrate(II) into (III) and *viceversa*. Therefore, after a few Gy of radiation dose, both hexacyanoferrate(II) and (III) are participating in the reaction mechanism.

The effect of other cyanocomplexes of transition elements on the free-radical oligomerization of HCN is expected to be similar to that found for hexacyanoferrate(II) and (III). This is because the rates and modes of reactions of cyanocomplexes of transition elements with hydroxyl radicals (Figure 4.37), hydrogen atoms (Figure 4.38), and hydrated electrons (Figure 4.39) are very similar.

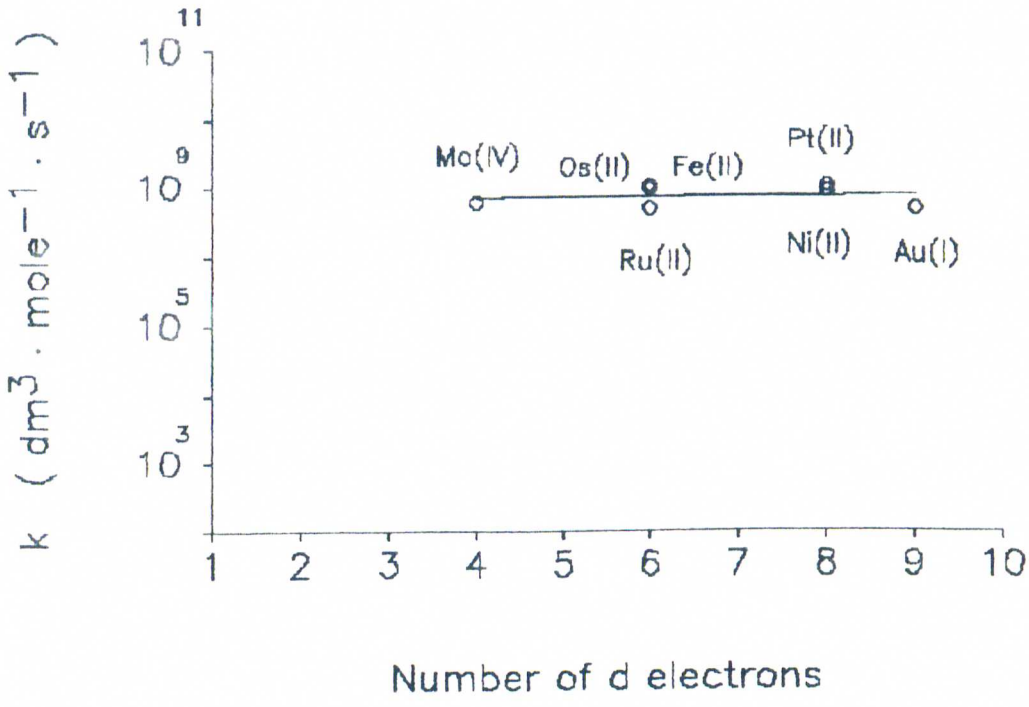

Figure 4.37. Dependance of the rate of reaction (k) of hydroxyl radicals with cyanocomplexes of transition elements. Values were taken from Ross and Ross, 1977, and Buxton *et al.*, 1988.

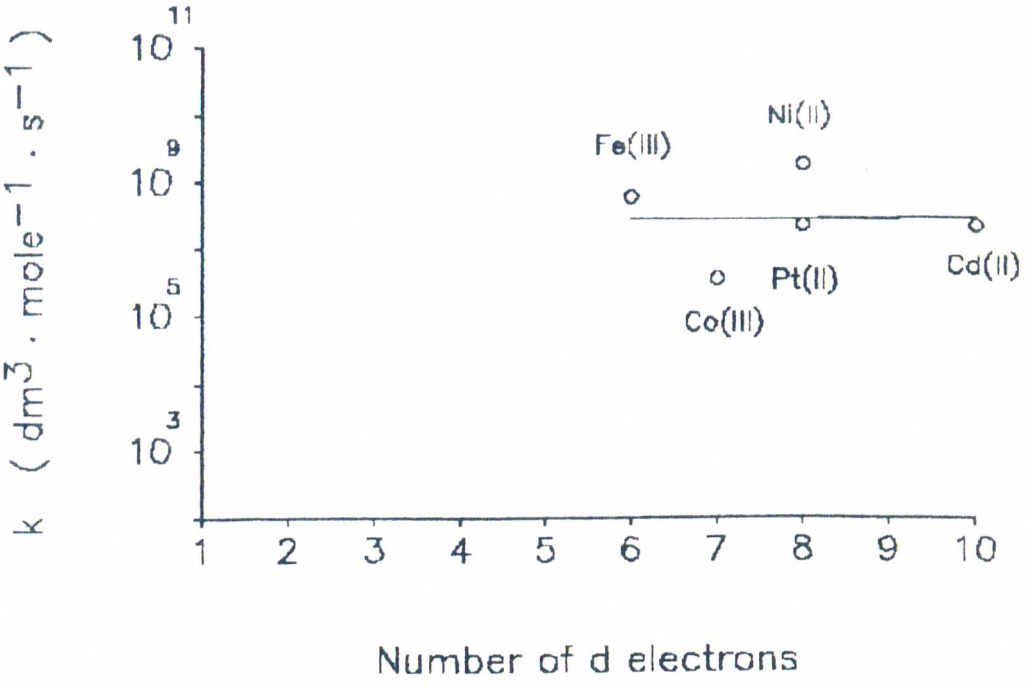

Figure 4.38. Dependance of the rate of reaction (k) of hydrogen atoms with cyanocomplexes of transition elements. Values were taken from Anbar and Ross, 1975, and Buxton *et al.*, 1988.

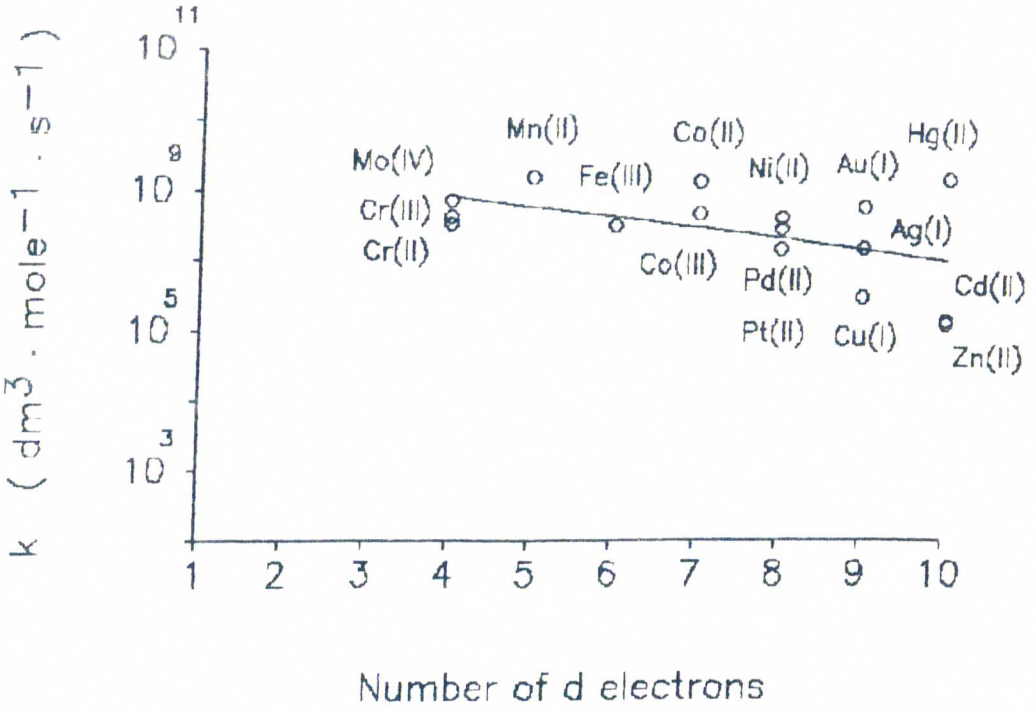

Figure 4.39. Dependance of the rate of reaction (k) of hydrated electrons with cyanocomplexes of transition elements. Values were taken from Anbar *et al.*, 1973, Ross, 1975, and Buxton *et al.*, 1988.

4.6 Conclusions

A comprehensive investigation of the effect of hexacyanoferrate(II) and (III) on the free-radical oligomerization of HCN was carried out. The γ-radiolysis of aqueous solutions of 0.02 mole dm^{-3} $K_4Fe(CN)_6$, 0.1 mole dm^{-3} HCN in the presence of (10^{-5}-10^{-3} mole dm^{-3}) $K_4Fe(CN)_6$ or 10^{-3} $K_3Fe(CN)_6$ were investigated in a wide dose range.

The radiation chemical yields for a variety of products were calculated, these included among others: H_2, CO_2, NH_3, $Fe(CN)_6^{3-}$, $Fe(CN)_6^{4-}$, and a variety of aldehydes and polycarboxylic acids.

The results indicated that hexacyanoferrate(II) or (III) have a significant effect on the free-radical oligomerization of HCN; however, rather than increasing the product yields and/or opening new synthetic pathways, re-formation of HCN, and predominant production of CO_2 and NH_3 were the principal pathways.

Computer simulations were performed to model the radiolysis of mixtures of aqueous solutions of hydrogen cyanide and hexacyanoferrates. The reaction mechanism consisted of about 110 simultaneous chemical equations.

Evaluation of the experimental data by computer simulation permitted the elucidation of the mechanism and the derivation of the rate for the following reactions:

$$HO\text{-}CH{=}N^{\cdot} + Fe(CN)_6^{4-} \longrightarrow Fe(CN)_6^{3-} + HCN + HO^{-}$$

$$^{-}O\text{-}CH{=}N^{\cdot} + Fe(CN)_6^{4-} \longrightarrow Fe(CN)_6^{3-} + HO^{-} + {}^{-}CN$$

The results obtained in this study provide an insight into the possible role of cyanocomplexes in chemical evolution.

CHAPTER 5

GENERAL CONCLUSIONS

Hydrogen cyanide is generally considered to have been a key molecule in the process of chemical evolution because:

1. It is widely distributed in the interstellar medium, in the comets, and in the atmospheres of Jupiter and Titan;

2. It is readily synthesized under a large variety of experimental conditions that are relevant to primitive Earth scenarios; and

3. It is an important precursor to the synthesis of a large array of biomolecules.

The extensive literature on the abiotic chemistry of hydrogen cyanide was reviewed in Chapter 1. At

present there is a significant understanding of several aspects of the abiotic chemistry of hydrogen cyanide. There were two areas of research, however that required further study:

1. The investigation of the electrosynthesis of hydrogen cyanide from a simulated primitive atmosphere; and,

2. The possible role of cyanocomplexes of transition metal ions on the free-radical oligomerization of hydrogen cyanide.

The main research objective of this dissertation was a comprehensive investigation into the chemistry of hydrogen cyanide. Although much work has been done in this field, it has been of a qualitative nature. To obtain a better understanding, we have concentrated on the quantitative and modeling aspects as well.

5.1 Electrolysis of a simulated primitive atmosphere: The synthesis of hydrogen cyanide.

5.1.1 Quantitative methods

Three new methods were developed to determine the precise dose rate supplied by high voltage, high frequency electric discharges:

1. Using methane as the chemical dosimeter;

2. Measurements of the electric discharge voltage and current through an oscilloscope; and,

3. Measurements of the electric discharge voltage and current by calorimetry.

The dose rate was determined to be 2.73 MGy hr^{-1} with a standard deviation of 15%. Knowledge of this parameter was essential to study the electrolysis of a simulated primitive atmosphere.

5.1.2 Quantitative results

The electrolysis of a CH_4-N_2-H_2O gas mixture was thoroughly investigated:

1. The initial chemical yields of decomposition of methane and nitrogen were determined to be 6.54 and 1.26, respectively.

2. About 96% of the initial methane and 10% of the initial nitrogen were converted into:
   a. C_2H_2 (G°=2.14);
   b. C_2H_6 (G°=0.57);
   c. HCN (G°=0.26);
   d. CH_3CHO (G°=0.13);
   e. CH_3CH_2CHO (G°=0.011);
   f. $CH_2(CH_2)_2CHO$ (G°=0.016); and
   g. Unidentified water-insoluble oligomeric material (G°=0.25 for carbon).

5.1.3 Computer modeling

A free radical mechanism was developed to account for the chemical changes produced by electric discharges. Computer modeling of such a mechanism could ef-

fectively predict the initial trends of experimental data.

1. Hydrogen cyanide originated according to the following mechanism:

$$CH_3\cdot + \cdot N: \longrightarrow HCN + H_2$$

$$:CH_2 + \cdot N: \longrightarrow HCN + H\cdot$$

2. Computer modeling of this system permitted an evaluation of the possible rate of production of hydrogen cyanide in the primitive atmosphere under a variety of conditions such as chemical composition, pressure, and temperature. $G°$ (HCN) could vary from 0.1 to 0.4 depending on the atmospheric conditions.

3. The possible rate of electrosynthesis of HCN in the primitive atmosphere was estimated to vary from 10^{-4} to 10^{-3} mole cm^{-3} y^{-1} depending on the atmospheric conditions.

5.2 The effect of cyanocomplexes on the free-radical oligomerization of hydrogen cyanide

Cyanocomplexes of transition elements are generally believed to have played a role in the catalysis and synthesis of biomolecules in the process of chemical evolution. The main research goal was to investigate the possible effect of cyanocomplexes of transition elements on the free-radical oligomerization of HCN. Specifically, we were interested in hexacyanoferrate (II) and (III), since they probably accumulated in the primitive oceans. There was great interest in this investigation since only a limited number of studies in abiotic chemistry has been devoted to examine the effects of metal ions in catalyzing reactions of significance to the origins of life.

A comprehensive investigation was undertaken to study the γ-irradiation of aqueous solutions of hydrogen cyanide in the presence of hexacyanoferrate(II) or (III).

5.2.1 Radiation chemical yields

The G° values for HCN, $K_4Fe(CN)_6$, $K_3Fe(CN)_6$, H_2, CO_2, HCHO, CH_3CHO, CH_3CH_2CHO, $CH_3(CH_2)_3CHO$, $(CO_2H)_2$ and

a variety of polycarboxylic acids were determined under different conditions.

5.2.2 Mechanism of reaction

Evaluation of the experimental data by computer simulations consisted of about 110 simultaneous chemical reactions. This study permitted the elucidation of the reaction mechanism:

1. Hexacyanoferrate(II) reacts with $HO-CH=N^{\cdot}$ and/or $^{-}O-CH=N^{\cdot}$ according to:

$$HO-CH=N^{\cdot} + Fe(CN)_6^{4-} \longrightarrow Fe(CN)_6^{3-} + HCN + HO^{-}$$

$$^{-}O-CH=N^{\cdot} + Fe(CN)_6^{4-} \longrightarrow Fe(CN)_6^{3-} + HO^{-} + {}^{-}CN$$

2. Hexacyanoferrate(III) competes with hydrogen cyanide for hydrogen atoms. 64% of hydrogen atoms react with hexacyanoferrate(II) according to:

$$H^{\cdot} + Fe(CN)_6^{3-} \longrightarrow \begin{cases} Fe(CN)_6^{4-} + H^{+} \\ Fe(CN)_5^{3-} + HCN \end{cases}$$

$$H^{\cdot} + HCN \longrightarrow H_2C=N^{\cdot}$$

5.2.3 Effect on the free-radical oligomerization of HCN

The decomposition of hydrogen cyanide was markedly decrease from 7.60 to 2.00 in the presence of hexacyanoferrates. Carbon dioxide and ammonia were the major products in the presence of hexacyanoferrates. About 76% of decomposed HCN molecules are built up into larger molecules in pure aqueous HCN solutions. The yield of this oligomeric material decreases to about 61% or 44% in the presence of hexacyanoferrate(II) or (III), respectively. The results obtained in this study provided an insight into the possible role of cyanocomplexes in chemical evolution.

REFERENCES

Abelson, P.H.: 1966, Proc. Nat. Acad. Sci. USA **55**, 1365.

Anbar, M. and Hart, E.J.: 1965, J. Phys. Chem. **69**, 973.

Anbar, M. and Neta, P.: 1967, Int. J. Appl. Rad. Isotopes 18, 493.

Anbar, M., Bambenek, M. and Ross, A.B.: 1971, Selected Specific Rates of Reactions of Transients From Water in Aqueous Solution. 1. Hydrated Electron, **NSRDS-NBS-43**, National Bureau of Standards, Washington, D.C.

Anbar, M., Ross, F. and Ross, A.B.: 1975, Selected Specific Rates of Reactions of Transients From Water in Aqueous Solution. II. Hydrogen Atom, **NSRDS-NBS-51**, National Bureau of Standards, Washington, D.C.

Arai, H., Nagai, S., Matsuda, K. and Hatada, M.: 1981a, Radiat. Phys. Chem. **17**, 151.

Arai, H., Nagai, S., Matsuda, K. and Hatada, M.: 1981b, Radiat. Phys. Chem. **17**, 217.

Armstrong, D.A. and Winkler, C.A.: 1955, Canad. J. Chem. **33**, 1649.

Bada, J.L. and Miller, S.L.: 1968, Science **159**, 423.

Balestic, F.: 1974, Synthése Abiotique d'acides Aminés par voie Radiochimique, Thése de Doctorat d'Etat es Sciences, Université de Paris Sud, Orsay.

Bamford, C. H. and Wayne, R. P.: 1967, in Ashmore, P.G., Dainton, F.S. and Sugden, T.M. (eds.), Photochemistry and Reaction Kinetics, Univ. Press, Cambridge, p. 26.

Bar-Nun, A. and Tauber, M.E.: 1972, Space Life Sciences 3, 254.

Bar-Nun, A. and Shaviv, A.: 1975, Icarus **24**, 197.

Bar-Nun, A.: 1981, in Lifshitz, A., ed., Shock Waves in Chemistry, Marcel Dekker, Inc., New York, 183.

Basset, J. (ed.): 1978, Vogel's Textbook of Quantitative Inorganic Analysis, Longman, London.

Baulch, D.L., Cox, R.A., Crutzen, P.J., Hampson, R.F. Jr., Kerr, J.A., Troe, J. and Watson, R.T.: 1982, J. Phys. Chem. Ref. Data 11, 327.

Beck, M.T.: 1978, in Sigel, H. (ed.), Metal Ions in Biological Systems, Marcel Dekker, New York, 1978, Vol. 7, p. 1.

Behar, D. and Fessenden, R.W.: 1972, J. Phys. Chem. 76, 3945.

Behar, D.: 1974, J. Phys. Chem. 78, 2660.

Bielski, B.H.J. and Allen, A.O.: 1977, J. Am. Chem. Soc. 99, 5931.

Bielski, B.H.J., Cabelli, D.E. and Arudi, R.L.: 1985, J. Phys. Chem. Ref. Data 14, 1041.

Borisova, E.N. and Eremin, E.N.: 1968, in Pechuro, N.S. (ed.), Organic Reactions in Electric Discharges, Consultants Bureau, New York, 52.

Bossard, A. and Toupance, G.: 1980, Nature 288, 243.

Bosaard A., Raulin, F., Mourey, D. and Toupance, G.: 1981, in Wolman, Y. (ed.), Origin of Life, D. Reidel Publ. Co., Holland, 83.

Bosaard, A., Raulin, F., Mourey, D. and Toupance, G.: 1982, J. Mol. Evol. 18, 173.

Bosaard, A., Mourey, D. and Raulin, F.: 1983, Adv. Space Res. 3, 39.

Braun, W., Welge, K.H. and McNesby, J.R.: 1966, J. Chem. Phys. 45, 2650.

Braun, W., McNesby, J.R. and Bass, A.M.: 1967, J. Chem. Phys. 46, 2071.

Braun, W., Herron, J.T. and Kahaner, D.K.: 1988, International J. Chem. Kinetics 20, 51.

Brewer, P.R.: 1975, in Riley J.P. and Skirrow, G. (eds.), Chemical Oceanography, Academic Press, London, 415.

Buchler, H., Buhler, R.E. and Cooper, R.: 1976, J. Phys. Chem. 80, 1549.

Buxton, G.V. and Sellers, R.M.: 1978, Compilation of Rate Constants for the Reactions of Metal Ions in Unusual Valency States, NSRDS-NBS-62, National Bureau of Standards, Washington, D.C.

Buxton, G.V., Greenstock, C.L., Helman, W.P. and Ross, A.B.: 1988, J. Phys. Chem. Ref. Data 17, 513.

Canuto, M.V., Levine, J.S., Augustsson, T.R., and Imhoff, C.L.: 1982, Nature 296, 816.

Canuto, V.M., Levine, J.S., Augustsson, T.R., Imhoff, C.L. and Giampapa, M.S.: 1983, Nature 305, 281.

Castellan, G.W.: 1983, Physical Chemistry, 3rd. Edition, Addison-Wesley Publishing Company, Massachusetts, 943 p.

Castillo, S.: 1983, Radiolysis of Malic Acid in Aqueous Solution, Tesis de Maestria de la Facultad de Química, Universidad Nacional Autonoma de México. Mexico D.F., 15.

Chang, S., Scattergood, T., Arowitz, S. and Flores, J.: 1979, Rev. Geophys Space Phys. 17, 1923.

Chen, C.J., Back, M.H. and Back, R.A.: 1975, Canad. J. Chem. 53, 3580.

Cochran, E.L., Adrian, F.J. and Bowers, V.: 1962, J. Chem. Phys. 36, 1938.

Cohen, N. and Westberg, K.R.: 1983, J. Phys. Chem. Ref. Data 12, 531.

Day, R.A.Jr. and Underwood, A.L.: 1980, Quantitative Analysis, 4th edition, Prentice-Hall, Inc., N.J.

Davies, G. and Garafalo, A.R.: 1976, Inorg. Chem. 15, 1101.

Ditchburn, R.W.: 1955, Proc. Roy. Soc. (London) A229, 44.

Dodonova, N. Y.: 1966, Russ. J. Phys. Chem. 40, 523.

Dorfman, L.M. and Adams, G.E.: 1973, Reactivity of the Hydroxyl Radical in Aqueous Solutions, NSRDS-NBS-46, National Bureau of Standards, Washington, D.C.

Draganic, I.G. and Draganic, Z.D.: 1971, The Radiation Chemistry of Water, Acad. Press, New York, 242 p.

Draganic, I., Draganic, Z., Petkovic, L. and Nikolic, A.: 1973, J. Am. Chem. Soc. 95, 7193.

Draganic, Z.D., Draganic, I.G. and Borovicanin, M.: 1976a, Rad. Res. 66, 42.

Draganic, I.G., Draganic, Z.D. and Markovic, V.M.: 1976b, Int. J. Radiat. Phys. Chem. 8, 339.

Draganic, Z.D. and Draganic, I.G.: 1977, Rad. Res. 69, 223.

Draganic, Z., Draganic, I., Shimoyama, A. and Ponnamperuma, C.: 1977a, Origins of Life 8, 371.

Draganic, I.G., Draganic, Z.D., Jovanovic, S., and Ribnikar, S.V.: 1977b, J. Mol. Evol. 10, 103.

Draganic, I.G. and Draganic, Z.D.: 1980, Memorias del III Simposio sobre Quimica Nuclear, Radioquimica y Quimica de Radiaciones, C.E.N., U.N.A.M., 137.

Draganic, Z.D., Niketic, V., Jovanovic, S. and Draganic, I.G.: 1980, J. Mol. Evol. 15, 239.

Duffey, S.S: 1981, in Vennesland, B., Conn, E.E., Knowless, C.J., Westley, J. and Wissing, F. (eds), Cyanide in Biology, Academic Press, London, 385.

Eaton, D.R. and Pankratz, M.: 1985, CAN. J. Chem. 63, 793.

Fegly, B.Jr., Prinn, R.G., Hartman, H. and Watkins, G.H.: 1986, Nature 319, 305.

Ferris, J.P., Donner, D.B. and Lotz, W.: 1972, J. Am. Chem. Soc. 94, 6968.

Ferris, J.P. and Ryan, T.J.: 1973, J. Org. Chem. 38, 3302.

Ferris, J.P., Sanchez, R.A. amd Mancuso, R.W.: 1973, Organic Syntheses 5, 32.

Ferris, J.P. and Nicodem, D.E.: 1974, in Dose, K., Fox, S.W., Deborin, G.A. and Pavlvskaya, T.E. (eds.), The Origin of Life and Evolutionary Biochemistry, Plenum Press, New York, 107.

Ferris, J.P., Williams, E.A., Nicodem, D.E., Hubbard, J.S. and Voecks, G.E.: 1974a, Nature 249, 437.

Ferris, J.P., Wos, J.D. and Lobo, A.P.: 1974b, J. Mol. Evol. 3, 311.

Ferris, J.P. and Chen, C.T.: 1975, Nature 258, 587.

Ferris, J.P. and Joshi, P.C.: 1978, Science 201, 361.

Ferris, J.P. and Edelson, E.H.: 1978, J. Org. Chem. 43, 3989.

Ferris, J.P., Joshi, P.C., Edelson, E.H. and Lawless, J.G.: 1978, J. Mol. Evol. 11 , 293.

Ferris, J.P., Alwis, K.W., Edelson, E.H., Mount, N. and Hagan, W.J.Jr.: 1981a, in Wolman, Y. (ed.), Origin of Life, D. Reidel Publ. Co., 125.

Ferris, J.P., Edelson, E.H., Auyeung, J.M. and Joshi, P.C.: 1981b, J. Mol. Evol. 17, 69.

Ferris, J.P., Hagan, W.J.Jr., Alwis, K.W. and McCrea, J.: 1982, J. Mol. Evol. 18, 304.

Ferris, J.P. and Hagan, W.J.Jr: 1984, Tetrahedron 40, 1093.

Field, F.H., Franklin, J.L. and Munson, M.S.D.: 1963, J. Am. Chem. Soc. 85, 3575.

Fox, S.W., and Dose, K.: 1977, Molecular Evolution and the Origin of Life, Revised Ed., Marcel Dekker Inc., New York, 370 p.

Fripiat, J.J. and Cruz-Cumplido, M.I.: 1974, Ann. Rev. Earth and Planet. Sci. 2, 239.

Froben F.W.: 1974, Ber. Bunsen-Gesellschaft Phys. Chem. 78, 184.

Fugio, C.: 1930, Bull. Chem. Soc. (Japan) 5, 249.

Garrison, W.M., Morrison, D.C., Hamilton, J.G., Benson, A.A. and Calvin, M.: 1951, Science 114, 416.

Gordon, R. and Ausloos, P.: 1967, J. Phys. Chem. 46, 4823.

Groth, W. and Suess, H.: 1938, Naturwissenschaften 26, 77.

Haissinsky, M., Koulkes, A.M. and Masri, E.: 1966, J. Chim. Phys. 63, 1129.

Haldane, J.B.S.: 1929, The Origin of Life, The Rationalist Annual. (in J.D.: 1967, The Origin of Life, Weidenfeld and Nicolson, London, 242).

Hanel, R.A., Conrath, B., Flaser, F.M., Kunde, V., Maguire, W., Pearl, J., Pirraglia, J., Samuelson, R., Herath, L., Allison, M., Cruikshank, D., Gautier, D., Gierasch, P., Horn, L., Koppany, R. and Ponnamperuma, C.: 1981, Science 18, 157.

Harada, K. and Fox, S.W.: 1964, Nature 201, 335.

Harada, K. and Iwasaki, T.: 1975, Chem. Letters 185.

Harada, K., Suzuki, S. and Ishida, H.: 1978, Experientia **34**, 17.

Harada, K., Hasegawa, N. and Shimoyama, A.: 1984, Origins of Life **14**, 115.

Harkins, W. and Jackson, J.M.: 1933, J. Chem. Phys. **1**, 37.

Harteck, P. and Dondes, S.: 1957, J. Chem. Phys., **27**, 546.

Harteck, P. and Dondes, S.: 1958a, J. Chem. Phys., **28**, 975.

Harteck, P. and Dondes, S.: 1958b, J. Phys. Chem., **63**, 956.

Harting, R., Troe, J. and Wagner, H.G.G.: 1971, 13th Symposium on Combustion, Combustion Institute, Pittsburgh, 147.

Harting, K.J. and Getoff, N.: 1980, J. Photochem. **13**, 207.

Hauser, W.P.: 1964, J. Phys. Chem. **68**, 1576.

Hoing, E.R. and Sheppard, C.W.: 1946, J. Phys. Chem. **50**, 119.

Hug, G.L.: 1981, Optical Spectra of Nonmetallic Inorganic Transients Species in Aqueous Solution, **NSRDS-NBS-69**, National Bureau of Standards, Washington, D.C.

James, A.D. and Murray, R.S.: 1975, J. Chem. Soc. Dalton 1530.

Kammaludin, Singh, M. and Deopujari, S. W.: 1986, Origins of life 17, 59.

Kevorkian, V., Heath, C.E. and Boudart, M.: 1960, J. Phys. Chem. **64**, 964.

Kliss, R. M. and Matthews, C. N.: 1962, Proc. Nat. Acad. Sci. USA **48**, 1130.

Kobayashi, K. and Ponnamperuma, C.: 1985a, Origins of Life 16, 41.

Kobayashi, K. and Ponnamperuma, C.: 1985b, Origins of Life 16, 57.

Kobayashi, K. and Ponnamperuma, C.: 1986, Viva Origino 14, 41.

Koberstein, E.: 1973, Ind. Engng. Chem. Process. Des. Dev. 12, 444.

Kondratiev, V.N.: 1965, 10th Symposium on Combustion, Combustion Institute, Pittsburgh, 319.

Kozlov, G.I. and Knorre, V.G.: 1963, Russ J. Phys. Chem. 9, 1128.

Kraljic, I. and Trumbore, C.N.: 1965, J. Am. Chem. Soc. 87, 2547.

Kuhn, W.R. and Atreya, S.K.: 1979, Icarus 37, 207.

Lampe, F.W.: 1957, J. Am. Chem. Soc. 79, 1055.

Laufer, A. and Bass, A.: 1978, Combustion and Flame 32, 215.

Lasaga, A.C., Holland, H.D. and Dwyer, M.J.: 1971, Science 174, 53.

Levine, J.S.: 1982, J. Mol. Evol. 18, 161.

Levine, J.L., Augustsson, T.R. and Natarajan, M.: 1982, Origins of Life 12, 245.
Lind, S.C. and Bardwell, D.C.: 1926, J. Am. Chem. Soc. 48, 2335.

Lind, S.C. and Glockler, G.: 1929, J. Am. Chem. Soc. 51, 2811.

Lind, S.C. and Glockler, G.: 1930, J. Am. Chem. Soc. 52, 4450.

Lind, S.C. and Schltze, G.R.: 1931, J. Am. Chem. Soc. 53, 3355.

Loew, G.H. and Chang, S.: 1971, Tetrahedron 27, 298.

Loew, G.H.: 1971, J. Theor. Biol. 33, 121.

Long, D.A., George, W.O. and Williams, A.E.: 1960, Proc. Chem. Soc., 285.

Lowe, C.U., Rees, M.W. and Markham, F.R.S.: 1963, Nature 199, 219.

Mackenzie, F.T.: 1975, in Riley J.P. and Skirrow, G. (eds.), Chemical Oceanography, Academic Press, London, 1.

Magee, E.M.: 1963, J. Chem. Phys. 39, 855.

Mahan, B.H. and Mandal, R.: 1962, J. Chem. Phys. 37, 207.

Malmstadt, H.V., Enke, C.G. and Crouch, S.R.: 1981, Electronics and Instrumentation for Scientists, The Benjamin/Cummings Publishing Co., Inc., Menlo Park, p. 543.

Masri, E. and Haissinsky, M.: 1963, J. Chim. Phys. 60, 397.

Matthews, C.N. and Moser, R.E.: 1966, Proc. Nat. Acad. Sci. 56, 1087.

Maurin, J.: 1962, J. Chim. Phys. 59, 15.

McGovern, W.E.: 1969, J. Atmos. Sci. 26, 623.

Miller, S.L.: 1953, Science 117, 528.

Miller, S.L.: 1957a, Biochim. et Biophys. Acta 23, 480.

Miller, S.L.: 1957b, Ann. N.Y. Acad. Sci. 69, 260.

Miller, S.L.: 1974, in Oro, J., Miller, S.L., Ponnamperuma, C. and Young, R.S. (eds.), Cosmochemical Evolution and the Origins of Life, I.D. Reidel Pub. Co., Holland, p. 139.

Miller, S.L., and Orgel L.E.: (1974) The Origins of Life on the Earth, Prentice-Hall, Inc., New Jersey, 229 p.

Moffat, J.B.: 1975, J. Chem. Soc. Chem. Commun. 888.

Mourey, D., Raulin, F. and Toupance, G.: 1981, in Wolman, Y. (ed.), Origin of Life, D. Reidel Publishing Co., Holland, 73.

Narty, F.: 1981, in Vennesland, B., Conn, E.E., Knowless, C.J., Westley, J. and Wissing, F. (eds), Cyanide in Biology, Academic Press, London, 115.

Navarro-González, R.: 1983, Identification of Carboxylic Acids in Irradiated Samples of Simple Nitriles and Cyanides, Bachelor Science Thesis, Universidad Nacional Autonoma de México, C.U. México.

Navarro-González, R. and Negrón-Mendoza, A.: 1983a, Analysis of Carbonyl Compounds. Part I. Paper Chromatography of Aldehydes and Ketones, Technical Report Q-05-83, Center of Nuclear Studies, U.N.A.M., C.U., México D.F. 08500.

Navarro-González, R. and Negrón-Mendoza, A.: 1983b, Analysis of Carbonyl Compounds. Part II. Gas Chromatography of Aldehydes and Ketones, Technical Report Q-06-83, Center of Nuclear Studies, U.N.A.M., C.U., México D.F. 08500.

Navarro-González, R., Negrón-Mendoza, A. and Ponnamperuma, C.: 1986, Origins of Life 16, 301.

Navarro-González, R., Negrón-Mendoza, A., Aguirre-Calderón, M.E. and Ponnamperuma, C.: 1989, Advances in Space Research in press.

Nazly, N., Collins, P.A. and Knowles, C.J.: 1981, in Vennesland, B., Conn, E.E., Knowless, C.J., Westley, J. and Wissing, F. (eds), Cyanide in Biology, Academic Press, London, 289.

Negrón-Mendoza, A. and Navarro-González, R.: 1982, Determination of Carboxylic Acids by Gas Chromatography, Technical Report Q-12-82, Center of Nuclear Studies, U.N.A.M., C.U., México D.F. 08500.

Negrón-Mendoza, A., Navarro-González, R., Draganic, Z. and Draganic, I.: 1982, Resumenes del IV Simposio sobre Quimica Nuclear, Radioquimica y Quimica de Radiaciones, U.N.A.M., Mexico, 34.

Negrón-Mendoza, A., Draganic, Z.D., Navarro-González, R. and Draganic, I.G.: 1983, Rad. Res. **95**, 248.

Negrón-Mendoza, A. and Draganic, Z.D.: 1984, Adv. Space Res. **4**, 121.

Negrón-Mendoza, A., Navarro-González, R. and Azamar, J.A.: 1984, Analysis of Aldehydes, Ketones, Alcoholes, and Monocarboxylic Acids by Gas-Solid Chromatography, Technical Report Q-04-84, Center of Nuclear Studies, U.N.A.M., C.U., México D.F. 08500.

Neta, P. and Fessenden, R.W.: 1970, J. Phys. Chem. **74**, 3362.

Niketic, V., Draganic, Z., Neskovic, S. and Draganic, I.: 1982, J. Mol. Evol. **18**, 130.

Niketic, V., Draganic, Z.D., Neskovic, S. and Draganic, I.G.: 1983, J. Mol. Evol. **19**, 184.

Niketic, V.: 1984a, Origins of Life **14**, 251.

Niketic, V.: 1984b, Adv. Space Res. **4**, 107.

Ogura, H. and Kondo, M.: 1967, Bull. Chem. Soc. Japan **40**, 2448.

Ogura, H.: 1968, Bull. Chem. Soc. Japan **41**, 2871.

Ogura, H., Fujimura, T., Murozono, S. Hirano, K. and Kondo, M.: 1972, J. Nuclear Sci. Technology **9**, 339.

Oparin, A.I.: 1924, Proiskhozhdenie zhizny, Moscow. Izd. Moskovshii Rabochii. (Translation in Bernal, J.D.: 1967, The Origin of Life, Weidenfeld and Nicolson, London, 199).

Oparin, A.I.: 1938, The Origin of Life, Dover, New York.

Oparin, A.I.: 1957, The Origin of Life on the Earth, 3rd Ed. Oliver & Boyd, London.

Oparin, A.I.: 1972, in Ponnamperuma, C., (ed.), Comparative Planetology, Academic Press, New York, 1.

Oró, J.: 1960, Biochem. Biophys. Res. Comm. **2**, 407.

Oró, J.: 1961, Nature **191**, 1193.

Oró, J. and Kimball, A.P.: 1961, Arch. Biochem. Biophys. **94**, 217.

Oró, J. and Kamat, S.S.: 1961, Nature **190**, 442.

Oró, J., Miller, S.L., and Urey, H.C.: 1977, in Buvet, R., ed., Living Systems as Energy Converters, Elsevier/North-Holland Biomedical press, Amsterdam, 7.

Owen, T.: 1982, J. Mol. Evol. **18**, 150.

Palm, C. and Calvin, M.: 1962, J. Am. Chem. Soc. **84**, 2115.

Palmer, H.B. and Hirt, T,J.: 1963, J. Phys. Chem. **67**, 709.

Park, W.K., Hochstim, A.R. and Ponnamperuma, C.: 1975, Origins of Life **6**, 99.

Perrin, D.E., Amarego, W.L. and Perrin, D.R.: 1966, Purification of Laboratory Chemicals, Pergamon Press, Oxford.

Peters, K. and Wagner, O.H.: 1931, Z. Phys. Chem. **A153**, 161.

Ponnamperuma, C.: 1965, in Fox, S.W. (ed.), The Origin of Prebiological Systems and of Their Molecular Matrices, Academic Press, New York, 221.

Ponnamperuma, C., Lemmon, R.M., Mariner, R. and Calvin, M.: 1963, Proc. Nat. Acad. Sci. USA **49**, 737.

Ponnamperuma, C. and Woeller, F.: 1964, Nature **203**, 272.

Ponnamperuma, C. and Pering, K.: 1966, Nature 209, 979.

Ponnamperuma, C., Woeller, F., Flores, J., Romiez, M. and Allen, W.: 1969, Adv. Chem Ser. 80, 280.

Rabani, J. and Matheson, M.S.: 1966, J. Phys. Chem. 70, 761.

Rabani, J. and Meyerstein, D.: 1968: J. Phys. Chem. 72, 1599.

Rao, V.V., Mackay, D. and Trass, O.: 1967, Canad. J. Chem. Eng. 45, 61

Rasmussen, O.L. and Bjergbakke, E.: 1984, CHEMSIMUL- A Program Package for Numerical Simulation of Chemical Reaction Systems, Risø-R-395, Risø National Laboratory, DK-4000 Roskilde, Denmark.

Raulin, F. and Toupance, G.: 1975a, Origins of Life 6, 91.

Raulin, F. and Toupance, G.: 1975b, Origins of Life 6, 507.

Raulin, F., Bossard, A. and Toupance, G.: 1979, Icarus 38, 358.

Raulin, F., Mourey, D. and Toupance, G.: 1982, Origins of Life 12, 267.

Rebbert, R.E. and Ausloos, P.: 1972, J. Photochem. 1, 171.

Rebbert, R.E. and Ausloos, P.: 1973, J. Res. N.B.S. 77A, 109.

Roscoe, J.M. and Thompson, M.J.: 1985, Int. J. Chem. Kinetics 17, 967.

Ross, A.B.: 1975, Selected Specific Rates of Reactions of Transients From Water in Aqueous Solution. 1. Hydrated Electron, Supplemental Data, NSRDS-NBS-43 Supplement, National Bureau of Standards, Washington, D.C.

Ross, F. and Ross, A.B.: 1977, Selected Specific Rates of Reactions of Transients From Water in Aqueous Solution. III. Hydroxyl Radical and Perhydroxyl Radical and Their Radical Ions, **NSRDS-NBS-59**, National Bureau of Standards, Washington, D.C.

Ross, A.B. and Neta, P: 1979, Rate Constants for Reactions of Inorganic Radicals in Aqueous Solution, **NSRDS-NBS-65**, National Bureau of Standards, Washington, D.C.

Ross, A.B. and Neta, P: 1982, Rate Constants for Reactions of Aliphatic Carbon-Centered Radicals in Aqueous Solution, **NSRDS-NBS-70**, National Bureau of Standards, Washington, D.C.

Sanchez, R.A., Ferris, J.P. and Orgel, L.E.: 1966, Science **154**, 784.

Sanchez, R.A., Ferris, J.P. and Orgel, L.E.: 1967, J. Mol. Biol. **30**, 223.

Schaefer, F.C.: 1970, in Zuirappoport, S. (ed.), The Chemistry of the Cyano Group, Interscience, N.Y., 240.

Sharpe, A.G.: 1976, The Chemistry of Cyano Complexes of the Transition Metals, Academic Press, London, 113.

Shimoyama, A., Blair, N. and Ponnamperuma, C.: 1978, in Noda, H. (ed), Origin of Life, Japan Scientific Societies Press, Tokyo, p. 95.

Sidle, A.B.: 1967, Nature **216**, 408.

Sieck, L.W. and Johnsen, R.H.: 1963, J. Phys. Chem. **67**, 2281.

Skinner, G.B. and Ruehrwein, R.A.: 1959, J. Phys. Chem. **63**, 1736.

Slanger, T.G. and Black, G.: 1982, J. Chem. Phys. **77**, 2432.

Smith, R.M. and Martell, A.E.: 1976, Critical Stability Constants, Volume 4: Inorganic Complexes, Plenum Press, New York, 26.

Snyder, L.E. and Buhl, D.: 1971, Astrophys. J. Lett. 163, L47.

Spinks J.W.T. and Woods, R.J.: 1976, An Introduction to Radiation Chemistry, John Wiley & Sons, New York, 503 p.

Stanley, J.B., Brown, D.F., Senn, V.J. and Dollean, F.G.: 1975, J. Food Sci. 40, 1134.

Stribling, R. and Miller, S.L.: 1986, Origins of Life 16, 279.

Stribling, R. and Miller, S.L.: 1987, Origins of Life 17, 261.

Sun, H., and Weissler, G.L.: 1955, J. Chem. Phys. 23, 1160.

Swallow, A.: 1960, Radiation Chemistry of Organic Compounds, Pergamon Press, New York, 45, 243.

Tain-Jen, Y., Sutherland, R. G. and Verrall, R. E.: 1980, Can J. Chem. 58, 1909.

Terasawa, J. and Harada, K.: 1980, Chem. Letters 73.

Thomas, J.K. and Hart, E.J.: 1962, Rad. Res. 17, 408.

Tokunaga, A.T., Beck, S.C., Geballe, T.R., Lacey, L.H. and Serabyn, E.: 1981, Icarus 48, 283.

Torres, J.L., Negrón-Mendoza, A. and Castillo, S.: 1982, Calibration of Carbon Monoxide, Methane, Ethane, and Carbon Dioxide by Gas Chromatography, **Technical Report Q-11-82**, Center of Nuclear Studies, U.N.A.M., C.U., México D.F. 08500.

Toupance, G., Sebban, G. and Buvet, R.: 1970, J. Chim. Phys. Physicochim. Biol. 67, 1870.

Toupance, G., Raulin, F. and Buvet, R.: 1975, Origins of Life 6, 83.

Toupance, G., Bossard, A. and Raulin, F.: 1977, Origins of Life 8, 259.

Tsang, W. and Hampson, R.F.: 1986, J. Phys. Chem. Ref. Data 15, 1087.

Ulich, B.L. and Conklin, B.K.: 1974, Nature 248, 121.

Vennesland, B., Pistorius, E.K. and Gewitz, H.S.: 1981, in Vennesland, B., Conn, E.E., Knowless, C.J., Westley, J. and Wissing, F. (eds), Cyanide in Biology, Academic Press, London, 349.

Voet, A.B. and Schwartz, A.W.: 1982, Origins of Life 12, 45.

Voet, A.B. and Schwartz, A.W.: 1983, Bioorg. Chem. 12, 8.

Volker, T.: 1957, Angew. Chem. 69, 728.

Volker, T.: 1960, Angew. Chem. 72, 379.

Weast, R.C., Astle, M.J. and Beyer, W.H. (eds.): 1985, CRC Handbook of Chemistry and Physics, CRC Press, Florida.

Weissler, A.: 1953, J. Acoustical Soc. Amer. 25, 651.

Wiener, H. and Burton, M.: 1953, J. Am. Chem. Soc. 75, 5815.

Wiley, E.J.: 1934, Trans. Farady Soc. 30, 230.

Wilson, W. E.: 1972, J. Phys. Chem. Ref. Data 1, 535.

Wilson, I.R.: 1972a, in Bamford, C.H. and Tipper, C.F.H (eds), Chemical Kinetics, Elsevier Publishing Company, Amsterdam, 217.

Yang, W., Minard, R. and Matthews, C.: 1976. J. Theor. Biol. 56, 111.

Yuasa, S. and Ishigami, M.: 1975, Origins of Life 6, 75.

Yung, Y.L., Allen, M. and Pinto, J.P.: 1984, Astrophisical J. Supplement Series 55, 465.

Zehavi, D. and Rabani, J.: 1972, J. Phys. Chem. 76, 3703.

Zehavi, D. and Rabani, J.: 1974, J. Phys. Chem. 78, 1368.

Zhdamirov, G.G., Kornienko, V.N., Borosov, E.A., Rumyantsev, Y.M. and Dzantiev, B.G.: 1971, High Energy Chemistry **5**, 475.

CURRICULUM VITAE

Name: Rafael Navarro-González

Permanent address: Instituto de Ciencias Nucleares, Universidad Nacional Autonoma de Mexico, Ciudad Universitaria, Mexico D.F. 04510 MEXICO

Degree and date to be conferred: Ph.D., 1989

Date of birth: April 25, 1959

Place of birth: Mexico, D.F., Mexico

Collegiate Institutions attended:

INSTITUTION	DATES ATTENDED	DEGREE	DATE OF DEGREE
University of Maryland, College Park	1984-1989	Ph.D.	1989
Major: Biochemistry			
Universidad Nacional Autonoma de Mexico, Mexico City	1978-1981	B. Sci.	1983
Major: Biology			

Honors:

1. 1980-1982. Research Fellowship from The National Autonomous University of Mexico.

2. 1984-1989. Research Fellowship from The National Autonomous University of Mexico.

Memberships:

1. International Society for the Study of Origins of life. Associate Member, 1981-

2. Mexican Chemical Society. Member, 1986-

3. Radiation Research Society. Student Member, 1986-

Publications:

1. Negrón-Mendoza, A., Z.D. Draganić, Navarro-González, R. and Draganić, I,G. (1983). Aldehydes, Ketones, and Carboxylic Acids Formed Radiolytically in Aqueous Solutions of Cyanides and Simple Nitriles. Rad. Res. **95**, 248-261.

2. Torres, J.L., Negrón-Mendoza, A. and Navarro-González, R. (1985). γ-Radiation of Aqueous Solutions of Urea (Spanish). J. Mexican Chem. Soc. **29**, 163.

3. Draganić, Z.D., Draganić, I.G., Negrón-Mendoza, A., Sehested, K., Navarro-González, R. and Albarrán-Sánchez, M.G. (1986). Radiolysis of Aqueous Solutions of Ammonium Bicarbonate over a Large Dose Range. Risø-M-2621. 16 pages.

4. Navarro-González, R., Negrón-Mendoza, A. and Ponnamperuma, C. (1986). Methane as a Chemical Dosimeter in Prebiotic Experiments. I. Electrical Discharges, Heat and Shock Waves. Origins of Life **16**, 301-302.

5. Negrón-Mendoza, A., Navarro-González, R. and Ponnamperuma, C. (1986). Influence of Na-Montmorillonite in the Gamma Radiolysis of Acetic Acid. Implications in Prebiotic Chemistry. Origins of Life **16**, 303-304.

6. Negrón-Mendoza, A., Navarro-González, R. and Torres, J.L. (1986). Some Aspects of the Gamma Radiolysis of Aqueous Solutions of Urea in the Context of Chemical Evolution. Origins of Life **16**, 305-306.

7. Draganić, Z.D., Negrón-Mendoza, A., Navarro-González, R. and Vujosević, S.I. (1987). The Presence of Polymeric Material in Radiolysed Aqueous Solutions of Ammonium Bicarbonate. Radiat. Phys. Chem. **30**, 229-231.

8. Navarro-González, R., Negrón-Mendoza, A., Chacón, E. and Honda, Y. (1989). The γ-Radiolysis of Aqueous Solutions of Urea. Implications for Chemical Evolution. Radiat. Phys. Chem. (in press).

9. Honda, Y., Navarro-González, R. and Ponnamperuma, C. (1989). Chemical Yields of Biologically Important Compounds from Electric Discharges. Radiat. Phys. Chem. (in press).

10. Honda, Y., Navarro-González, R. and Ponnamperuma, C. (1989). A Quantitative Assay of Biologically Important Compounds in Simulated Primitive Earth Experiments. Advances in Space Research (in press).

11. Navarro-González, R., Negrón-Mendoza, A., Aguirre-Calderon, M.E., and Ponnamperuma, C. (1989). The γ-Irradiation of Hydrogen Cyanide in the Presence of Ferrocyanide or Ferricyanide. Implications to Prebiotic Chemistry. Advances in Space Research (in press).

12. Navarro-González, R., Negrón-Mendoza, A. and Chacón, E. (1989). The γ-Irradiation of Aqueous Solutions of Urea. Implications for Chemical Evolution. Origins of Life and Evolution of the Biosphere (in press).

13. Navarro-González, R. and Ponnamperuma, C. The Mechanism of Bacterial Luminescence (Spanish) (1989). J. Mexican Chem. Soc. (in press).

14. Negrón-Mendoza, A., and Navarro-González, R. The γ-Irradiation of Aqueous Acetic Acid-Clay suspensions. Submitted to Radiation Effects.

15. Navarro-González, R. and Negrón-Mendoza, A. Microdetermination of Formic Acid. Submitted to J. Mexican Analytical Chem. Soc.

16. Navarro-González, R., Honda, Y., and Ponnamperuma, C. Dosimetry of High Voltages Electric Discharges. In preparation.

Contributions presented at Scientific Meetings:

1. Navarro-González, R., Negrón-Mendoza, A., Draganić, Z. and Draganić, I. (1982). Carboxylic Acids and Carbonyl Compounds Formed Radiolytically in Aqueous Solutions of Nitriles (Spanish). Abstracts for the IV Symposium on Nuclear Chemistry, Radiochemistry and Radiation Chemistry. U.N.A.M., Mexico. p. 33.

2. Negrón-Mendoza, A., Navarro-González, R., Draganić, Z. and Draganić, I. (1982). Carboxylic Acids and Carbonyl Compounds Formed Radiolytically in Aqueous Solutions of Cyanides (Spanish). Abstracts for the IV Symposium on Nuclear Chemistry, Radiochemistry and Radiation Chemistry. U.N.A.M., Mexico. p. 34.

3. Navarro-González, R., Negrón-Mendoza, A., Torres, J.L., and Ponnamperuma, C. (1986). The Effect of Some Cyanocomplexes of Transition Elements in the Radiolysis of Hydrogen Cyanide. I. Iron (Spanish). Abstracts for the VI Symposium on Nuclear Chemistry, Radiochemistry and Radiation Chemistry. Puebla, Mexico, Dec. 1-5.

4. Navarro-González, R. and Negrón-Mendoza, A (1986). Products from the Decomposition of Methane under different Energy Sources (Spanish). Abstracts for the VI Symposium on Nuclear Chemistry, Radiochemistry and Radiation Chemistry. Puebla, Mexico, Dec. 1-5.

5. Honda, Y., Navarro-González, R. and Ponnamperuma, C. (1988). Dosimetry of Electric Discharge Experiments in Chemical Evolution. Abstracts for the Thirty-Sixth Annual Meeting of the Radiation Research Society. Philadelphia, PA. p. 144.

6. Navarro-Gonzalez, R., Negrón-Mendoza, A. and Ponnamperuma, C. (1988). γ-Radiolysis of Hydrogen Cyanide in the Presence of Cyanocomplexes. Implications for Chemical Evolution. Abstracts for the Thirty-Sixth Annual Meeting of the Radiation Research Society. Philadelphia, PA. p. 149.

7. Honda, Y., Navarro-González, R. and Ponnamperuma, C. (1988). A Quantitative Assay of Biologically Important Compounds in Simulated Primitive Earth Experiments. Abstracts from the XXVII Plenary Meeting of the Committee on Space Research, Espoo, Finland, July 18-29. p. 383.

8. Navarro-González, R., Negrón-Mendoza, A., Aguirre-Calderon, M.E., and Ponnamperuma, C. (1988). The γ-Radiolysis of Hydrogen Cyanide in the Presence of Ferro- and Ferricyanide. Implications to Prebiotic Chemistry. Abstracts from the XXVII Plenary Meeting of the Committee on Space Research, Espoo, Finland, July 18-29. p. 383.

9. Navarro-González, R., Negrón-Mendoza, A., Chacón, E. and Honda, Y. (1988). The γ-Radiolysis of Aqueous Solutions of Urea. Implications for Chemical Evolution. Abstracts from the VII Symposium on Nuclear Chemistry, Radiochemistry and Radiation Chemistry. Zacatecas, Mexico, July 25-29.

10. Honda, Y., Navarro-González, R. and Ponnamperuma, C. (1988). Chemical Yields of Biologically Important Compounds from Electric Discharges. Abstracts from the VII Symposium on Nuclear Chemistry, Radiochemistry and Radiation Chemistry. Zacatecas, Mexico, July 25-29.

11. Navarro-González, R. and Ponnamperuma C. (1988). HCN and Biochemical Evolution. The Possible Role of Iron in Prebiological Evolution. The Ninth Virginia Biochemists Meeting. Airlie, Virginia, October 7-9, 1988.

12. Honda, Y., Navarro-González, R. and Ponnamperuma, C. (1988). Studies on Biochemical Evolution. I. Quantitative Assay of Biologically Important Compounds in Electric Discharge Experiments. The Ninth Virginia Biochemists Meeting. Airlie, Virginia, October 7-9, 1988.

13. Navarro-González, R., Negrón-Mendoza, A. and Ponnamperuma, C. Clay-Mediated Decarboxylation of Acetic Acid. The Role of Radiation Heterogeneous Catalysis in Prebiotic Chemistry. To be presented at the 9th International Clay Conference. Strasbourg, France, August 28, 1989.

Professional positions held:

1. 1989- . Associate Research Professor. Institute of Nuclear Sciences, Universidad Nacional Autonoma de Mexico.

2. 1987-1989. Research Assistant. Department of Chemistry. University of Maryland at College Park.

3. 1984-1986. Teaching Assistant. Department of Chemistry. University of Maryland at College Park.

4. 1983-1984. Research Associate. Center of Nuclear Studies, Universidad Nacional Autonoma de Mexico.

5. 1980-1983. Research Assistant. Center of Nuclear Studies, Universidad Nacional Autonoma de Mexico.

6. 1980-1983. Teaching Assistant. Faculty of Sciences. Universidad Nacional Autonoma de Mexico.